Katarzyna Krystyna Berkowicz

Bachelor of Science

Metabolism studies on emerging novel psychoactive substances (NPS) – Synthetic cathinones buphedrone and N-ethylhexedrone

Dissertação para obtenção do Grau de Mestre em Bioquímica para a Saúde

Orientador: Cristina Mello-Sampayo, Faculty of Pharmacy, University of Lisbon

Co-orientador: Maria Rosário Bronze, ITQB, NOVA University of Lisbon

Dezembro, 2019

Katarzyna Krystyna Berkowicz

Bachelor of Science

Metabolism studies on emerging novel psychoactive substances (NPS) – Synthetic cathinones buphedrone and N-ethylhexedrone

Lisbon, 2019

Metabolism studies on emerging novel psychoactive substances (NPS)

This page left blank intentionally

Agradecimentos/Acknowledgements

I would like to thank all the people that supported me during the process of writing this thesis, primarily my Professors Cristina Sampayo and Maria de Jesus Perry who carried out the laboratory work with me and provided guidance and insightful feedbacks. My great thanks go to Joana Quintela Carrola who performed an extraordinary work with HPLC-MS analysis and this thesis would not be possible to complete without her help. I also wanted to thank Professor Maria Rosário Bronze for her support and Pedro Florindo for the synthesis of the investigated compounds, as well as the institution of Faculty of Pharmacy from University of Lisbon, for providing the conditions for the research.

Finally, I cannot thank enough all my friends and family that supported me during this time, the projects Check!n and Kosmicare for providing additional background to the topic of this thesis and giving me possibilities to explore the world of Harm Reduction. Many thanks to the Futurize Project that enabled presentation of some parts of this work at Lisbon Addictions 2019 Conference.

This work was financially supported by Fundação para a Ciência e a Tecnologia (FCT), through PTDC-SAU-TOX/32515/2017 and, in part, UID/DTP/04138/2013 (iMed.ULisboa). The authors acknowledge the financial support from FCT and Portugal 2020 to the Portuguese Mass Spectrometry Network (Rede Nacional de Espectrometria de Massa – RNEM; LISBOA-01-0145-FEDER-402-022125).

Abstract

Novel Psychoactive Substances (NPS) started emerging around two decades ago as a response to strict prohibition laws on common illicit drugs. They have been marketed as legal alternatives, sold openly in smartshops, dark web as adulterants of other drugs. The trend rose noticeably in the last decade, as the number of NPS monitored by the European Monitoring Centre for Drugs and Drug Addiction (EMCDDA) rose from 13 in 2008 to 730 in 2018. Among them, synthetic cathinones (SC) became the most sought for class of NPS between users. They are particularly appealing to partygoers as some of the drugs from this class, such as Mephedrone, give effects similar to Ecstasy (MDMA) and cocaine, and were often cheaper and easier to obtain. As countries started to introduce restriction laws on the use of emerging SC, in response, new modified molecules would appear right after.

Two of the newly appeared cathinones: Buphedrone and N-ethylhexedrone were investigated in this study. The aim was to evaluate their metabolic profiles in order to get an idea of their rate of metabolism and possible metabolites that may later be used for screening and monitoring the use of those drugs. For this purpose, available *in silico* prediction tools combined with *in vitro* metabolic assays using mice and human microsomes, in vitro human plasma as well as the stability at 37ºC of the selected compounds were studied. HPLC-MS/MS was the technique used for the detection of selected metabolites in samples. Both SC were stable in plasma (t½ ~ > 24h). In vitro, N-dealkylation was the main metabolic reaction, but NEH also underwent beta-keto reduction, which could be followed by hydroxylation in the para position of the aromatic ring. These results add knowledge to create a map of metabolites and probable metabolic routes that can be used in future for SC use screening and monitoring purposes.

Keywords: Novel Psychoactive Substances, Synthetic Cathiones, Buphedrone, N-ethylhexedrone, Metabolism Studies, Metabolites.

Resumo

As novas Substâncias Psicoactivas (NPS) começaram a surgir há cerca de duas décadas como resposta a leis de proibição rigorosas sobre drogas ilícitas comuns. Foram comercializadas como alternativas legais, frequentemente vendidas abertamente em smartshops, dark-web ou usadas como adulterantes de outras drogas. A tendência aumentou consideravelmente na última década, tendo o número de novas substâncias psicoativas monitorizadas pelo Observatório Europeu da Droga e da Toxicodependência aumentado de 13 em 2008 para 730 em 2018. Entre elas, as catinonas sintéticas (SC) ganharam popularidade significativa tornando-se uma das classes de NPS mais procurada entre os utilizadores. São particularmente atraentes para os "partygoers", uma vez que algumas das drogas desta classe, como a mefedrona, podiam dar os efeitos tanto do ecstasy (MDMA) como da cocaína, e eram frequentemente mais baratas e mais fáceis de obter. À medida que os países começaram a introduzir leis de restrição ao uso das SC emergentes, em resposta novas moléculas modificadas surgiram logo a seguir.

Duas das novas catinonas emergentes: Buphedrone e N-Etilhexedrona foram investigados neste projecto. O objectivo era avaliar os seus perfis metabólicos de modo a ter uma ideia da sua taxa de metabolismo e possíveis metabolitos que possam mais tarde ser utilizados para rastreio na monitorização do uso destas drogas. Para isso, foram utilizadas ferramentas de predição de *in silico* disponíveis combinadas com ensaios metabólicos *in vitro* com microssomos humanos e de ratinhos, estudos *in vitro* em plasma humano bem como estudos de estabilidade a 37ºC dos compostos selecionados. A técnica de HPLC-MS/MS foi usada na deteção desses metabolitos nas amostras. Ambos compostos eram estáveis em plasma (t½ ~ > 24h). *In vitro*, N-dealquilação foi a principal reação metabólica, mas a NEH também sofreu redução de grupo cetona, podendo ser seguida de hidroxilação na posição para do anel aromático. Esses resultados contribuem para conhecimento do mapa de metabolitos e prováveis vias metabólicas, que poderão ser usados no futuro para fins de pesquisa e monitorização do uso de SC.

Palavras-chave: Novas Substâncias Psicoativas, Catinonas Sintéticas, Bufedrona, N-etilhexedrona, Estudos de Metabolismo, Metabolitos.

Table of Contents

1 INTRODUCTION 1

1.1 HISTORICAL BACKGROUND OF SYNTHETIC CATHINONES 1

1.2 INTERNET AND DARK WEB 9

1.3 CHEMISTRY 11

1.4 MECHANISM OF ACTION 13

1.5 METABOLISM 14

2 OBJECTIVES 20

3 METHODS AND MATERIALS 21

3.1 *IN SILICO* METABOLISM STUDIES: 21

3.1.1 SWISSADME TOOL 21

3.1.2 SMARTCYP PROGRAM 21

3.1.3 XENOSITE PROGRAM 22

3.1.4 BIOTRANSFORMER PROGRAM 22

3.2 STRUCTURE DRAWINGS 23

3.3 CHEMICALS AND MATERIALS 23

3.4 *IN VITRO* METABOLISM STUDIES 26

3.4.1 MICE LIVER MICROSOMAL ASSAY USING SYNTHETIC CATHINONES BUPHEDRONE AND N-ETHYLHEXEDRONE AS SUBSTRATES 26

3.4.2 MICE LIVER MICROSOMAL ASSAY USING N-ETHYLHEXEDRONE METABOLITES AS SUBSTRATES 27

3.4.3 HUMAN LIVER MICROSOMAL ASSAY USING SYNTHETIC CATHINONES BUPHEDRONE AND N-ETHYLHEXEDRONE AS SUBSTRATES 28

3.5 *IN VITRO* BLOOD PLASMA STUDIES 28

3.6 *IN VITRO* STABILITY STUDIES 29

3.6.1 STABILITY OF SYNTHETIC CATHINONES IN PHOSPHATE BUFFER (SHORT-TERM) 29

3.6.2 STABILITY OF SYNTHETIC CATHINONES IN PHOSPHATE BUFFER (LONG-TERM) 30

3.7 HPLC-MS/MS ANALYSIS 30

4 RESULTS AND DISCUSSION 32

4.1 *IN SILICO* AND LITERATURE METABOLISM PREDICTION OF SELECTED SCS: 32

4.1.1 METABOLITE PREDICTION BASED ON LITERATURE REVIEW 32

4.1.2 PROPERTIES PREDICTION OF BUPHEDRONE AND N-ETHYLHEXEDRONE USING SWISSADME 33

4.1.3 PREDICTION OF BUPHEDRONE AND N-ETHYLHEXEDRONE SITE OF METABOLISM USING SMARTCYP: 35

4.1.4 PREDICTION OF BUPHEDRONE AND N-ETHYLHEXEDRONE SITE OF METABOLISM AND POSSIBLE REACTIONS USING XENOSITE: 39

4.1.5 METABOLITE PREDICTION USING BIOTRANSFORMER PROGRAM. 41

4.2 *IN VITRO* STABILITY STUDIES 45

4.2.1 SHORT TERM STABILITY STUDY OF BUPHEDRONE AND N-ETYLHEXEDRONE 45

4.2.2 LONG TERM STABILITY STUDY OF BUPHEDRONE AND N-ETHYLHEXEDRONE 46

4.3 *IN VITRO* PLASMA STABILITY STUDIES 50

4.4 IN VITRO METABOLISM STUDIES USING LIVER MICROSOMES 58

4.4.1 MICROSOMAL METABOLISM STUDIES WITH MICE LIVER MICROSOMES USING BUPHEDRONE AND N-ETHYLHEXEDRONE AS SUBSTRATES 59

4.4.2 MICROSOMAL METABOLISM STUDIES WITH MICE LIVER MICROSOMES USING N-ETHYLHEXEDRONE BETA-KETO-REDUCED METABOLITE AS A SUBSTRATE 65

4.4.3 MICROSOMAL METABOLISM STUDIES WITH MICE LIVER MICROSOMES USING N-ETHYLHEXEDRONE N-DEALKYLATED METABOLITE AS A SUBSTRATE 66

4.4.4 MICROSOMAL METABOLISM STUDIES WITH HUMAN LIVER MICROSOMES USING BUPHEDRONE AND N-ETHYLHEXEDRONE AS SUBSTRATES 67

5 CONCLUSIONS 72

APPENDIX 1 – STRUCTURES OF SELECTED SYNTHETIC CATHINONES 75

APPENDIX 2 – STRUCTURES OF SELECTED MDMA PRECURSORS AND ADULTERANTS..... 80

APPENDIX 3 – POSITIVE CONTROL STUDIES PERFORMED DURING *IN VITRO* MICE AND HUMAN LIVER MICROSOMAL ASSAYS. 82

BIBLIOGRAPHY 85

List of Figures

Figure 1.1 Structures of cathinone, cathine and pseudoephedrine 3

Figure 1.2 Synthesis of methcathinone from pseudoephedrine as described by Sikk & Taba (2015) 4

Figure 1.3 Examples of some synthetic cathinones and their similarity between each other and to common illicit drugs such as amphetamine, methamphetamine and MDMA. 7

Figure 1.4 Structures of buphedrone (left) and N-ethylhexedrone (right) 9

Figure 1.5 Google search trends of selected synthetic cathinones from June 2009 until October 2019, as of 11th of November, 2019. 10

Figure 1.6: Structure of cathinone (A) and general structure of synthetic cathinones (B) 11

Figure 1.7 Examples of 4 different structural classes of synthetic cathinones 13

Figure 1.8 Reduction reaction of cathinones' β-Ketone Moiety (adapted from Zaitsu, 2018). 16

Figure 1.9 N-Dealkylation reaction of synthetic cathinones (adapted from Zaitsu, 2018) 17

Figure 1.10 Demethylenation reaction of synthetic cathinones followed by O-Methylation Pathways (adapted from Zaitsu, 2018) 17

Figure 1.11 Hydroxylation reaction of synthetic cathinones followed by dehydrogenation, and ring opening for the N- pyrrolidine cathinone derivative (adapted from Zaitsu, 2018) 18

Figure 1.12 O-demethylation reaction of 4'-methoxy group of synthetic cathinones and hydroxylation of the 4'-methyl group followed by oxidation to the corresponding carboxylic acid (adapted from Zaitsu, 2018) 18

Figure 3.1 Chemical structures of selected N-ethylhexedrone and buphedtone metabolites 24

Figure 3.2 Schematic representation of microsome assay proceedings 27

Figure 4.1 Buphedrone phase I metabolism prediction based on literature 33

Figure 4.2 N-ethylhexedrone phase I metabolism prediction based on the literature 33

Figure 4.3 SwissADME properties prediction for buphedrone 34

Figure 4.4 SwissADME properties prediction for N-ethylhexedrone 35

Figure 4.5 SmartCyp prediction for buphedrone metabolic transformation by CYP3A4 Isoform (Note that the atoms are numbered by their score) 36

Figure 4.6 SmartCyp prediction for buphedrone metabolic transformation by CYP2D6 isoform (Note that the atoms are numbered by their score) 36

Figure 4.7 SmartCyp prediction for buphedrone metabolic transformation CYP2C9 (Note that the atoms are numbered by their score) 37

Figure 4.8 SmartCyp prediction for NEH metabolic transformation by CYP3A4 isoform (Note that the atoms are numbered by their score) 37

Figure 4.9 SmartCyp prediction for NEH metabolic transformation by CYP2D6 isoform 38

Figure 4.10 SmartCyp prediction for NEH metabolic transformation by CYP2C9 isoform (Note that the atoms are numbered by their score) 38

Figure 4.11 XenoSite site of metabolism prediction for buphedrone 39

Figure 4.12 Site of metabolism prediction for N-ethylhexedrone performed by XenoSite 40

Figure 4.13 Rainbow Phase I prediction of the possible reactions, example of N-ethylhexedrone 41

Figure 4.14 Buphedrone metabolites with corresponding reaction types and metabolic enzymes inolved in the reaction predicted by BioTransformer 42

Figure 4.15 N-ethylhexedrone metabolites with corresponding reaction types and metabolic enzymes inolved in the reaction predicted by BioTransformer 43

Figure 4.16 Assessed amount (%) of tested compounds during the short-term (2h) stability study at 37 ºC in 20% of 0.01M phosphate buffer, pH ~7 46

Figure 4.17 Long-term stability of buphedrone at 37 ºC in 0.01 M isotonic phosphate buffer, pH 7.4 (starting concentration 100 μM) 47

Figure 4.18 Detection and assessment of buphedrone N-dealkylated metabolite (B2) during the long-term stability study of buphedrone 100 μM at 37 ºC in 0.01 M isotonic phosphate buffer, pH 7.4 47

Figure 4.19 Long-term stability of N-ethylhexedrone at 37 ºC in 0.01 M isotonic phosphate buffer, pH 7.4 (starting concentration 100 μM) 48

Figure 4.20 Detection and assessment of N-ethylhexedrone N-dealkylated metabolite (H2) during the long-term stability study of N-ethylhexedrone 100 μM at 37 ºC in 0.01 M isotonic phosphate buffer, pH 7.4. 48

Figure 4.21 Comparison of the stability of Buph and NEH in phosphate buffer (0.01 M)..... 49

Figure 4.22 Plasma Stability of buphedrone at a final concentration of 10^{-5} M. 50

Figure 4.23 Plasma stability of buphedrone at starting concentration of 10^{-5} M and 10^{-4} M 51

Figure 4.24 Plasma stability of buphedrone at final concentration 10^{-4} M. 51

Figure 4.25 Buphedrone kinetics assessment in plasma at concentration 10^{-5} M (left) and 10^{-4} M (right). 52

Figure 4.26 Detection and assessment of buphedrone N-dealkylated metabolite (B2) during the plasma stability study of buphedrone at final concentration of 10^{-4} M. 52

Figure 4.27 Stability of buphedrone in phosphate buffer (0.01 M, pH 7.4) and in plasma.. ... 53

Figure 4.28 Plasma stability of N-ethylhexedrone at final concentration at 10^{-4} M.. 53

Figure 4.29 N-ethylhexedrone kinetics assessment in plasma at concentration 10^{-4} M..... 54

Figure 4.30 Detection and assessment of NEH N-dealkylation metabolite (H2) during the plasma stability study of NEH (10^{-4} M). 55

Figure 4.31 Detection and assessment of NEH metabolite resulting from β-keto-reduction and oxidation in the para position of the aromatic ring (H4) during the plasma stability study of NEH (10^{-4} M)..... 55

Figure 4.32 Stability of N-ethylhexedrone in phosphate buffer (0.01 M, pH 7.4) and in plasma. Starting concentration 100 μM..... 56

Figure 4.33 Buphedrone *in vitro* metabolism assay using mice liver microsomes: buphedrone content variations (left) and detected metabolite resulting from N-dealkylation (B2, right). 59

Figure 4.34 N-ethylhexedrone *in vitro* metabolism assay using mice liver microsomes: N-ethylhexedrone content variation (left) and detected metabolite resulting from N-dealkylation (H2, right). 60

Figure 4.35 Buphedrone *in vitro* metabolism assay using mice liver microsomes: Buphedrone content variations (left) and detected metabolite resulting from N-dealkylation (B2, right) . 61

Figure 4.36 N-ethylhexedrone *in vitro* metabolism assay using mice liver microsomes: N-ethylhexedrone content variation (left) and detected metabolite resulted from N-dealkyation (H2, right) 61

Figure 4.37 Buphedrone *in vitro* metabolism assay using mice liver microsomes: Buphedrone content variations (left) and detected metabolite resulting from N-dealkylation (B2, right) . 62

Figure 4.38 N-ethylhexedrone *in vitro* metabolism assay using mice liver microsomes: N-ethylhexedrone content variation (left) and detected metabolite resulted from N-dealkylation (H2, right) 63

Figure 4.39 Formation of the metabolite resulting from β-keto reduction (H1) in the N-ethylhexedrone *in vitro* metabolism assay using mice liver microsomes 64

Figure 4.40 Variation of formed N-dealkylated metabolites B2 and H2. Start substrate concentrations of 15μM 65

Figure 4.41 *In vitro* metabolism assay of the β-keto-reduced N-ethylhexedrone metabolite (H1) using mice liver microsomes: H1 content variation (left) and detected metabolite resulted from hydroxylation in the *para* position (H4, right)..... 66

Figure 4.42 *In vitro* metabolism assay of the N-dealkylated N-ethylhexedrone metabolite (H2) using mice liver microsomes: H2 content variation (left) and detected metabolite resulted from β-keto-reduction (H3, right)..... 67

Figure 4.43 Buphedrone content variation during *in vitro* metabolism assay using human liver microsomes..... 68

Figure 4.44 N-ethylhexedrone content variation during *in vitro* metabolism assay using human liver microsomes. 68

Figure 4.45 Metabolite H1 content variation during in vitro metabolism assay using human liver microsomes (left) and in the negative control without cofactors (right)..... 69

Figure 4.46 Proposed metabolic pathway of N-ethylhexedrone in mice liver microsomes as predicted by the carried-out in vitro metabolism experiments..... 70

Figure 5.1 Comparison of the primarily predicted pathway for N-ethylhexedrone with the reactions actually observed in the *in vitro* mice microsomal assay..... 74

List of Tables

Table 3.1 Standard composition of the microsomal reaction mixture and of the stability assay 27

Table 3.2 Optimized MS/MS parameters for NEH and BUPH and metabolites..... 31

Table 3.3 Limits of detection for selected compounds. For H2 and B1 values were not obtained due to an interfering peak at concentrations below 0.05μg mL^{-1} 31

Table 4.1 Chemical properties of buphedrone and N-ethylhexedrone predicted by SwissADME 34

Table 4.2 Amount (%) of tested compounds present at different times of the stability study in phosphate buffer (0.01 M). 49

Table 4.3 Assessement of buphedrone content of samples collected from human plasma incubated at 37ºC 51

Table 4.4 Assessement of N-ethylhexedrone content of samples collected from human plasma incubated at 37ºC. 54

Table 4.5-Assessment of the content of investigated compounds present in samples collected from human plasma incubated at 37ºC 56

Table 4.6 Percentage of the initial amount of substrate remaining in the microsomal reaction mixture after 2h. 69

List of Abbreviations

3,4-DMMC	3′,4′-dimethylmethcathinone
4-FMC	Flephedrone, 4-fluoromethcathinone
4-MEC	4-Methylethcathinone
ADME	Administration, distribution, metabolism and excretion (of a drug)
BBB	Blood Brain Barrier
BZP	Benzylpiperazine
BUPH	Buphedrone
DAT	Dopamine transporter
DME	Drug metabolizing enzymes
EMCDDA	European Monitoring Centre for Drugs and Drug Addiction
FMO	Flavin containing monooxygenases
hDAT	Human dopamine transporter
HLM	Human liver microsomes
IFR	Institute of Forensic Research
MABP	α-methylamino-butyrophenone – Buphedrone
mCPP	meta-Chlorophenylpiperazine
MDMA	3,4-methylenedioxymethamphetamine
MDPBP	3',4'-Methylenedioxy-α-pyrrolidinobutyrophenone
MDPPP	3',4'-Methylenedioxy-α-pyrrolidinopropiophenone
MDPV	Methylenedioxypyrovalerone
MLM	Mice Liver Microsomes
MPHP	4'-Methyl-α-pyrrolidinohexiophenone
NEH	N-ethylhexedrone
NPS	Novel Psychoactive Substances
PBS	Phosphate-buffered saline
PMA	para-Methoxyamphetamine
PMK	Piperonyl Methyl Ketone - 3,4-Methylenedioxyphenylpropan-2-one
PMMA	para-Methoxy-N-methylamphetamine
SC	Synthetic Cathinones
SERT	Serotonin transporter
SOM	Site of Metabolism
TFMPP,	Trifluoromethylphenylpiperazine
UNDOC	United Nations Office on Drugs and Crime
α-PBP	alpha-Pyrrolidinobutiophenone
α-PPP	α-Pyrrolidinopropiophenone
α-PVP	alpha-Pyrrolidinopentiophenone

1

1 Introduction

1.1 Historical background of synthetic cathinones

New Psychoactive Substances (NPS) is the term coined to describe new substances producing psychoactive effects similar to the already known drugs that are controlled by international laws, or 'Narcotic or psychotropic drugs that are not scheduled under the United Nations 1961 or 1971 Conventions, but which may pose a threat to public health comparable to scheduled substances' (King & Kicman, 2011). Those drugs interact with central nervous system in a similar way to traditional drugs to produce the desired effect. The substances controlled under the 1961 and 1971 Conventions, while diverse in chemistry, can be placed into six distinct groups based on the major psychoactive effect they produce. These are opioids (e.g. heroin, morphine, and fentanyl), cannabimimetics (e.g. cannabis and delta-9-THC), dissociatives (e.g. phencyclidine), classic hallucinogens (e.g. LSD, 2C-B), sedatives/hypnotics (e.g. diazepam) and stimulants (e.g. cocaine and amphetamine-type stimulants such as methamphetamine) (United Nations Office on Drugs and Crime, 2018). NPS primarily started to emerge as a response to strict antidrug laws and often propose a cheaper, more easily available and legal alternative. On internet forums and in physical shops they are widely described as "plant food", "research chemicals" or "bath salts" and labelled as "not for human consumption" in order to escape legislative control. The first NPS to appear on a bigger scale and to be widely covered in media were synthetic cannabinoids. They were supposed to mimic the effects of marijuana and proposed a legal alternative for those seeking the drug. Subsequently, the market of the party drug "ecstasy" (MDMA – 3,4-methylenedioxymethamphetamine) suffered a crash, which prompted the vendors to look for

its substitutes. After 2004, when safrole, isosafrole, PMK and piperonal, common precursors for MDMA production, were banned in Europe under Regulation (EC) No 273/2004 of the European Parliament and of the Council of 11 February 2004 on drug precursors (European Monitoring Centre for Drugs and Drug Addiction, 2016), substances such as PMA and PMMA produced from anethole, legal at the time, started to appear. The impact of United Nations' massive seizure of 33 tonnes of safrole in Cambodia in 2008, and another one on a smaller scale in Thailand in 2010 also cannot be underestimated. The Cambodian safrole was supposed to yield estimated 245 million ecstasy tablets with a street value of nearly $8 billion (Barron, 2015), so after that event there has been a significant, rapid surge in synthesis of "legal highs" in order to satisfy the market demand for stimulants and entactogens. Those were produced from non-scheduled precursors and their role was to mimic the action of MDMA and other controlled stimulants like amphetamine and cocaine. One of the class of substances that gained major popularity among users as giving fairly stimulating and empathogenic effects were synthetic cathinones (SC) (Karila et al., 2014).

Synthetic cathinones chemically derive from cathinone, a stimulant alkaloid found in the leaves of khat (*Catha edulis),* an evergreen plant growing naturally in some parts of Africa and Arabian Peninsula. The plant has been used there for centuries. It is believed to have been introduced to Yemen, currently one of the biggest exporters in those regions next to Ethiopia and Kenya ("Khat is big business in Ethiopia | Africa | DW | 10.07.2019," n.d.) as early as in 13th century (Al-motarreb et al., 2002). In some of those countries in recent years khat cultivation has outgrown coffee production, being a more lucrative business. Interestingly, khat is not banned by Quran and is considered a typically Muslim drug (Krikorian, 1984). Fresh leaves and shoots are traditionally chewed in long sessions, especially among men, who often gather together after work to chew the leaves, but the practice is also common among women, who often hold their own chewing sessions. That ritual plays a significant role in social life of many communities and thanks to the export of khat leaves it is also practiced among emigrants from those regions. The tradition is reported to be typically performed in a social or festive context, such as weddings and birth parties, and is often accompanied by drinking large quantities of water (Litman et al., 1986). Although being a social phenomenon with rarely reported solitary use, khat use can still lead to dependency and can manifest withdrawal symptoms after abrupt cessation of prolonged use, similar to those of amphetamine dependency and withdrawal (Kalix, 1992). Chewing of the leaves helps extract cathinone and cathine, psychoactive chemicals present in the plant, through the action of salivary enzymes. It is important for the leaves to be fresh as cathinone, being an α-aminopropiophenone, is quite unstable and decomposes to cathine, a less active compound, within about 36-72 hours after the leaves have been picked up, losing therefore most of its psychoactive properties (Figure 1.1). Chewing of the leaves promotes alertness, sociability and increases feeling of well-being, therefore Khat has often been described as a natural

amphetamine. The effects on peripheral nervous system include increase in respiration, body temperature, blood pressure, heart rate and mydriasis (Patel, 2000). Similarly to other stimulants, excess use can result in insomnia, anorexia, hyperactivity, and may even lead to psychosis, paranoia and maniac-like behaviours (Patel, 2000).

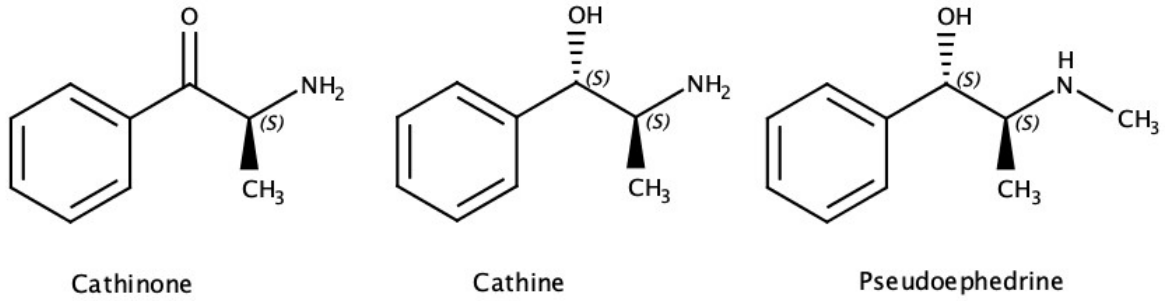

Figure 1.1 Structures of cathinone, cathine and pseudoephedrine

Cathinone was first identified as a main compound of Khat only in 1975 by the United Nations' Narcotics Laboratory and it was a ground-breaking discovery, as for decades cathine was thought to be the main psychoactive ingredient of the Khat plant because of its structural resemblance to pseudoephedrine (Figure 1.1). As it was later confirmed, cathine is much less potent than cathinone and is a product of its degradation. Even before those findings synthetic cathinones have been known and researched primarily as potential medications for therapeutic purposes. Bupropion (Wellbutrin, Zyban) found medical application as antidepressants and smoking cessation help. Interestingly, it has also been suggested as a form of treatment of cathinone withdrawal (Coppola & Mondola, 2012). It is currently the only cathinone analogue widely prescribed for many psychiatric disorders without causing significant dependence. Pyrovalerone has been used in clinical trials to treat lethargy and chronic fatigue syndrome and is sometimes prescribed as anorectic in short-term management of obesity. The same application was found for amfepramone (Diethylpropion, marketed as Tenuate). Methylone was first synthetized and patented by Peyton Jacob III and Alexander Shulgin in 1996 as a potential antidepressant and anti-Parkinsonian agent, but it has never been marketed (Patent No. WO9639133A1, 1996).

Cathinone's derivatives are closely related to the phenetylamine family of compounds. New synthetic cathinones are β-ketoamphetamine analogues of common stimulants or new substances on its own and produce euphoric, stimulating effects. They are obtained by modification in the ring or aliphatic chain of the molecule, therefore maintaining the active groups but at the same time escaping the common prohibition laws (King & Kicman, 2011).

Methcathinone, also described as ephedrone, "Jeff" or "mulka", was the first synthetic cathinone to be reported as a drug of abuse. It was marketed in Russia in the 30's and 40's as an antidepressant and substantially developed into a common stimulant among drug users in the '70s and '80s. It quickly became popularized in the USA in the '90s due to its easy production from ephedrine or pseudoephedrine (Figure 1.2) (Emmerson & Cisek, 1993). It is worth noting that in the US more often used as oxidizing agents in the clandestine production of methcathinone were chromium compounds as opposed to potassium permanganate, widely used as an oxidizing agent in Europe. Potassium permanganate has been linked to the Parkinson syndrome in chronic synthetic cathinone users (Sikk & Taba, 2015). As the final product often undergoes almost no purification, it contains high amounts of manganese that can cause severe neurotoxicity and irreversible brain damage. The risk is especially high among injecting drug users. In 1992 methcathinone was placed by the Drug Enforcement Administration into Schedule I of the United Nations Controlled Substance Act and is currently a controlled substance worldwide.

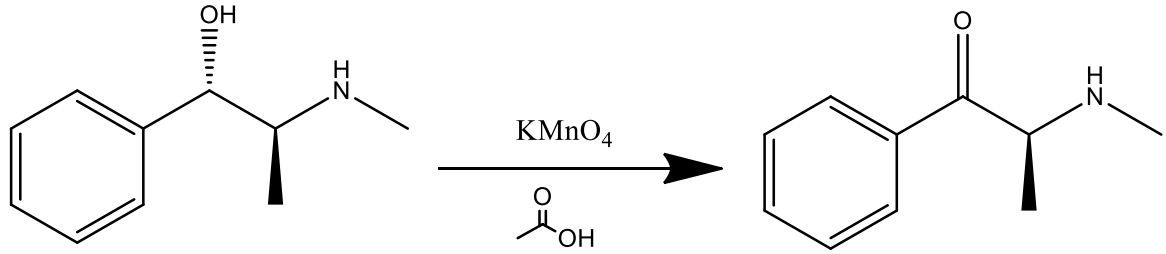

Figure 1.2 Synthesis of methcathinone from pseudoephedrine as described by Sikk & Taba (2015)

In 2003 and 2004 Israel experienced a boom in sales of the newly emerged capsules named "Hagigat" (Hebrew for "party"), labelled as "Natural stimulant and aphrodisiac for men and women, contains no chemicals; drink fluids liberally" (Bentur et al. 2008). In fact, as later analysed by the Israel Police, they contained 200mg of cathinone. They were commonly sold in small kiosks and convenience stores open 24/7 and supposedly primarily marketed as a substitute of khat. The plant was popularized by Yemenite Jews, who immigrated to Israel in 1950s, shortly after formation of the state, and kept the tradition of chewing leaves alive (Litman et al., 1986). During a typical chewing session around 100-300 g of khat leaves are used over a period of 3-4 hours (Toennes et al. 2003). According to the habit of Yemen, only the juice from chewed leaves is swallowed and the leaves are spit out. During chewing most of the alkaloids present in the leaves are extracted to the saliva and only about 10% of the original content is found in the leaf residue (Toennes et al., 2003). Fresh khat contains on average 36 mg of cathinone, 120 mg of cathine and 8 mg of norepinephrine per 100 g of leaves (Geisshusler & Brenneisen, 1987), although higher (78-343 mg/100 g) levels of cathinone in

fresh leaves have been reported (Al-motarreb et al., 2002). It shows that the dose of cathinone found in "Hagigat" was much higher than ingested during a common chewing session and it was taken at once instead over a prolonged period of time, thus posing a higher threat in terms of toxicity and poisonings. The capsules were described by the users as producing significant stimulating, euphoric effects and increasing sociability and self-confidence, therefore they quickly gained extreme popularity in the party scene. Because of its fame, the party drug quickly became an interest of the regulatory instances and was soon banned. Its replacement was a slightly modified version of the cathinone molecule, synthetized by an Israeli company Neorganics, sold under the names such as Neodoves. It is sometimes speculated that it was this company that brought cathinone and its possible synthetic derivatives to the attention of clandestine chemists that were looking for alternative party drugs. The pills and liquids they were producing contained 4-methyl methcathinone, more widely known as Mephedrone, and were banned in Israel in 2008, at the time when they were only gaining popularity in Europe and other parts of the world.

Methylone (Figure 1.3), previously mentioned as a potential antidepressant and anti-Parkinsonian agent, was one of the first generation of synthetic cathinones to appear on illicit drug markets in Europe in the mid-2000s, usually sold under the brand name 'Explosion', marketed on the dark net and sold in smartshops. However, the drug that really brought synthetic cathinones to a wider attention of the public and users was mephedrone. The appearance of mephedrone (4-methyl methcathinone - 4-MMC, also called Meow Meow, M-CAT or MMCAT) (Figure 1.3) is a phenomena on its own and has been compared to the revolution on the drug scene as that of rediscovery of MDMA by Alexander Shulgin in the 70's and it's popularization in the 80's club scene. It appeared in Europe at the time of the MDMA "drought", after widespread banning of precursors for production of that drug and massive seizure of safrole oil in Cambodia. The first reports of mephedrone come from 2007 and it was primarily found as an adulterant of ecstasy (MDMA) pills. Shortage of precursors for MDMA-like drugs forced clandestine chemists to look for alternatives. In that period many other substances were sold as ecstasy, among them piperazines, such as mixture of BZP/TFMPP or mCPP, infamous for inducing severe headaches and generally unpleasant effects as well as long lasting hangovers. Another notorious drugs at the time were PMA and PMMA. Produced from legal precursor anethole, the flavour compound of anise, fennel and liquorice, although more similar in structure to MDMA than piperazines, they had little psychoactive effect. Instead, they were responsible for numerous deaths, as they are both more potent than MDMA and take longer to exert any effect. Because of that many users would redose them shortly after taking the first pill. Their mechanism of action is also different. PMA and PMMA lead to significant increase in body temperature and can easily induce a serotonin syndrome in the users, and thus are still responsible for many deaths. That is why among those substances sold as Ecstasy pills mephedrone quickly gained popularity.

Mephedrone was first synthetized in 1929 by Saem de Burnaga Sanchez (Europol & EMCDDA, 2005), only to be rediscovered seventy years later as a party drug. The formula for synthesis of Mephedrone was first published in 2003 on the drug forum "The Hive" by the user nicknamed Kinetic, who described himself as a mathematician and a chemist. As reported by Professor David Nutt in his book *Drugs –Without the Hot Air: Minimising the Harms of Legal and Illegal Drugs* mephedrone was also researched by Israeli scientists working for a pesticide company as a potential insecticide, hence the marketed name of synthetic cathinones as "plant food". Mephedrone produces pleasant, euphoric effects with a quick onset when insufflated, very similar of those of ecstasy, but its shorter lasting (1-2h) and more socializing effect, as well as high redosing potential make it also similar to cocaine. It is no wonder then that many users started to prefer that drug even over MDMA and it quickly established its position as the most common and sought for synthetic cathinone, ranking as the fourth most used drug in the UK in the club scene in 2009, after cannabis, cocaine and MDMA (Dargan & Wood, 2013).

Mephedrone's golden age did not last for long. In 2010 European Union decided to submit 4-methylmethcathinone (mephedrone) to control measures under council decision of 2 December 2010 (2010/759/EU). Shortly after the US followed and in 2011 scheduled mephedrone as a Schedule I drug. Those bans, as previously in the case of MDMA, sparked an avalanche of new synthetic cathinones appearing on drug markets worldwide, where each banned drug is quickly substituted by a new one (Valente et al., 2013). Clandestine chemists rushed to modify the structures of banned psychoactive substances more and more escaping the prohibitionist laws and the original drugs, thus making new substances' action less predictive. New synthetic cathinones are usually encountered in pill or powder form and the most common route of consumption is insufflation, ingestion or vaporization, although there are reports of injection of cathinones, especially among high risk drug users (EMCDDA, 2015, 2017)

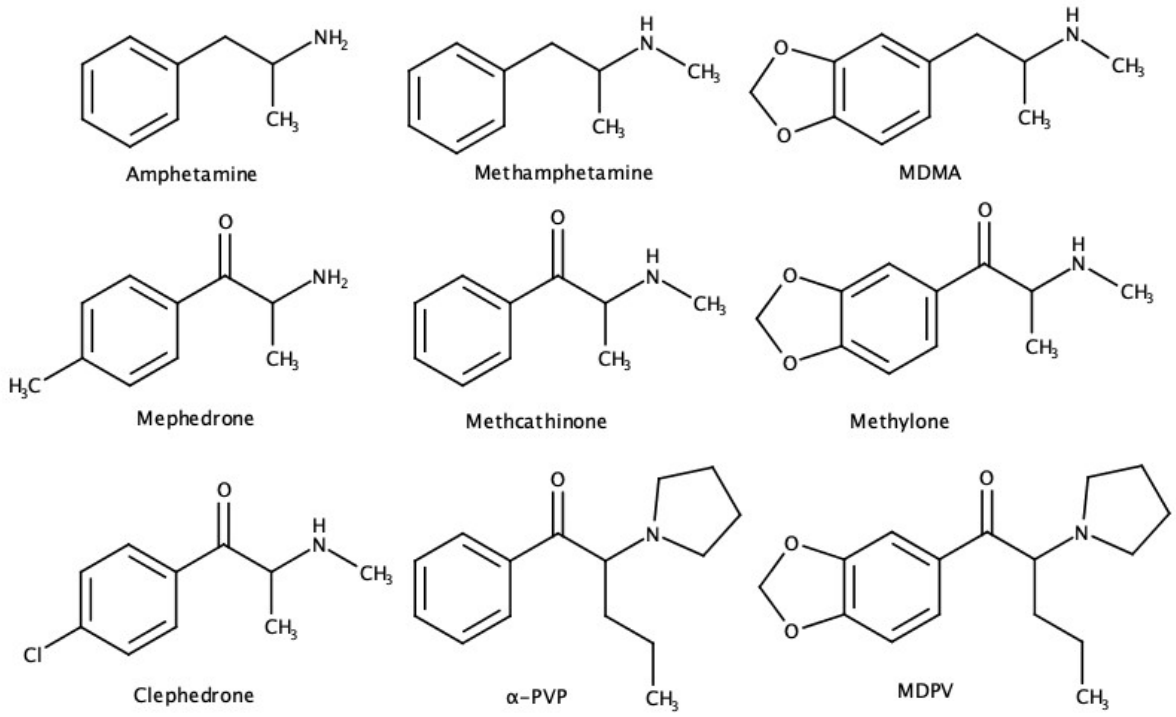

Figure 1.3 Examples of some synthetic cathinones and their similarity between each other and to common illicit drugs such as amphetamine, methamphetamine and MDMA.

For the purpose of this study two synthetic cathinones have been chosen to be researched: **buphedone** and **N-ethylhexedrone** (Figure 1.4). Buphedrone, also known as α-methylamino-butyrophenone (MABP), is an interesting substance to investigate, as it is a positional isomer of mephedrone and gained popularity as a recreationally used stimulant shortly after mephedrone was banned. It is still legal in most countries as a research chemical. Just like other synthetic cathinones, in its free base it is very unstable, and the ketone group is easily reduced to hydroxyl group, forming a corresponding alcohol. Because of that it is often sold in the form of various salts, principally hydrochloride salt. The substance is usually snorted, smoked or taken orally. It was first synthetized in 1928 (Hyde et al., 1928) but has not been much heard of until its reappearance as a recreational stimulant in headshops and online markets. Comparably to other synthetic cathinones, the effects of buphedrone include elevated mood, euphoria, increased talkativeness, motivation, alertness, stimulation and insomnia, although it appears to be less euphoric than mephedrone (Zuba et al., 2013). While there is data available on methods of detection of buphedrone (Maheux & Copeland, 2012; Zuba et al., 2013), still very little research has been made on buphedrone's metabolism, toxicology, addiction potential, long term effects and possible harms associated with the use. Most of the reports of self-administration can be found on Internet fora, but they often should

not be treated as a solid reference as the users might have reported using a substance they believed to be buphedrone, but in fact containing a different compound or a mixture. According to the harm reduction website TripSit ("TripSit Factsheets - Buphedrone," 2019) the light oral dose of Buphedrone is 10-30mg, common is 30-50mg and heavy – 50-80mg. It can be both used orally and insufflated and in both cases the effects start to appear after 10-20min. When used orally, the effects last for about 2-3 hours and after-effects can be felt until up to 8 hours. When snorted, the effects last up to 2 hours with a similar duration of after-effects as when taken orally.

After banning of mephedrone in 2010, Buphedrone was identified in 15 products seized by Polish law enforcement and analysed in the Institute of Forensic Research (IFR), but was mostly found mixed with other cathinones, such as 4-MEC and MDPV (Zuba et al., 2013).

N-ethylhexedrone (HEX-EN, NEH) only appeared on drug markets around 2016, so it is a fairly new substance, but already in 2017 it was the most seized stimulant designer drug in Hungary (Kovács et al., 2019) and in 2018 it was reported as the second most common drug of the cathinone class to be identified by the US DEA-DOJ (Expert Committee on Drug Dependence, 2019). Also in China, N-ethylhexedrone was described as the 5th most commonly identified novel psychoactive substance according to the NPS Monitoring Programme in 2017 (UNODC, 2015). It is structurally similar to other popular cathinones such as pentedrone. NEH was first described in a patent by Boehringer Ingelheim in Germany in 1965 (Herbert et al., 1965), together with other derivatives of aminoketone. Nowadays it is sold as white, grey or yellow powder or fine crystals. The common way of administration is via insufflation or inhalation, as well as orally. There are also reports of rectal, intravenous, smoked or *Hot rails* (inhaling through the nose through a heated glass tube) ingestion (Mikołajczyk et al., 2017). The threshold doses of N-ethylhexedrone described on internet sources when taken orally are in the range of 5–15 mg; light doses: 15–25 mg; typical doses: 25–40 mg; high doses: 40mg and more ("TripSit Factsheets - Hexen," 2019); although some reports describe the dosage as much higher, with very high doses reaching the level of 100–150 mg, and even 250 mg (Mikołajczyk et al., 2017). The effects are reported to be rather short lasting, reaching the peak after about 50-60 minutes and ceasing after 2-3 hours, which leads to frequent redosing, although some people report that after more frequent redosing the effects switch to be very unpleasant. The psychoactive effects are sometimes compared to cocaine, giving the users feelings of euphoria, stimulation, empathy, enhanced sense of well-being, increased talkativeness, sociability, insomnia, and sensory enhancement (Expert Committee on Drug Dependence, 2019). The adverse effects are similar to those of other cathinones and include hypertension, pains in the chest, tachycardia, paranoia, elevated temperature, bruxism (teeth grinding) (Mikołajczyk et al., 2017). Because the effects of NEH appear to be rather short-lived, it might be suspected that the substance is absorbed,

distributed, metabolized and excreted relatively quickly. It has been involved in some cases of non-fatal and fatal intoxications (Kovács et al., 2019; Mikołajczyk et al., 2017).

A toxicology screening test has been developed in order to measure the toxicity of synthetic cathinones: 4-FMC, 4-MEC, buphedrone, methedrone, and N-ethylhexedrone. In the assay two models were used: yeast *S. cerevisiae* and differentiated SH-SY5Y (human derived cell line often used as in vitro models of neuronal function and differentiation) cells. In the SH-SY5Y viability assay N-ethylhexedrone showed to have the lowest IC_{50} (measure that indicates how much of a particular inhibitory substance is needed to inhibit, in vitro, a given biological process or biological component by 50%) of all of the investigated SCs (98.1 μM), thus being the most toxic of all the investigated SCs. For buphedrone that value was 148.0 μM. The yeast assay showed that N-ethylhexedrone inhibited the growth of *S. cerevisiae* already at the concentration of 75mM, making it the second most toxic substance, after 4-FMC, of all the SCs tested (Ferreira et al., 2019). In this study buphedrone was shown to significantly decrease the yeast growth curve at the concentration of 75mM. Higher concentrations however did not completely inhibit the yeast growth, contrary to N-ethylhexedrone (Ferreira et al., 2019).

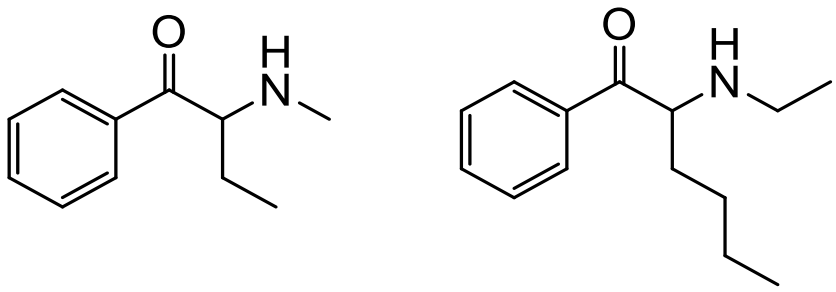

Figure 1.4 Structures of buphedrone (left) and N-ethylhexedrone (right)

1.2 Internet and Dark Web

The phenomena of research chemicals, such as synthetic cathinones, and its ever-growing market, would not be possible without emergence of the internet culture and dark web. It made purchase of new substances much easier and online vendors started offering a wider range of compounds, often also the new and legal ones, of very high purity. First drug fora emerged as early as in 1994 and focused mostly on exchange of the information about substances and their action, as well as tips and recipes for home-based production. These fora were also used to exchange harm reduction practices, describe the effects and dosages of psychoactive substances and create a certain community for the drug users, who often would

call themselves "psychonauts", that is people who explore altered states of consciousness, especially through the use of psychoactive drugs (Chatwin et al., 2017).

Legal NPS were primarily sold on the surface web, but with the progression of legislative measures to criminalize their use and selling, the market moved to the deep web. The most valuable advantage of the deep web is that it allows the users and vendors to remain anonymous thanks to various encryption methods and allows anonymous payments with cryptocurrencies, which creates a sense of security and escape from the criminal law. Anonymous darknet markets emerged in 2010, so their appearance is closely correlated in time with the appearance of synthetic cathinones and other NPS. Since then it is estimated that over 100 darknet markets have been in existence at various time-points since then (European Monitoring Centre for Drugs and Drug Addiction, 2019). The first cryptomarket that achieved the biggest success was Silk Road, taken down by FBI in October 2013. It has been estimated that since the closure of Silk Road until the end of 2016 the number of transactions of illicit drugs on the cryptomarkets has tripled and the revenues doubled, even in spite of various law enforcement interventions (RAND Europe, 2013). In 2017 due to large-scale international police operation AlphaBay, the largest marketplace to have existed so far, and Hansa, another large market, have been taken down. Nevertheless, it was shown that one year later the scale of sales and revenues related to drug sales in darknet has returned to pre-enforcement levels and trading of illegal drugs remains the most widespread activity on the Darknet (European Monitoring Centre for Drugs and Drug, 2019).

It is worth noting that crypto markets are not only used by individuals, but very often,

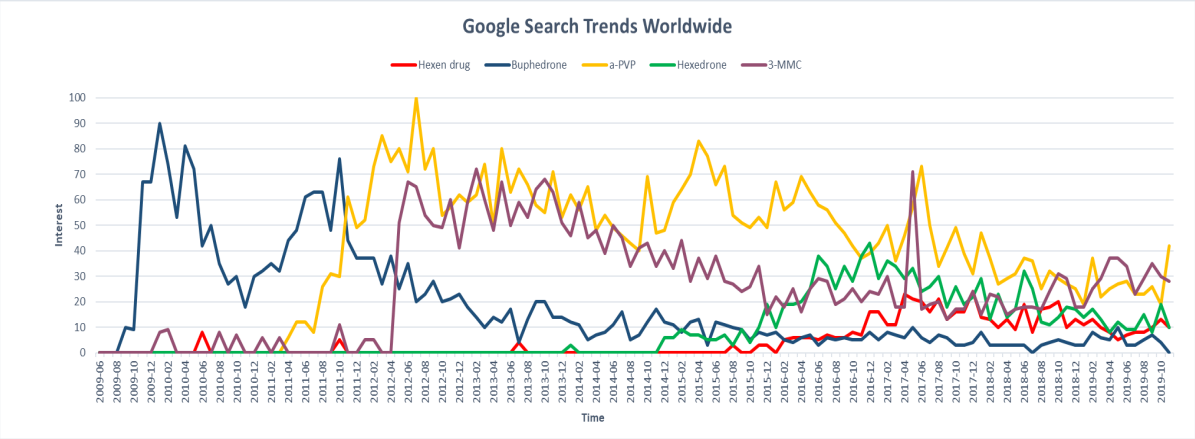

Figure 1.5 Google search trends of selected synthetic cathinones from June 2009 until October 2019, as of 11th of November, 2019.

especially in case of MDMA, by local dealers that purchase large quantities of the drugs to sell them to their clients. Concerning individual purchases, on the crypto markets buyers had the possibility to choose the vendor and product based on the price, opinion from other buyers, "trip reports" (individual reports from the experience and effects of the drug) and vendor

reputation. The fact that vendors could be rated and that the sold substances were often submitted for testing by the buyers in the available drug checking services created a somehow trustworthy atmosphere and community where vendors make sure to satisfy their clients and the clients leave feedback to guide other potential buyers (Mirea et al., 2019). Some argue that crypto markets reduced the violence normally associated with drug trades, but on the other hand they made the purchase of illicit substances easily available for the underage (Mirea et al., 2019). The full social impact of the dark web markets is still difficult to assess.

The interest in different synthetic cathinones has been changing a lot in the last decade, and it is clearly visible that as soon as one substance is banned, a new one appears in google searches, as illustrated on the Figure 1.5. The general tendency to search for those particular cathinones is declining, but this trend can mean that the interest in SC is lower due to easier availability of other common illicit drugs, or that the searches have moved from "clean web" to the dark web and it is very difficult to track them.

1.3 Chemistry

Synthetic cathinones are closely related to amphetamine (Figure 1.3) and are being often called β-keto-amphetamines. The difference in structure is that synthetic cathinones contain a keto group in the β position of the alkyl chain (Zaitsu, 2018). Chemically, all synthetic cathinones are derivatives of cathinone, with different substituents added to one or more of the 5 possible positions as represented on the Figure 1.6.

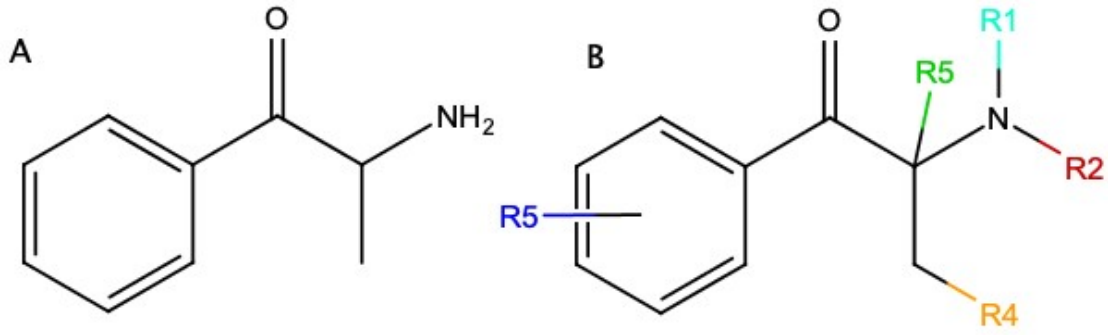

Figure 1.6: Structure of cathinone (A) and general structure of synthetic cathinones (B)

While investigating cathinones' metabolism it is important to remember that synthetic cathinones often vary in structure (**Error! Reference source not found.**) and thus will have d ifferent metabolic pathways. According to Valente and colleagues (2013), synthetic cathinones can be separated into four different categories depending on the structure and, thus, metabolic similarities within each group:

N-Alkylated cathinone derivatives with/without ring substituents.

The first group is composed of N-alkylated derivatives at R_1 and/or R_2, some with ring substituents at R_3, that were primarily synthetized for therapeutic purposes, for example antidepressant bupropion and anorectics like diethylpropion (Valente et al., 2013).This group was also the first one to reach the drug markets, as the modification is relatively easy to carry out, like in case of mephedrone, buphedrone and methcathinone (**Error! Reference source not found.**). Flephedrone, clephedrone and 3′,4′-dimethylmethcathinone (3,4-DMMC) also belong to this group.

N-Pyrrolidine cathinone derivatives with ring substituents.

This group can be distinguished by a substitution of a N-pyrrolidine ring at the nitrogen atom instead of N-alkyl chain. That includes compounds such as pyrovalerone (Figure 1.7), α-PVP, MPHP and α-PPP.

3′,4′-Methylenedioxy-N-alkylated cathinones.

This category is characterized by the presence of 3,4-methylenedioxy group added to the benzene ring, which is characteristic for other drugs of abuse, primarily MDMA. It includes synthetic cathinones such as methylone (bk-MDMA) (Figure 1.7), ethylone (bk-MDEA), butylone (bk-MBDB), and pentylone (bk-MBDP) etc.

3′,4′-Methylenedioxy-N-pyrrolidine cathinone derivatives.

The last group is described as derivatives of 3,4-methylenedioxy-N-pyrrolidine cathinone MDPPP, containing both substitution at the benzene ring with 3,4-methylenedioxy group and an N-pyrrolidine moiety. The most known representants of this class are MDPV (Figure 1.7), MDPPP and MDPBP.

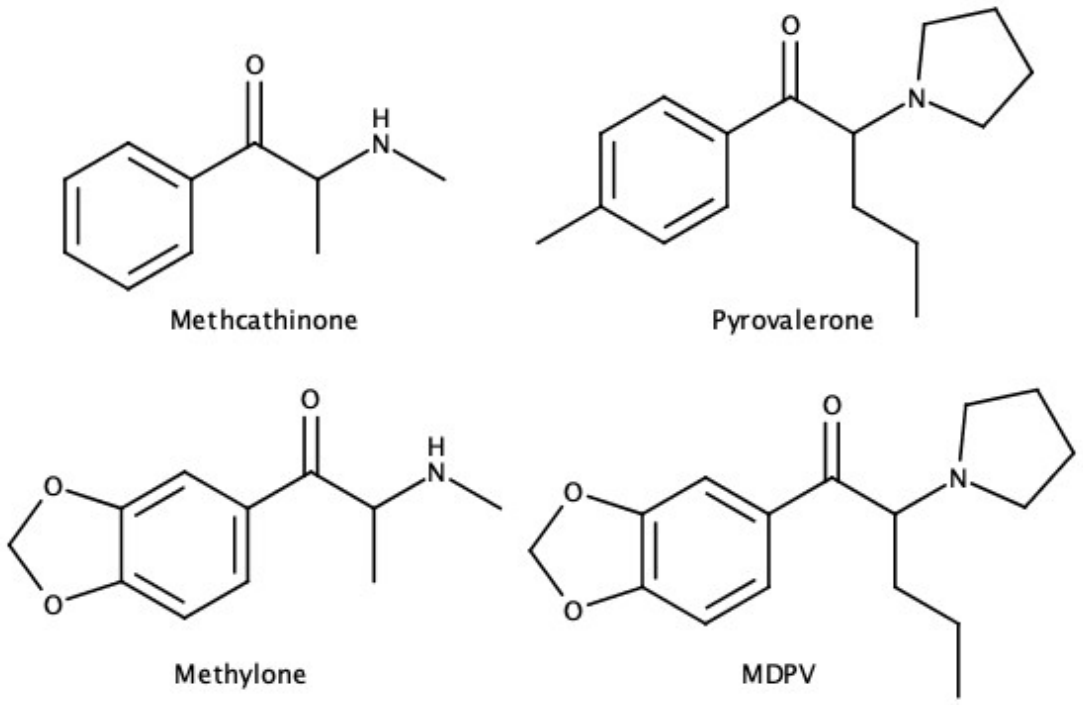

Figure 1.7 Examples of 4 different structural classes of synthetic cathinones: N-alkylated without ring substitutes – Methcathinone, N-pyrrilodine cathinone derivatives with ring substituents – Pyrovalerone, 3',4'-Methylenedioxy-N-alkylated synthetic cathinones – Methylone, 3',4'-Methylenedioxy-N-pyrrolidine cathinone derivatives - MDPV

1.4 Mechanism of action

All synthetic cathinones act by increasing extracellular monoamine concentration in the brain, and therefore increasing the cell-to-cell signalling (Baumann et al., 2018). Generally, the presence of the β-keto group increases the polarity of the synthetic cathinones in comparison to amphetamines and MDMA, resulting in a decrease in their ability to cross the blood–brain barrier (BBB) (Lindsay & White, 2012). That is the case in synthetic cathinones with N-alkylated groups, where the dose taken by the users must be usually higher than their amphetamine analogue or repeated more often in order to sustain the effect. On the contrary, the presence of the pyrrolidine ring in the structure decreases polarity and those compounds would have a lower active dose. Cathinones can also be divided in two categories depending on the way they act in the synapse. They can increase the concentration of monoamines by promoting neurotransmitter release and reversing the normal transportation flux or they can act by inhibiting neurotransmitter reuptake from the synaptic cleft by binding to the orthosteric site of the transporter. Ring substituted cathinones such as mephedrone usually fall in the first cathegory of **releasers**, whereas pyrrolidine-containing cathinones like α-PVP and MDPV are potent **blockers**. Both types can significantly increase the extracellular

concentrations of monoamines, increasing the cell-to-cell signalling. Releasers are particularly important to distinguish because of their properties to enter into cells together with sodium ions and reverse the direction of transporter flux to promote release of neurotransmitters. They can also disrupt normal neurotransmitter synthesis by accumulating in the cytoplasm and interacting with neuronal proteins, which may lead to neurotransmitter deficiency (Baumann et al., 2018).

Baumann and colleagues (2011) have shown that ring-substituted cathinones are transporter substrates (releasers). They used examples of mephedrone and methylone to show that they both trigger release of dopamine and serotonin, having the molecular mechanism of action very similar to that of MDMA. However, it has been suggested that the bulkier the substituents of the phenyl ring, the higher the potency for serotonin transporter (SERT) relative to dopamine transporter (DAT). Buphedrone is known to have a DAT/SERT inhibition ratio above 10 (higher than methamphetamine), which indicates greater relative dopaminergic vs serotonergic activity similar to methamphetamine, and it has been proven to induce dopamine D1 receptor activation (Oh et al., 2018). A high DAT/SERT inhibition ratio is a pharmacological characteristic associated with more stimulant effects and with higher potential for addiction (Liechti, 2015). NEH has been shown to have a high preference for the human dopamine transporter (hDAT) with the ratio of DAT/SERT equal to 100 (Eshleman et al., 2018). As it appears to act primarily on dopamine transporters, it might be another reason why it induces a high desire of redosing. In addition, it was shown that the carbon chain length on the alpha carbon affects DAT affinity and potency, with compounds containing tails with three to six carbons having very high affinity.

1.5 Metabolism

Majority of drugs, as well as other xenobiotics, undergo primary elimination through hepatic metabolism. Metabolism is a determinant of drug bioavailability, clearance, elimination half-life, and thus, dose and dosing frequency (Knights et al., 2016). Generally, metabolism of xenobiotics, such as drugs, can be divided in two phases. Phase 1 usually consists of hydroxylation reactions primarily catalysed by polymorphic Cytochrome P450s enzymes, monooxygenases capable of metabolizing a broad range of substrates (Stanley, 2017). Those enzymes, apart from hydroxylation, can catalyse a wide range of different reactions, such as deamination, dehalogenation, desulfuration, epoxidation, peroxygenation, and reduction (Wood, 1996). In phase 2 the metabolites of phase one are conjugated with a bulky polar molecule such as glucuronic acid or glutathione. The main objective of those reactions is to increase the drug's solubility in water in order to facilitate its excretion and

make them less active (although it is not the case when considering prodrugs, where the phase 1 reactions actually turn the drug active).

In laboratory setting, hepatic microsomes, derived largely from the smooth endoplasmic reticulum, are commonly used as the enzyme source for metabolic studies, as they contain the main drug-metabolizing enzymes (DMEs) cytochrome P450 (CYP) and UDP-glucuronosyltransferase (UGT), together with other DMEs, including flavin containing monooxygenases (FMO) and esterases (hCE1, hCE2) (Penner et al. 2012).

The available literature on synthetic cathinones' metabolism mostly focuses on the drug mephedrone, due to its popularity. In a study evaluating in vitro metabolism of mephedrone CYP450 isoenzyme 2D6 was indicated as primarily responsible for the metabolism of mephedrone, especially involved in the hydroxylation of the *p*-totyl group and N-dealkylation (Pedersen et al., 2012). The study also mentions isoforms 1A2 and 2C19 as capable of performing the same reactions, although in the inhibition test it was confirmed that neither 1A2, 2C19, 2C9 nor 3A4 contributed significantly to the metabolism of the compound. Incubation with human liver microsomes (HLM) also resulted in formation of hydroxytolyl-mephedrone, but to a lower degree. The study also suggests that most of the drug is excreted unchanged. In the analysis of four traffic cases the parent drug was found in urine, along with metabolites Nor-mephedrone, dihydro-mephedrone and 4-carboxy- mephedrone (those three were also detected in blood), hydroxytolyl- and 4-carboxy-dihydro-mephedron. Hydroxytolyl mephedrone and nor-hydroxytolyl mephedrone were partly excreted as glucuronides and/or sulfates (Pedersen et al., 2012).

Another study investigating metabolism of mephedrone in rat and human urine samples further confirmed the predicted metabolic pathway: N-dealkylation to the primary amine, reduction of the β-keto group to the corresponding alcohol and oxidation of the totyl moiety (Meyer & Maurer, 2010). Further metabolite 4-carboxy-dihydro mephedrone was only found in human samples.

Uralets and colleagues (2014) examined the metabolic profiles of 16 synthetic cathinones excreted in human urine. According to their investigation, a large group of SC appears to be metabolized by carbonyl reduction into corresponding substituted ephedrines and further N-dealkylated into norephedrines. While investigation over 34000 random urine samples, they were able to obtain characteristic patterns of metabolites and parent drugs. They suggested that the group of designer cathinones, including mephedrone, buphedrone, 4-methylbuphedrone, pentedrone, 4-methyl-N-ethylcathinone, DMMC, N-ethylbuphedrone, flephedrone and ethcathinone, follows metabolic path of previously investigated drugs cathinone and methcathinone. They seem to be first metabolized into respective alcohols (substituted ephedrines and norephedrines), followed by N-dealkylation. In the study, that group of SC was mostly found in urine samples as metabolites resulting from those reactions

or as unchanged parent drug, although parent drugs were less abundant than metabolites or not present at all (Uralets et al., 2014). It has been suggested that for this group β -keto reduced metabolites appear to be the essential markers of the parent drug use (Uralets et al., 2014). However, it is worth noting that sometimes the same metabolites can be formed from different parent drug (e.g. buphedrone, ethylbuphedrone and α-PBP share metabolite 2-Amino-1-phenylbutan-1-ol).

Recently, a study investigating human metabolism of alpha-cathinone-derived drugs of abuse identified cytochrome P450 isoforms (CYP) CYP1A2, CYP2B6, CYP2C9, CYP2C19, CYP2D6, and CYP3A4 as responsible for performing initial metabolic steps of four selected alpha-pyrrolidine cathinone derivatives (Meyer et al., 2018).

It is important to note that although the drugs seem to be often excreted unchanged, parent drugs are detected in urine only for a short period after administration or not at all in some cases, so knowledge of the extent of metabolism and the metabolites of novel SCs is essential (Pedersen et al., 2012; Uralets et al., 2014; Valente et al., 2013). It is also worth remembering that synthetic cathinones seem to be metabolized differently depending on their chemical structures, because of different chemical properties, but similar metabolic pathways are present intragroup (Zaitsu, 2018).

According to Zaitsu (Zaitsu, 2018), the main steps of cathinone metabolism are described as follows:

Reduction of the β-Ketone Moiety

As synthetic cathinones are characterized by the presence of the β-ketone moiety, practically all of them undergo reduction to the hydroxyl group. That step also causes diastereomerization of the generated metabolite as the β-carbon becomes chiral (Figure 1.8). Metabolites generated in this step can further undergo by phase II metabolism reactions, such as glucuronidation and/or sulfation.

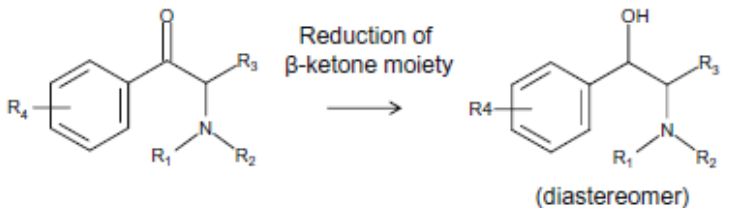

Figure 1.8 Reduction reaction of cathinones' β-Ketone Moiety (adapted from Zaitsu, 2018)

N-dealkylation

This step is mainly catalysed by CYP2D6. The N-alkyl cathinone derivatives commonly suffer N-dealkylation (Figure 1.9), just as their corresponding N-alkyl amphetamine derivatives (Valente et al., 2013).

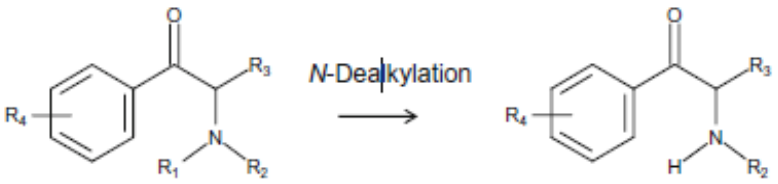

Figure 1.9 N-Dealkylation reaction of synthetic cathinones (adapted from Zaitsu, 2018)

Demethylenation Followed by O-Methylation Pathways for 3′,4′-Methylenedioxyphenyl Cathinone Derivatives

In this step first the 3′,4′-methylenedioxy moiety is demethylated to dihydroxy metabolite (Figure 1.10), generally mediated by CYP2D6 and CYP2C19 (Meyer, Peters, & Maurer, 2008), followed by O-methylation pathway of the dihydroxy metabolite mediated by the catechol O-methyl transferase (COMT) (Zaitsu, 2011).

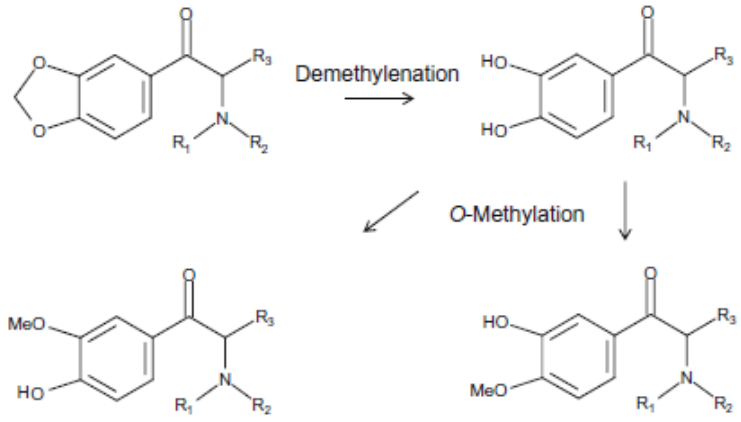

Figure 1.10 Demethylenation reaction of synthetic cathinones followed by O-Methylation Pathways (adapted from Zaitsu, 2018)

Hydroxylation Followed by Dehydrogenation, and Ring Opening for the N-Pyrrolidine Cathinone Derivatives.

N-pyrrolidine cathinone derivatives can suffer hydroxylation at the pyrrolidine moiety (primarily at 2″-postion). The resulting metabolite can be further dehydrogenated to a lactam, and open to generate an aliphatic aldehyde metabolite, which can be further oxidized to carboxylic acid metabolite (Figure 1.11).

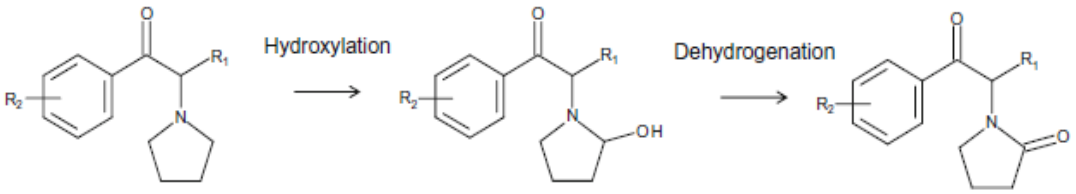

Figure 1.11 Hydroxylation reaction of synthetic cathinones followed by dehydrogenation, and ring opening for the N- pyrrolidine cathinone derivative (adapted from Zaitsu, 2018)

Metabolism of Benzene Ring Substituents

Ring substituents of cathinones can also undergo metabolic reactions. Depending on their structure, they can either undergo O-Demethylation or hydroxylation and further oxidation to a corresponding carboxylic acid (Figure 1.12).

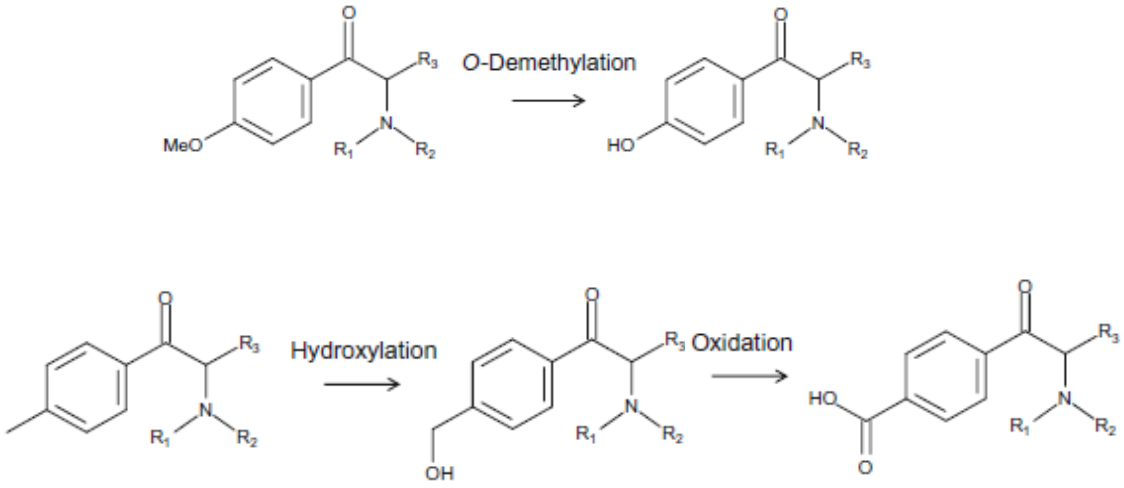

Figure 1.12 O-demethylation reaction of 4'-methoxy group of synthetic cathinones and hydroxylation of the 4′-methyl group followed by oxidation to the corresponding carboxylic acid (adapted from Zaitsu, 2018)

It is important to investigate the use of SCs and other NPS and find new analytical methods for their efficient and rapid detection and quantification required in clinical and forensic toxicology, which demands knowledge of the substances' chemistry and metabolism. Especially important is to developed the knowledge of possible metabolites, as the parent compounds are sometimes less stable and not excreted in urine, excreted to a lower extend than their metabolites or excreted only for a short period of time after the consumption (Uralets et al., 2014). Currently, the methods of choice for detection and quantification of SCs are gas chromatography-mass spectrometry (GC-MS) and liquid chromatography-tandem mass spectrometry (LC-MS-MS). (Majchrzak et al., 2018; Mikołajczyk et al., 2017; Pedersen et al., 2012; Uralets et al., 2014; Zuba et al., 2012). The rapid evolution of this drug class, however, poses identification and characterization difficulties for forensic drug chemistry laboratories as reference standards often do not exist (Cuimei et al., 2017).

2

2 Objectives

As NPS metabolites are markers of parent drugs consumption in environmental and biological samples, the knowledge about their metabolites and degradation products is of major relevance, among other reasons, to improve the detection and monitoring the pattern of consumption of this type of drugs. The main objective of this study is to contribute with knowledge to help building the map of metabolites and degradation products of selected NPS. For that propose the prediction of metabolites, attained by in silico metabolism studies and available data from the literature, will be followed by detection of main metabolites/degradation products present in reaction mixtures samples of studied SC buphedrone (Buph) and N-etylhexedrone (NEH), for confirmation. For that *in vitro* metabolism studies using either human or mice liver microsomes will be performed in order to find possible metabolites of those SC. The aim will be also to investigate the drugs' stability and for that purpose stability studies were performed in human plasma and in PBS over time.

3

3 Methods and Materials

3.1 *In silico* metabolism studies:

3.1.1 SwissADME tool

For primary identification and characterization of the two chosen compounds, buphedrone and N-ethylhexedrone, SwissADME tool was used. That open access, web-based program allows computation of physicochemical descriptors of small molecules and prediction of ADME parameters, pharmacokinetic properties and medicinal chemistry parameters, and is perfect for primary screening and characterization of the molecule (Daina et al., 2017). Bioavailability Radar displayed as first step of the characterization allows a rapid analysis of drug-likeness. It can be seen next to the molecule in the results of the analysis and combines physicochemical properties such as: lipophilicity (partition coefficient between n-octanol and water (log Po/w)), size, polarity, solubility, flexibility and saturation and presents them in a form of net.

3.1.2 SmartCyp program

SmartCyp is a free program that predicts site of the metabolism rather than the exact metabolites. It estimates which sites in a molecule are most liable to metabolism by Cytochrome P450 (Rydberg et al., 2010). It is applicable to metabolism of the isoforms CYP1A2, CYP2A6, CYP2B6, CYP2C8, CYP2C19, CYP2E1, isoform CYP3A4, CYP2C9 and CYP2D6. The last three represent the three most important enzymes involved in drug metabolism (Rydberg et al., 2010). The program uses the available data of the 2D structure of the molecule to calculate the distances between the atoms and energies required for oxidation

and applies an algorithm that consists of reactivity descriptor (*E*) and accessibility descriptor (*A*). The first one is an estimation of the energy required for the enzyme to react at this position and is calculated from SMARTS patterns and lookup table which contains information about the reaction energies in kJ/mol, corresponding to the known reaction energies of CYP enzymes with the molecular sub-structure. The accessibility is approximated as the relative spatial distance of an atom from the center of the molecule, or the longest bond path distance from a given atom divided by the longest bond path distance in the whole molecule, and it always gives a value between 0.5 and 1. The final score (*S*) is computed as $S=E - 8A - 0.04$*SASA. Solvent Accessible Surface Area (SASA) describes the local accessibility of an atom and is computed using the 2DSASA algorithm, which predicts this value from the molecular topology. The lower final score indicates a higher probability of being a Site of Metabolism (SOM) (Rydberg et al., 2010).

3.1.3 XenoSite program

XenoSite, like SmartCyp, is also an open access program that predicts the atomic sites at which xenobiotics will undergo metabolic modification by Cytochrome P450 enzymes (Sites of Metabolism, SOMs) (Zaretzki et al., 2013). It combines the data of reactivity of atomic sites generated by the SmartCyp software with the computation of multiple quantitative descriptions of a molecule. It uses a neuronal-network model that is based on those molecular descriptors and fingerprint-based search using a technique known as Influence Relevance Voting (Swamidass et al., 2009), thus achieving a high cross-validated accuracy. XenoSite models are trained on the largest set of publicly available P450 metabolism data consisting of over 680 compounds annotated with SOMs for the P450 CYP isozymes: 1A2, 2A6, 2B6, 2C8, 2C9, 2C19, 2D6, 2E1 and 3A4, as well as human liver microsomes (HLM), which combines the individual P450 models to represent the expected metabolism of compounds in vivo (Zaretzki et al., 2013).

3.1.4 BioTransformer program

BioTransformer is an open access tool created for *in silico* metabolism prediction and metabolite identification. It combines a machine learning approach with knowledge-based approach to predict small molecule metabolism . It can be used for CYP450, EC-Based, Phase II, Human Gut Microbial and Environmental Microbial transformations prediction. It is a knowledge-based system consisting of three major components: a biotransformation database (MetXBioDB) containing detailed annotations of experimentally confirmed metabolic reactions, a reaction knowledge base containing generic biotransformation rules, preference rules, and other constraints for metabolism prediction; a reasoning engine that implements

both generic and transformer-specific algorithms for metabolite prediction and selection (Feunang, Fiamoncini, Gil, Fuente, & Greiner, 2019).

3.2 Structure drawings

All structures of compounds and metabolites, other than extracted from the above tools or literature, were drawn using ChemSketch v2018 ADC/Labs and MarvinSketch 19.25 ChemAxon Ltd. Programs.

3.3 Chemicals and materials

Studied synthetic cathinones and selected metabolites shown in Figure 3.1 were kindly synthetized by the Medicinal Chemistry Group of Faculty of Pharmacy of Universidade de Lisboa. Both synthetic cathinones, N-ethylhexedrone (**NEH**) [2-(ethylamino)-1-phenyl-1-hexanone hydrochloride] and buphedrone (**Buph**) [2-(methylamino)-1-phenylbutan-1-one hydrochloride] were synthetized by initial bromination of starting hexanophenone and butyrophenone, respectively, and subsequent reaction with the appropriate amine. Corresponding metabolites 2-(ethylamino)-1-phenylhexan-1-ol hydrochloride (**H1**), 2-amino-1-phenylhexan-1-ol hydrochloride (**H2**) 4-(2-(ethylamino)-1-hydroxyhexyl)phenol hydrochloride (**H3**), 2-(methylamino)-1-phenylbutan-1-ol hydrochloride (**B1**), 2-amino-1-phenylbutan-1-one hydrochloride (**B2**), 2-amino-1-phenylbutan-1-ol hydrochloride (**B3**) were chemically obtained following the synthetic procedures used in the synthesis of the parent drug for introduction of the amine group. Sodium borohydride was used for carbonyl reduction. Phenolic metabolites 4-2-amino-1-hydroxyhexyl)phenol hydrochloride (**H4**), 4-(2-amino-1-hydroxyhexyl)phenol hydrochloride (**H5**) and 4-(1-hydroxy-2-(methylamino)butyl)phenol hydrochloride (**B4**) were obtained by acetylation of the starting 4'-hydroxyphenones to prevent bromination of the activated phenyl rings. This allowed basic hydrolysis during reaction with primary amines and/or sodium borohydride.

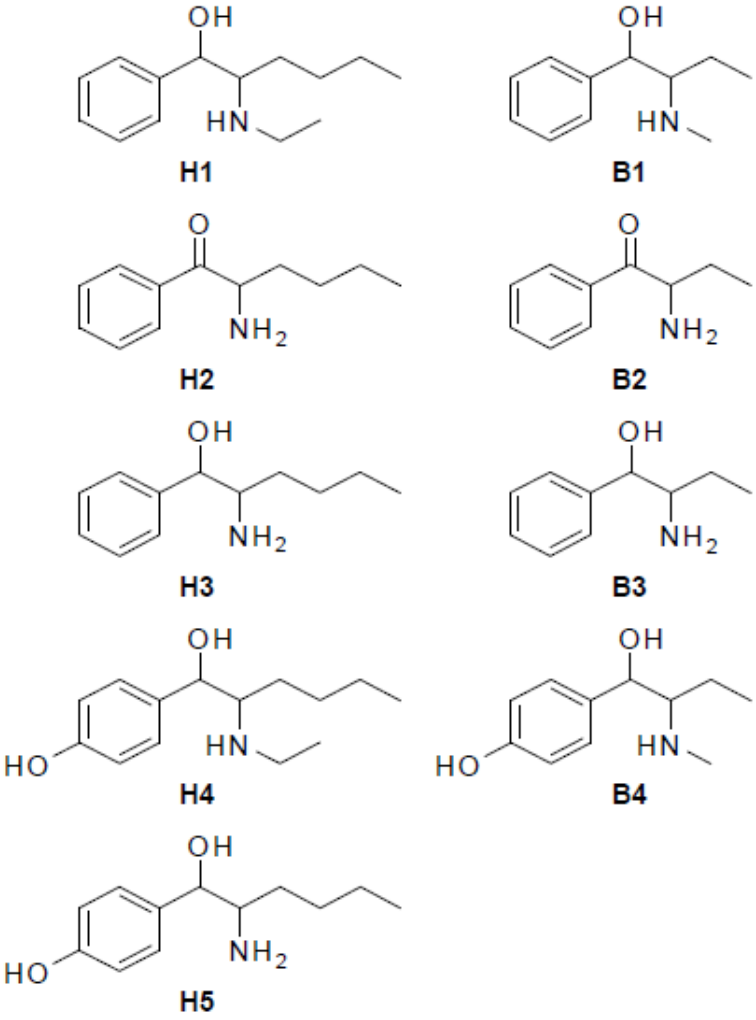

Figure 3.1 Chemical structures of selected N-ethylhexedrone and buphedtone metabolites: H1 – beta-keto-reduced, H2 – N-dealkylated, H3- beta-keto reduced and N-dealkylated, H4 – beta-keto reduced and hydroxylated in the para position of the aliphatic ring, H5- beta-keto reduced, N-dealkylated and hydroxylated in the para position of the aliphatic ring, B1 – beta-keto-reduced, B2 – N-dealkylated, B3- beta-keto reduced and N-dealkylated, B4 – beta-keto reduced and hydroxylated in the para position of the aliphatic ring

For *in vitro* metabolism studies the following chemicals were used: HPLC grade acetonitrile, methanol and formic acid 99-100% p.a. were obtained from Chem-Lab NV (Zedelgem, Belgium). Milli-Q water (18.2 MΩ cm^{-1} resistivity) was obtained from a Millipore-Direct Q3 UV system (Millipore ®, USA). Phosphate buffer saline (PBS) solution was prepared by dissolving one Phosphate Buffered Saline Tablet purchased from Fisher BioReagents® (Fair Lawn, New Jersey) in 200 mL of deionized water, yielding 0.01M Phosphate Buffer (containing 0.0027M Potassium Chloride, 0.137M Sodium Chloride, pH 7.4 at 25°C, stored at

4°C). Acetonitrile used as stop solution was purchased from CARLO ERBA Reagents S.A.S (Dasitgroup, France). Dimethyl Sulfoxide (DMSO) Reagent Grade ≥99.5% was purchased from Honeywell (Japan).

For human liver microsomes (HLMs) assay the microsomes used were BD Gentest™, catalogue No. 452156, obtained from 50-Donor Pool with Protein Content 20mg/mL in 250mM sucrose were stored at -80°C until used. Supplier analytical control (Western Blot) confirmed presence of CYP1A2, CYP2A6, CYP2B6, CYP2C8, CYP2C9, CYP2C19, CYP2D6, CYP2E1, CYP3A4, CYP3A5, CYP4A11, FMO, UGT1A1, UGT1A4, UGT1A6, UGT1A9, UGT2B7.

For Mice Liver Microsomes (MLMs) assay the microsomes used were Corning® Gentest™ Pooled Male Mouse Liver Microsomes, (B6C3F1), Catalogue No. 452220, obtained from around 77 mice, ~11 weeks of age, pooled, with Protein Content 20mg/mL in 250mM sucrose were stored at -80°C until used.

Used microsomes reaction cofactors consisted in two solutions, A and B, namely: Corning® Gentest™ NADPH Regenerating System (5 mL) and Corning® Gentest™ NADPH Regenerating System (1 mL), respectively.

For *in vitro* plasma studies used plasma was obtained from a pool of 7 healthy individuals' blood donors and stored in 3 mL aliquots at -80°C until needed.

For analytical studies (detection and quantification) the following chemicals were used: HPLC grade acetonitrile and methanol, and formic acid 99-100% *p.a.* obtained from Chem-Lab NV (Zedelgem, Belgium). Milli-Q water (18.2 MΩ cm^{-1} resistivity) was obtained from Millipore-Direct Q3 UV system (Millipore®, USA). High purity nitrogen was used as drying and nebulizing gas, and ultrahigh purity argon was used as collision gas.

Equipment

Heidolph™ Vortex Top Mix Stirrer, Water bath Julabo® F12-MP Refrigerated/Heating Circulator, Eppendorf® Centrifuge 5430, non-refrigerated, with Rotor FA-45-30-11 incl. rotor lid, rotary knobs, 230 V/50 – 60 Hz. Mettler Toledo AG135 5-Place Analytical Balance, VWR Signature™ Ergonomic High Performance Single-Channel Variable Volume Pipettors 0.5–10 μL, 10–100 μL and 100–1000 μL.

High Performance Liquid Chromatography (HPLC) coupled to mass spectrometry analysis was performed on a Waters Alliance HPLC system (Waters® 2695 separation module, Ireland) consisting on a system of quaternary pumps, degasser, autosampler and a column furnace. The mass spectrometer used was a MicroMass Quattromicro® API (Waters®,

Ireland). The column used was Waters XBridge BEH C18 XP (50 x 2.1 mm, 2.5 μm). MassLynx® 4.1 software (Waters, Ireland) was used for data acquisition and processing.

3.4 *In Vitro* Metabolism Studies

3.4.1 Mice liver microsomal assay using synthetic cathinones buphedrone and N-ethylhexedrone as substrates

In total, nine mice microsomal assays (some of them in duplicates) were performed during the course of the whole investigation. Two of them were carried out with the final concentration of buphedrone or N-ethylhexedrone at 10 μM, two with concentration of 5 μM and the rest was performed at final concentrations 15 μM. The standard solutions (mother solutions) of each studied SC were prepared by weighting around 1 mg of either Buphedrone or N-ethylhexedrone and dissolve it in 1 mL of isotonic 0.01 M PBS, pH 7.4. The standard solutions of substance used as positive control, either phenacetin or propanolol, were also prepared by weighting around 1 mg and dissolving it in DMSO/PBS 2:8 to the final volume of 1 mL. Stock solutions were later diluted in order to obtain a solution with a concentration of 3 mM (if the final solution was to be 15 μM of substrate in the microsomal reaction). From that dilution, 4 μL substrate solution was taken and added to the reaction mixture in order to obtain the desirable final concentration.

The final volume of the reaction mixture was always 802 μL and the reaction mixture consisted of 20 μM of Microsomes, 40 μL of Cofactor A (NADPH regenerating system A), 8 μL of Cofactor B (NADPH regenerating system B), 570 μL of water, 160 μL of isotonic 0.01 M PBS, pH 7.4 and the 4μL of the substrate solution.

The reaction mixture was first incubated at 37 °C for 5 min (usually without cofactors and in two cases without microsomes). Then the reactions were initiated by addition of NADPH regenerating system A and NADPH regenerating system B (or microsomes) to the mixture after incubation and the first time-point t0 was collected. At each time-point 120μL of the reaction mixture were taken and quenched with 120 μL of ice-cold acetonitrile to stop the reaction (Figure 3.2). The collection time-points were always: 0; 15; 30; 60; 90; 120 (in minutes). After the collection the samples were centrifuged at 10000 rpm for 5 min in order to separate the microsomes from the solution, supernatant collected and stored at -20°C until analyzed. The usual composition of the microsome assay mixture is presented in Table 3.1.

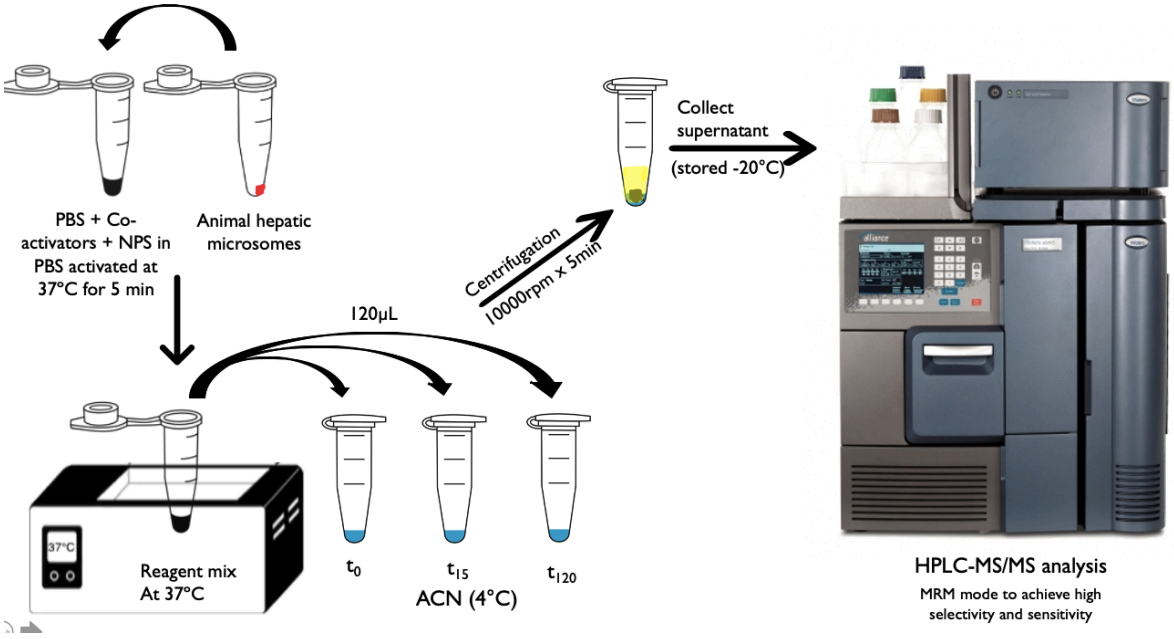

Figure 3.2 Schematic representation of microsome assay proceedings

Table 3.1 Standard composition of the microsomal reaction mixture and of the stability assay

	Buph (in duplicate)	NEH (in duplicate)	+control (phenacetin)	-control (NEH/Buph)	Stability control NEH	Stability control Buph
Cofactor A	40 µL	40 µL	40 µL	-	-	-
Cofactor B	8 µL	8 µL	8 µL	-	-	-
Microsomes	20 µL	20 µL	20 µL	20 µL	-	-
H20	570 µL	570 µL	570 µL	618 µL	620 µL	620 µL
PBS	160 µL	160 µL	160 µL	160 µL	178 µL	178 µL
Substrate	4 µL	4 µL	4 µL	4 µL	4 µL	4 µL
Final volume	802 µL	802 µL	802 µL	802 µL	802 µL	802 µL

3.4.2 Mice liver microsomal assay using N-ethylhexedrone metabolites as substrates

The in vitro metabolism studies using metabolites H1 and H2 as substrates of mice liver microsomes was performed in duplicate following the procedure previously described in section 3.4.1. The standard procedure was to weight around 1mg of H1 or H2 and dissolve

it in 1 mL of isotonic 0.01 M PBS, pH 7.4. The standard solution of phenacetine was used as positive control and it was also prepared by weighting around 1mg and dissolving it in DMSO/PBS 2:8 to the final volume of 1 mL.

The reaction mixture was first incubated at 37 ºC for 5 min. Then the reactions were initiated by addition of NADPH regenerating system A and NADPH regenerating system B to the mixture and the first time-point t0 was collected. The usual assay had the same composition as presented in Table 3.1 (but instead of Buph and NEH metabolites H1 – beta-keto reduced, and H2 – N-dealkylated, were used).

3.4.3 Human liver microsomal assay using synthetic cathinones buphedrone and N-ethylhexedrone as substrates

During the investigation two human microsomal assays (one in duplicate) were performed. All of them were carried out with the final concentration of buphedrone or N-ethylhexedrone at 15μM. The in vitro metabolism studies using HLMs was performed following the procedure previously described in section 3.4.1 for MLMs and the usual microsome reaction mixture had the same composition as presented in Table 3.1. The standard procedure was to weight around 1 mg of buphedrone or N-ethylhexedrone and dissolve it in 1 mL of isotonic 0.01 M PBS, pH 7.4. The standard solutions of substance used as positive control, either phenacetin or propanolol, were also prepared by weighting around 1mg and dissolving it in DMSO/PBS 2:8 to the final volume of 1 mL. Mother solutions were later diluted in order to obtain a working solution with a concentration of 3 mM. From that dilution, 0.004mL substrate solution was taken and added to the reaction mixture in order to obtain the desirable final concentration.

The reaction mixture was first incubated at 37 ºC for 5 min. Then in one case the reaction was initiated by addition of NADPH regenerating system A and NADPH regenerating system B, and in the other case addition of microsomes to the mixture and the first time-point t0 was collected.

3.5 *In vitro* Blood Plasma studies

To evaluate the stability of buphedrone and N-ethylhexedrone in human blood plasma, a study was carried out, twice for buphedrone and once for N-ethylhexedrone. The standard solution of buphedrone was prepared by dissolving 1.07 mg of BUPH in 0,05 mL of

PBS. From that solution 0.01 mL was later taken and added to plasma in order to obtain a concentration of 10^{-5} M. The standard solution of N-ethylhexedrone was prepared by dissolving 1.27 mg of NEH in 0,0 5mL of PBS. From that working solution 0,01 mL was used in the assay in order to obtain the final concentration of 10^{-5} M. The final volume in the samples was 3mL. Human blood plasma aliquots (2,5mL), stored at -80 ºC, were slowly defrosted and incubated for 5 min at 37 °C. Isotonic phosphate buffer, pH 7.4, (0.5 mL) was added to each used blood plasma aliquot in order to dilute the plasma to 80%.

In the first buphedrone blood plasma study, buphedrone (10^{-5} M final concentration) was incubated at 37 ºC in 3 mL 80% human plasma diluted with 0.01 M pH 7.4 isotonic phosphate buffer, and, at the time points: 0; 0.25; 0.75; 3.25; 5.25; 23.33; 29.45; 30 (in hours) 200μL aliquots of the incubation were quenched with 400 μl of ice cold acetonitrile. The sampling solutions were centrifuged for 5 min at 10000 rpm and the supernatants collected, stored frozen at -20 ºC until analyzed.

In the second blood plasma assay, buphedrone (10^{-4} M final concentration) and N-ethylhexedrone (10^{-4} M final concentration) were incubated at 37 °C for 48 h in 3 mL 80% human plasma according to the above-described procedure. At timepoints: 0.5; 1; 2; 3; 5; 7; 24; 29; 33; 48; (in hours), sampling volumes of 75 μL, instead of 200 μl, were collected and quenched with 150µL of ice-cold acetonitrile, maintaining the same dilution proportion. The collected samples were then centrifuged at 10000 rpm for 5 min, supernatant collected and stored at -20 °C.

3.6 *In vitro* stability studies

3.6.1 Stability of synthetic cathinones in phosphate buffer (short-term)

Stability of the compounds was first evaluated during 2 h in isotonic 0.01 M PBS, pH 7.4, at 37 ºC, diluted to 22,5% (0,0022 M), as indicated in the Table 3.1. Because the pH of the distilled water is around 7, and it constituted most of the testing solution, the final pH was most probably lower than 7.4. The same proceedings as described in section 3.5.1 were applied. The reaction mixture consisting of 620 μL of water, 178 μL of PBS and 4 μL of substrate, was first incubated at 37 ºC for 5 min. At each time-point 120 μL of the reaction mixture were taken and quenched with 120 μL of ice-cold acetonitrile to stop the reaction. The collection time-points were always: 0; 15; 30; 60; 90; 120 (in minutes). After the collection the samples stored at -20°C until analyzed.

3.6.2 Stability of synthetic cathinones in phosphate buffer (long-term)

Three studies were performed over the course of 48h in order to evaluate the stability of buphedrone and N-ethylhexedrone in isotonic 0.01 M PBS, pH 7.4, at 37 ºC. At first the standard solutions of 1 mg of buphedrone in 0.05 mL of PBS and 0.71 mg of N-ethylhexedrone in 0.05 mL of PBS were prepared. From those solution 0,004 mL of buphedrone solution was added to 1 mL of PBS, in duplicate. The same was performed with 0.006 mL of N-ethylhexedrone standard solution, in order to obtain a concentration of approximately 332 μM in each working solution and approximately 100 μM in each testing solution. The samples were kept in the water bath at 37 °C during 48 h. At each time-point 75 μL of the reaction mixture was collected and quenched with 150 μl of ice-cold acetonitrile. The time-points were: 0; 1; 2; 3; 5; 7; 20; 24; 30; 48 (in hours).

3.7 HPLC-MS/MS analysis

Before mass spectrometry analysis of the samples, separation and analysis of compounds was performed by liquid chromatography. The Waters XBridge BEH C18 XP (50 x 2.1 mm, 2.5 μm) column was used and the injection volume was 10 μL for all analyzed samples. The mobile phase consisted of a mixture of formic acid (0.5% v/v) in Milli-Q water (eluent A) and acetonitrile (eluent B). Method development consisted on varying the percentage of organic solvent so that optimal peak shape and adequate resolution of compounds were achieved.

For the analysis of NEH, its metabolites and phenacetine, in samples obtained during the stability and the microsome studies, the mobile phase was held isocratic at 18% B for 10 min, followed by 10min at 95% B, returning to 18%B in 1 min, and held isocratically at 18% for stabilization. Total run time was 25min at a flow rate of 0.3 mL min^{-1}. The gradient program used for the analysis of Buph and its metabolites, in samples obtained during the stability and the microsome studies, started with 1% B, increasing to 15% B in 1.5 min, then to 45% B in 5.5 min, and to 95% B in 0.5 min, held isocratic at 95% B for 9.5min, decreasing to 1% B in 1 min, and finally held isocratic at 1% B for 7 min. Total run time was 18 min at a flow rate of 0.3 mL min-1. For propranolol, the mobile phase was held isocratic at 10% B for 5 min, then increased to 90% for 3 min, decreased back to 90% after 3min and held isocratic at 18% B for stabilization. Total run time was 18 min at a flow rate of 0.3 mL min^{-1}.

In samples obtained during the in vitro plasma studies, for analysis of NEH and its metabolites, the mobile phase was held isocratic at 1% B for 3 min, then increased to 40% for

3 min, followed by 7 min at 95% and after held at 1% B for stabilization. Total run time was 10 min at a flow rate of 0.3 mL min^{-1}. The gradient program used for the analysis of Buph and its metabolites in plasma started with 1% B, increasing to 70% B in 3 min, then to 95% B after another 3 min, held isocratic at 95% B for 7 min, and finally held isocratic at 1% B for 3 min. Total run time was 15 min at a flow rate of 0.3 mL min^{-1}.

The mass spectrometry was performed using an electrospray ion source in positive ionization mode (ESI+) operating at 120ºC. High purity nitrogen was used as drying and nebulizing gas, and ultrahigh purity argon was used as collision gas. Individual standard solutions of each compound were infused into the mass spectrometer and different cone voltages (10-40V) and collision energies (7-25 eV) were tested, aiming to optimize the fragmentation of each compound. The two product ions with the highest signal (MRM1 and MRM2) were selected to choose the transitions to be monitored in MRM mode in order to achieve high selectivity and sensitivity (Table 3.2).

Limits of detection for each compound are presented in the Table 3.3.

Table 3.2 Optimized MS/MS parameters for NEH and BUPH and metabolites. [M+H]+: precursor ion; MRM1: quantification transition; C.E.: collision energy; MRM2: confirmation transition.

Compound	$[M+H]^+$	Cone Voltage/ V	MRM1 (C.E./ eV)	MRM2 (C.E./ eV)
NEH	220	12	220 > 202 (15)	220 > 175 (15)
H1	222	12	222 > 204 (15)	222 > 147 (15)
H2	192	12	192 > 118 (12)	192 > 91 (12)
H3	194	12	194 > 176 (10)	194 > 117 (10)
H4	238	12	238 > 220 (11)	238 > 163 (15)
H5	210	12	210> 192 (7)	210 > 175 (12)
BUPH	178	12	178 > 160 (15)	178 > 132 (15)
B1	180	12	180 > 162 (12)	180 > 133 (15)
B2	164	12	164 > 118 (12)	164 > 91 (12)
B3	166	12	166 > 148 (10)	166 > 131 (10)
B4	196	12	196 > 178 (9)	196 > 147 (12)

Table 3.3 Limits of detection for selected compounds. For H2 and B1 values were not obtained due to an interfering peak at concentrations below 0.05μg mL^{-1}

Compound	NEH	H1	H2	H3	H4	BUPH	B1	B2	B3
LOD (μg mL^{-1})	0.002	0.001	-	0.001	0.01	0.002	-	0.002	0.002
LOD (μM)	0.009	0.0045	-	0.005	0.04	0.011	-	0.012	0.012

4

4 Results and discussion

4.1 *In silico* and literature metabolism prediction of selected SCs:

There are few ways of predicting drug metabolism. The easiest non laboratory technique is to use *in silico* prediction tools or making metabolite prediction taking advantage of the literature already available on the topic, by comparing the metabolism of similar, previously investigated drugs. In this research four types of software have been used in order to predict possible metabolites of the selected synthetic cathinones: buphedrone and N-ethylhexedrone.

4.1.1 Metabolite prediction based on literature review

Based on literature review (Meyer & Maurer, 2010; Mikołajczyk et al., 2017; Uralets et al., 2014; Zaitsu, 2018) the following phase I metabolism pathways (Figure 4.1) (Figure 4.2) were predicted. It is common for N-alkylated synthetic cathinones, such as buphedrone, to first suffer β-keto reduction, as this can also be a spontaneous reaction resulting from degradation of the drug. The resulting metabolite can subsequently undergo N-dealkylation or hydroxylation of the aromatic ring. The N-dealkylated alcohol was the major phase I metabolite found in the urine study (Uralets et al., 2014). The compound can also first undergo N-dealkylation and both β-keto reduction and N-dealkylation are often mention as the main metabolic reactions for those type of synthetic cathinones (Uralets et al., 2014; Zaitsu, 2018).

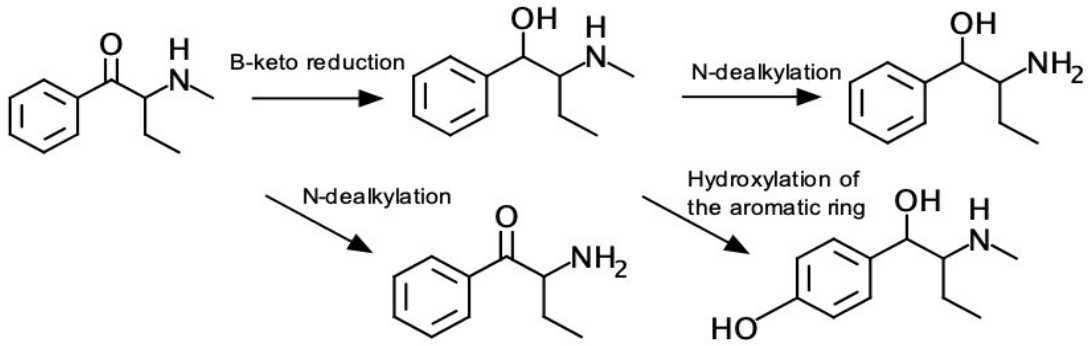

Figure 4.1 Buphedrone phase I metabolism prediction based on literature

N-ethylhexedrone is expected to follow the same metabolic pathways, as it belongs to the same group of N-alkylated synthetic cathinones as buphedrone, and accordingly, we predicted the following metabolic pathway based on the previously mentioned literature (Figure 4.2).

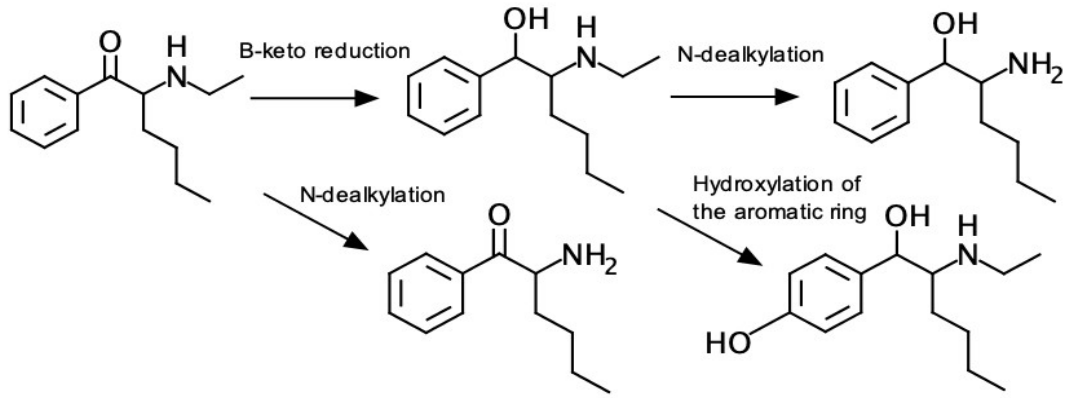

Figure 4.2 N-ethylhexedrone phase I metabolism prediction based on the literature.

4.1.2 Properties prediction of buphedrone and N-ethylhexedrone using SwissADME

When using the program SwissADME the following chemical properties were obtained for buphedrone and N-ethylhexedrone as shown in the Figure 4.3 and Figure 4.4. From the analysis it was predicted that buphedrone is a small molecule, not very polar, but soluble in water (values of Log *S* using three different models: -2.36; -2.38 and -3.62) and relatively lipophilic (average log $P_{o/w}$ = 2.8). It seems to be well absorbed in the gastro-

intestinal tract and permeable to Blood-Brain-Barrier. Buphedrone is also indicated as CYP1A2 inhibitor. It is also worth noting that it has been scored as relatively easy to synthetize (Synthetic accessibility - 1.60, on a scale 1- very easy to 10 – very difficult).

Table 4.1 Chemical properties of buphedrone and N-ethylhexedrone predicted by SwissADME

	Molecular weight	***Log $P_{o/w}$***	***Solubility (ESOL)***	***Inhibition***	***Bioavaila-bility score***	***Synthetic accessibility***
Buph	177.24 g/mol	2.08	-2.36	CYP1A2	0.55	1.60
NEH	219.32 g/mol	3.10	-3.16	CYP1A2 CYP2D6	0.55	2.11

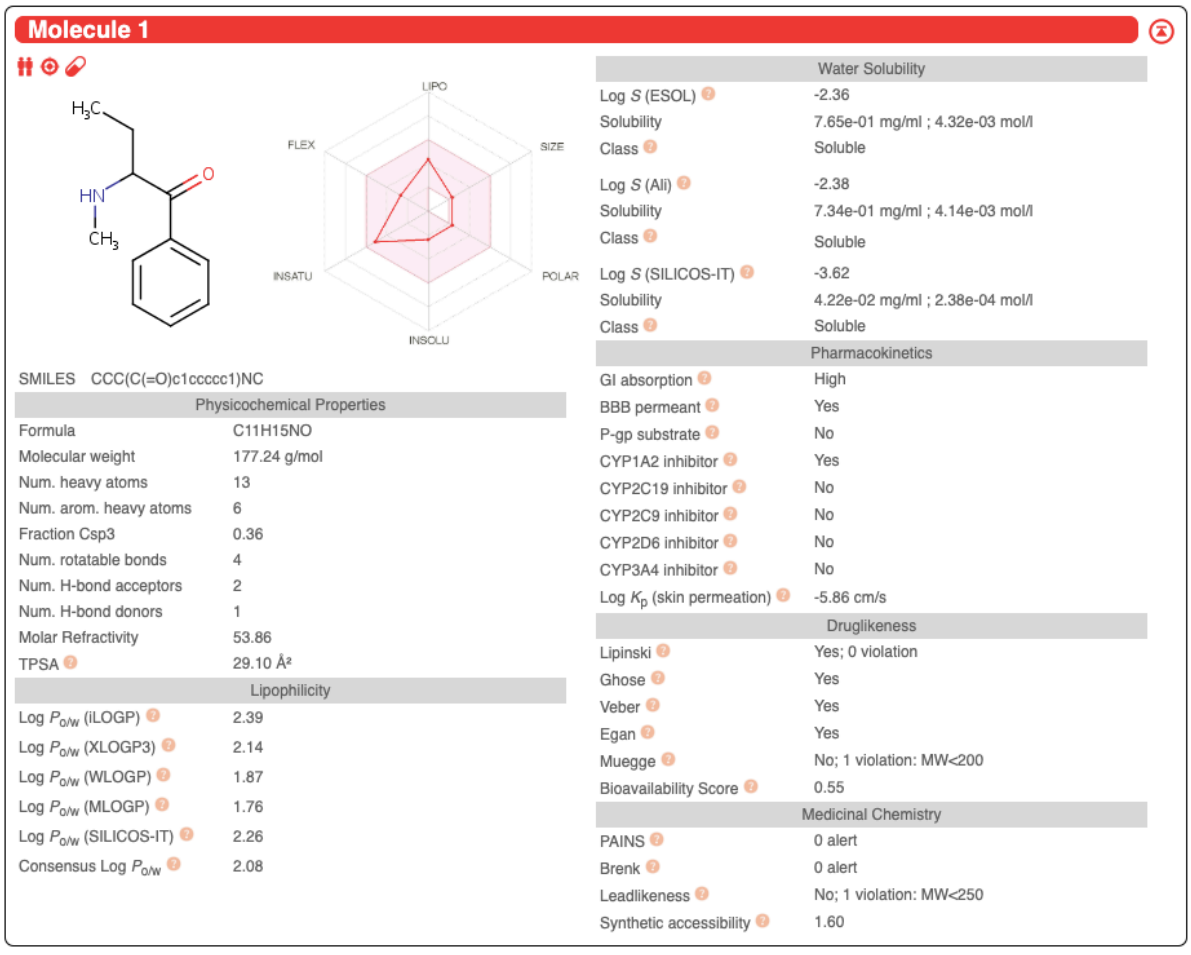

Figure 4.3 SwissADME properties prediction for buphedrone

N-ethylhexedrone has been predicted to be more liposoluble than buphedrone (average log $P_{o/w}$ = 3.1), with lower water solubility (values of Log *S* using three different models: -3.16; -3.69 and -4.85). It also is highly absorbed in the gastro-intestinal tract and permeates Blood-Brain-Barrier. It was indicated as a CYP1A2 and CYP2D6 inhibitor.

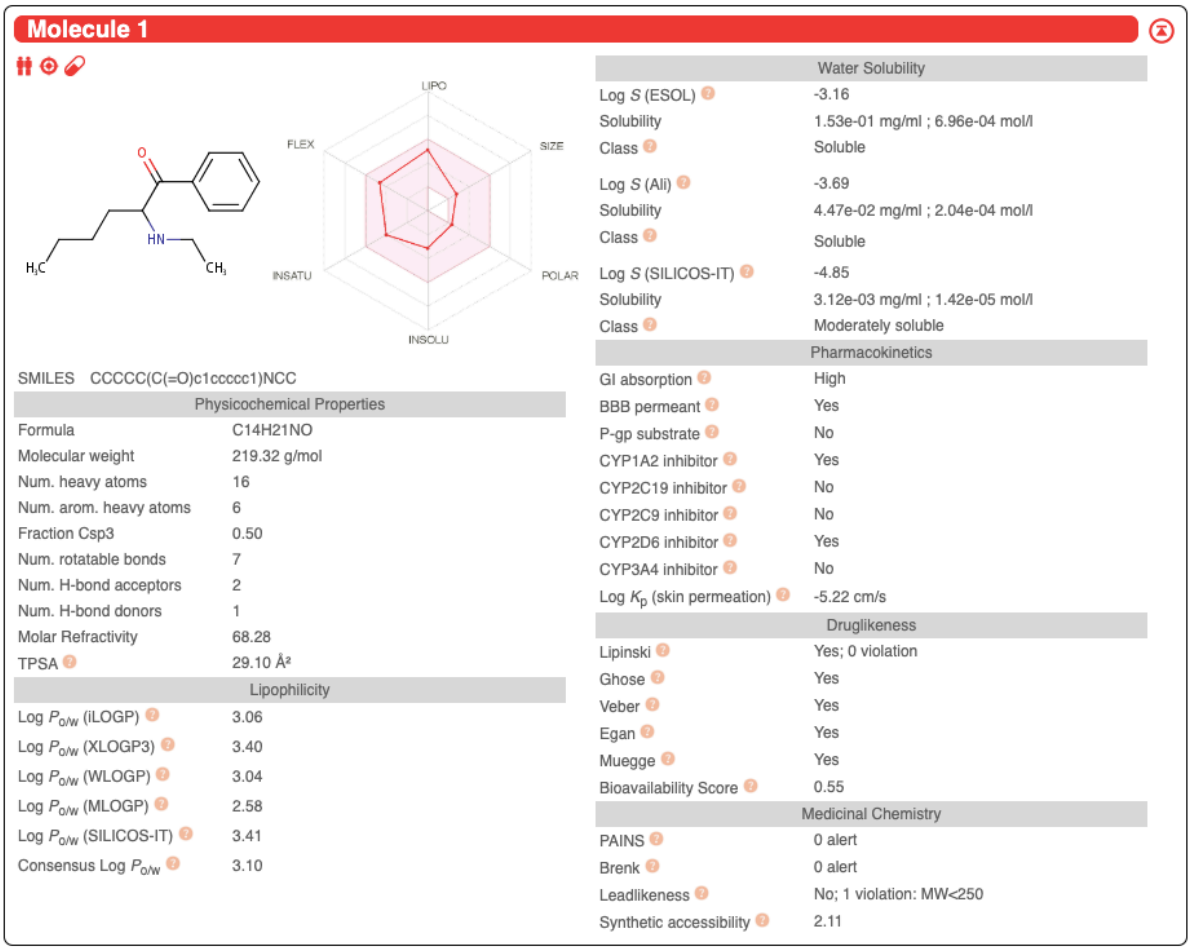

Figure 4.4 SwissADME properties prediction for N-ethylhexedrone

4.1.3 Prediction of buphedrone and N-ethylhexedrone site of metabolism using SmartCyp:

In the SmartCyp program, the top 3 atoms where the reaction is most probable to occure are highlighted at the top of the table. Atoms are ranked by score, with the lowest score resulting in the lowest rank, and thus the highest probability of being a site of metabolism.

For buphedrone, we can see that in all cases, the carbon atom C10, attached to the nitrogen, is most likely to undergo metabolic transformation. The score is particularly high

for the CYP3A4 family, as they are responsible for a range of N-dealkylation reactions (Figure 4.5). For 2D6 we can see that the scores are lower, but the possible indicated reactions are N-dealkylation and oxidation of the phenyl ring in the *para* position (Figure 4.6). The highest score for the isoform 2C9 is the N-dealkylation reaction.

Molecule

3A4 | 2D6 | 2C9

1

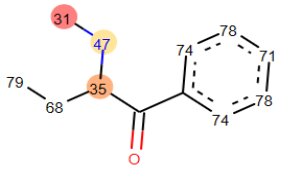

3A4 Ranking	Atom	3A4 Score	Energy	2DSASA	Span2end	Relative Span	Similarity
1	C.10	30.8	41.1	58.4	0	1.0	0.7
2	C.8	35	41.1	8.5	2	0.7	0.4
3	N.9	46.7	54.1	14.7	1	0.9	0.3
4	C.11	68	75.9	24.8	1	0.9	0.4
5	C.5	71.4	80.8	36.2	0	1.0	1.0
6	C.1	74	80.8	27.8	2	0.7	0.7
6	C.3	74	80.8	27.8	2	0.7	0.7
7	C.4	78.1	86.3	33.5	1	0.9	1.0
7	C.6	78.1	86.3	33.5	1	0.9	1.0
8	C.12	79.2	89.6	59.8	0	1.0	0.7
9	O.13	N/R	999.0	0.0	2	0.7	0.7
10	C.2	N/R	999.0	4.2	3	0.6	0.0
11	C.7	N/R	999.0	3.6	3	0.6	0.0

Figure 4.5 SmartCyp prediction for buphedrone metabolic transformation by CYP3A4 Isoform (Note that the atoms are numbered by their score)

Molecule

3A4 | 2D6 | 2C9

1

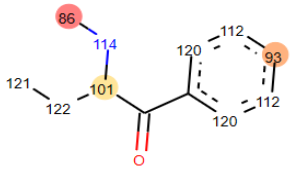

2D6 Ranking	Atom	2D6 Score	Energy	2DSASA	Span2end	N+dist	Similarity
1	C.10	85.7	41.1	58.4	0	1	0.7
2	C.5	92.8	80.8	36.2	0	6	1.0
3	C.8	101.1	41.1	8.5	2	1	0.4
4	C.4	111.8	86.3	33.5	1	5	1.0
4	C.6	111.8	86.3	33.5	1	5	1.0
5	N.9	113.8	54.1	14.7	1	0	0.3
6	C.1	119.9	80.8	27.8	2	4	0.7
6	C.3	119.9	80.8	27.8	2	4	0.7
7	C.12	120.7	89.6	59.8	0	3	0.7
8	C.11	121.8	75.9	24.8	1	2	0.4
9	O.13	N/R	999.0	0.0	2	3	0.7
10	C.2	N/R	999.0	4.2	3	3	0.0
11	C.7	N/R	999.0	3.6	3	2	0.0

Figure 4.6 SmartCyp prediction for buphedrone metabolic transformation by CYP2D6 isoform (Note that the atoms are numbered by their score)

Molecule

3A4 2D6 2C9

1

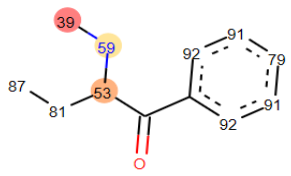

2C9 Ranking	Atom	2C9 Score	Energy	2DSASA	Span2end	COO-Dist	Similarity
1	C.10	38.8	41.1	58.4	0	0	0.7
2	C.8	52.6	41.1	8.5	2	0	0.4
3	N.9	59.4	54.1	14.7	1	0	0.3
4	C.5	79.4	80.8	36.2	0	0	1.0
5	C.11	80.8	75.9	24.8	1	0	0.4
6	C.12	87.2	89.6	59.8	0	0	0.7
7	C.4	90.9	86.3	33.5	1	0	1.0
7	C.6	90.9	86.3	33.5	1	0	1.0
8	C.1	91.5	80.8	27.8	2	0	0.7
8	C.3	91.5	80.8	27.8	2	0	0.7
9	O.13	N/R	999.0	0.0	2	0	0.7
10	C.2	N/R	999.0	4.2	3	0	0.0
11	C.7	N/R	999.0	3.6	3	0	0.0

Figure 4.7 SmartCyp prediction for buphedrone metabolic transformation CYP2C9 (Note that the atoms are numbered by their score)

Similarly, as in the case of buphedrone, also for N-ethylhexedrone the atom with the highest score for the CYP3A4 and CYP2C9 family is the carbon atom C7 attached to the nitrogen (Figure 4.8 and Figure 4.10), which suggest N-dealkylation reactions. The enzyme 2D6 is also indicated as possible of catalyzing oxidation reaction at the phenyl ring in the *para* position with the score almost the same as for buphedrone (~93) (Figure 4.9).

Smiles

3A4 2D6 2C9

1

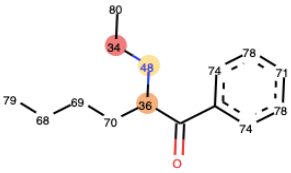

3A4 Ranking	Atom	3A4 Score	Energy	2DSASA	Span2end	Relative Span	Similarity
1	C.7	33.6	41.1	31.2	2	0.8	0.7
2	C.5	36.4	41.1	7.5	4	0.6	0.4
3	N.6	48.4	54.1	9.8	3	0.7	0.3
4	C.2	67.5	75.9	32.7	1	0.9	0.4
5	C.3	68.6	75.9	25.9	2	0.8	0.4
6	C.4	69.8	75.9	18.0	3	0.7	0.4
7	C.14	71.4	80.8	36.2	0	1.0	1.0
8	C.12	73.5	80.8	27.8	2	0.8	0.7
9	C.13	77.8	86.3	33.5	1	0.9	1.0
10	C.1	78.9	89.6	66.4	0	1.0	0.7
11	C.8	79.8	89.6	66.4	1	0.9	0.7

Figure 4.8 SmartCyp prediction for NEH metabolic transformation by CYP3A4 isoform (Note that the atoms are numbered by their score)

Smiles

3A4 | 2D6 | 2C9

1

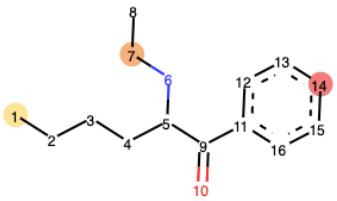

2D6 Ranking	Atom	2D6 Score	Energy	2DSASA	Span2end	N+dist	Similarity
1	C.14	92.8	80.8	36.2	0	6	1.0
2	C.7	100.2	41.1	31.2	2	1	0.7
3	C.1	107.0	89.6	66.4	0	5	0.7
4	C.2	108.1	75.9	32.7	1	4	0.4
5	C.13	111.8	86.3	33.5	1	5	1.0
6	C.5	114.5	41.1	7.5	4	1	0.4
7	C.12	119.9	80.8	27.8	2	4	0.7
8	C.3	121.8	75.9	25.9	2	3	0.4
9	N.6	127.4	54.1	9.8	3	0	0.3
10	C.8	133.8	89.6	66.4	1	2	0.7
11	C.4	135.5	75.9	18.0	3	2	0.4

Figure 4.9 SmartCyp prediction for NEH metabolic transformation by CYP2D6 isoform

Smiles

3A4 | 2D6 | 2C9

1

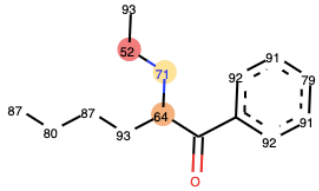

2C9 Ranking	Atom	2C9 Score	Energy	2DSASA	Span2end	COO-Dist	Similarity
1	C.7	51.7	41.1	31.2	2	0	0.7
2	C.5	64.4	41.1	7.5	4	0	0.4
3	N.6	71.4	54.1	9.8	3	0	0.3
4	C.14	79.4	80.8	36.2	0	0	1.0
5	C.2	80.5	75.9	32.7	1	0	0.4
6	C.3	86.7	75.9	25.9	2	0	0.4
7	C.1	86.9	89.6	66.4	0	0	0.7
8	C.13	90.9	86.3	33.5	1	0	1.0
9	C.12	91.5	80.8	27.8	2	0	0.7
10	C.8	92.8	89.6	66.4	1	0	0.7
11	C.4	92.9	75.9	18.0	3	0	0.4

Figure 4.10 SmartCyp prediction for NEH metabolic transformation by CYP2C9 isoform (Note that the atoms are numbered by their score)

4.1.4 Prediction of buphedrone and N-ethylhexedrone site of metabolism and possible reactions using XenoSite:

When using the Program XenoSite we were able to see possible sites of metabolism and enzymes that would catalyze the reaction. For buphedrone the program predicted N-dealkylation reaction as a most probable. According the program, the reaction can be catalyzed by various enzymes (1A2, 2A6, 2B6, 2C19, 2C8, 2C9, 2D6, 2E1, 3A4, HLM – human liver microsomes). The enzymes 3A4 and 2C9 also received a high score for the same reaction in the SmartCyp program. Additionally, it can be noticed that enzymes 2D6, 2E1 and HLM were predicted to catalyze the oxidation reaction of the phenyl ring in the *para* position and in SmartCYP we could also notice that prediction for 2D6. Enzymes 2A6 and 2E1 we can also notice a possible reaction on the side alkyl chain of the molecule (Figure 4.11).

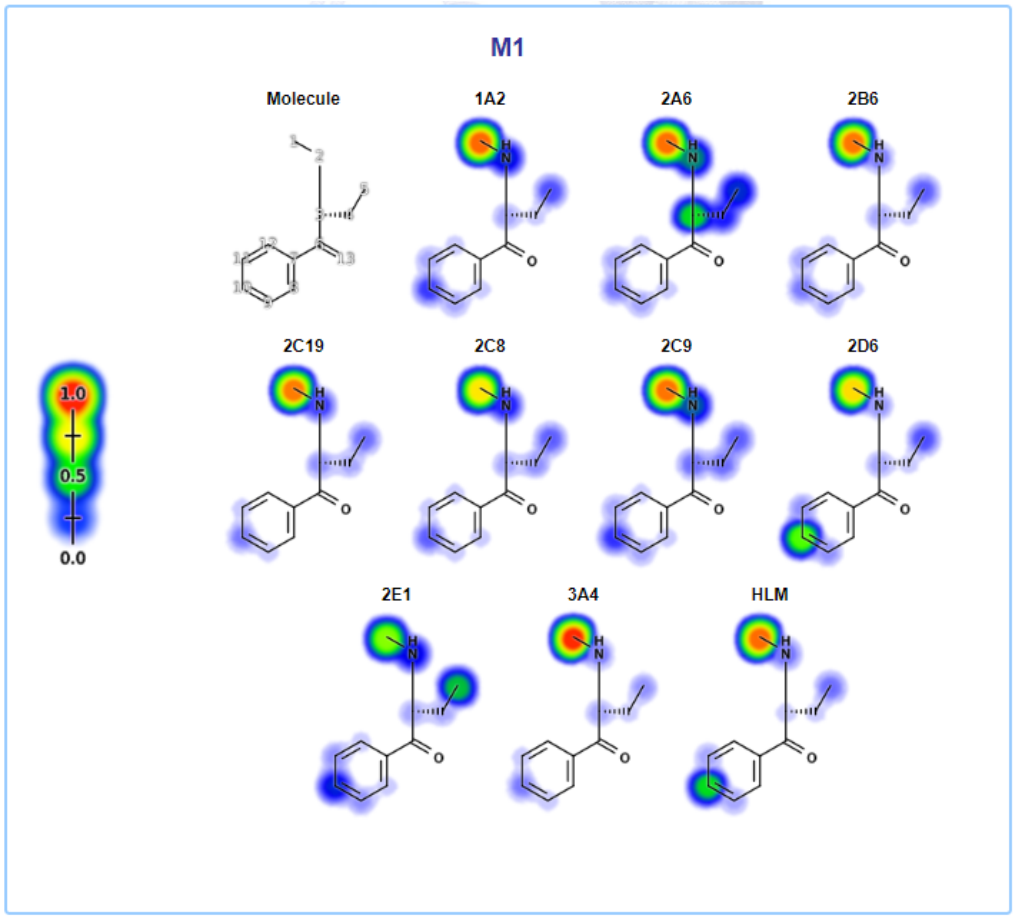

Figure 4.11 XenoSite site of metabolism prediction for buphedrone

For N-ethylhexedrone, the prediction using XenoSite indicates activity of the enzymes 1A2, 2A6, 2B6, 2C19, 2C8, 2C9, 2D6, 2E1, 3A4 and HLM as possible catalysts of the N-

dealkylation reaction as well as possible oxidation of the side chain. Enzymes 2A6, 2C9, 2D6, 2E1 and HLM also seem to catalyze oxidation reaction of the phenyl ring in the *para* position for this compound (Figure 4.12).

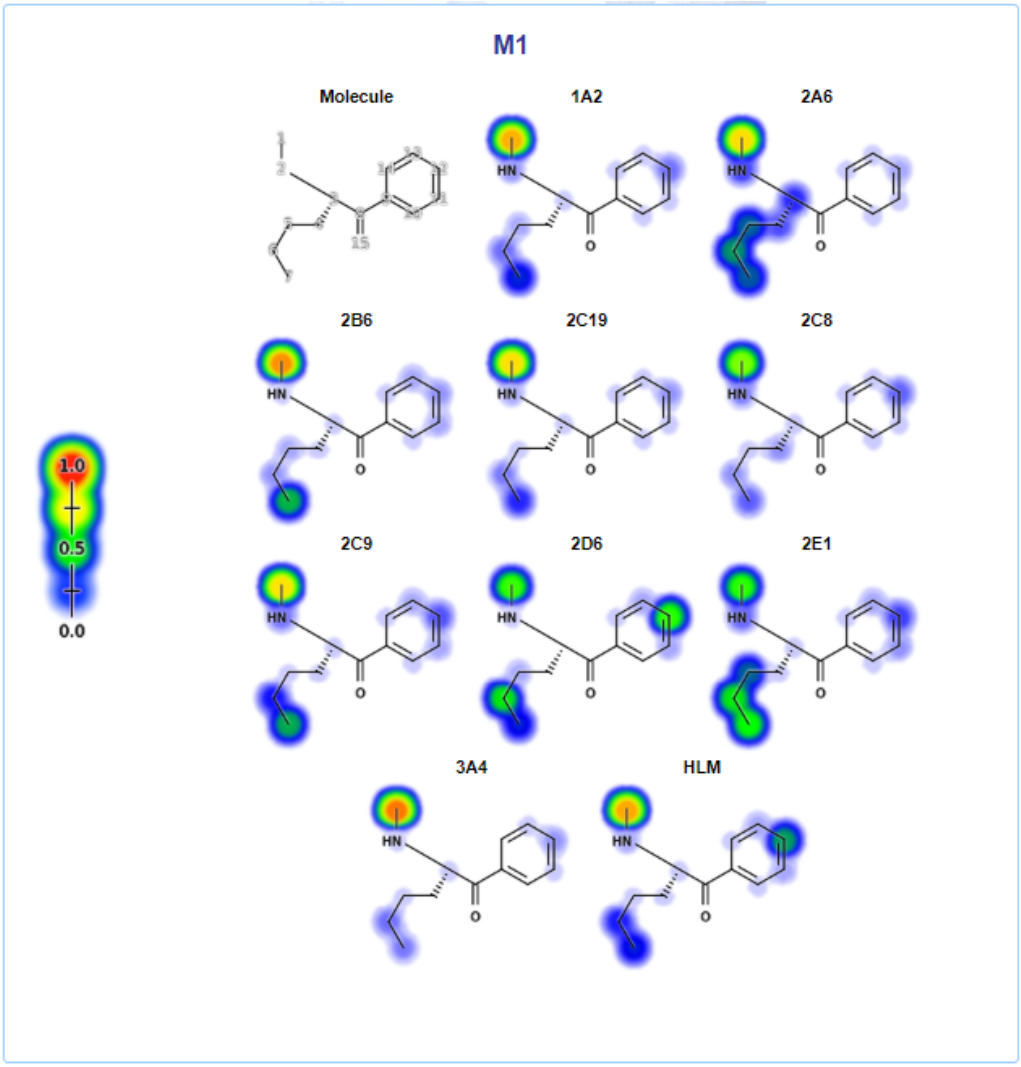

Figure 4.12 Site of metabolism prediction for N-ethylhexedrone performed by XenoSite

In the Rainbow Phase I prediction we can see the possible reactions N-ethylhexedrone can undergo. The most probable ones include oxidation of the side chain and the phenyl group, reduction of the β-keto moiety, dehydrogenation of the alkyl chain and unstable oxidation in the proximity of the amine group. The molecule does not seem to be able to suffer any hydrolysis as there is no group that could undergo such reaction (Figure 4.13).

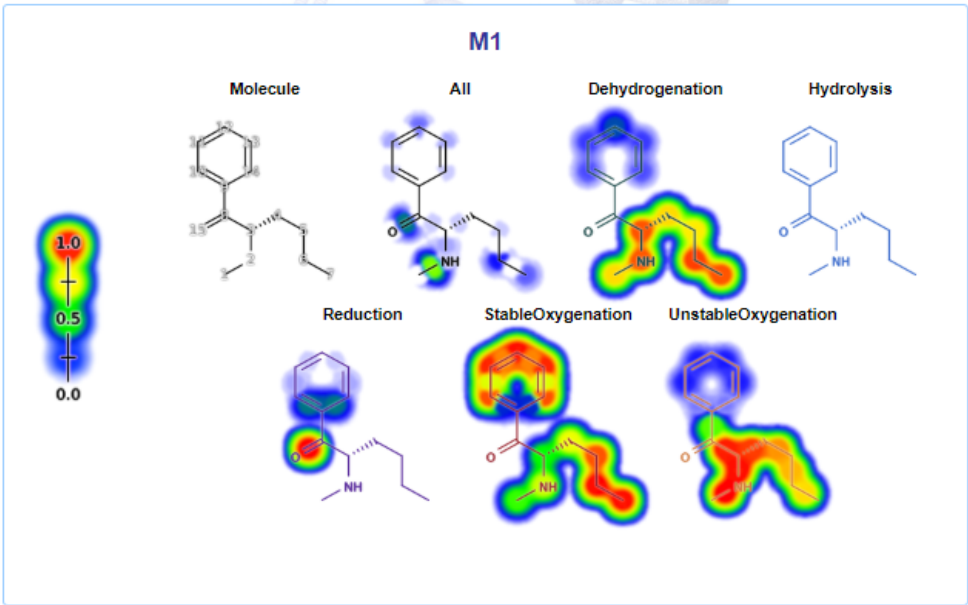

Figure 4.13 Rainbow Phase I prediction of the possible reactions, example of N-ethylhexedrone

4.1.5 Metabolite prediction using BioTransformer program.

BioTransformer, on the contrary to other used programs, predicts direct possible metabolites of the molecules, as well as probable enzymes catalyzing those transformations. For buphedrone, those predictions include metabolites formed by hydroxylation of the benzene group in the ortho and para position, hydroxylation of the aliphatic carbon (terminal or on the penultimate atom), terminal desaturation, epoxidation and N-dealkylation of the secondary amine (Figure 4.14).

Similarly, for N-ethylhexedrone the predicted metabolites result from *o*- or *p*-hydroxylation of the benzene ring, hydroxylation of the aliphatic chain, including both terminal carbons, epoxidation and N-dealkylation. The predicted metabolites match the possible sites of metabolism predicted previously by XenoSite, but some of the reactions does not seem to be energetically favorable (such as epoxidation of the benzene ring) and mostly they do not correspond to the metabolites predicted by literature (Figure 4.15).

BioTransformer:

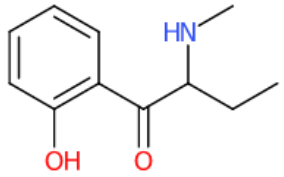

Reaction: o-Hydroxylation of monosubstituted benzene

Metabolic Enzyme(s):
CYP1A2 (Cytochrome P450 1A2)
CYP2C19 (Cytochrome P450 2C19)
CYP3A4 (Cytochrome P450 3A4)

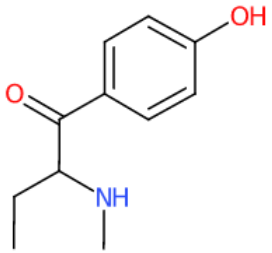

Reaction: p-Hydroxylation of monosubstituted benzene

Metabolic Enzyme(s):
CYP1A2 (Cytochrome P450 1A2)
CYP2D6 (Cytochrome P450 2D6)
CYP3A4 (Cytochrome P450 3A4)

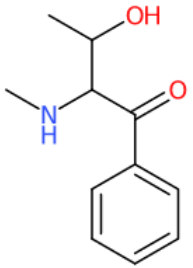

Reaction: Hydroxylation of penultimate aliphatic secondary carbon

Metabolic Enzyme(s):
CYP1A2 (Cytochrome P450 1A2)
CYP2B6 (Cytochrome P450 2B6)
CYP2C19 (Cytochrome P450 2C19)
CYP2D6 (Cytochrome P450 2D6)
CYP2E1 (Cytochrome P450 2E1)
CYP3A4 (Cytochrome P450 3A4)

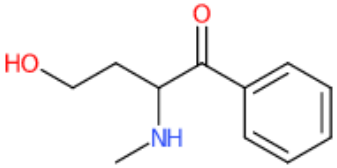

Reaction: Hydroxylation of terminal methyl

Metabolic Enzyme(s):
CYP1A2 (Cytochrome P450 1A2)
CYP2B6 (Cytochrome P450 2B6)
CYP2C19 (Cytochrome P450 2C19)
CYP2D6 (Cytochrome P450 2D6)
CYP2E1 (Cytochrome P450 2E1)
CYP3A4 (Cytochrome P450 3A4)

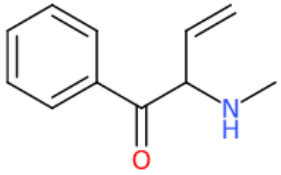

Reaction: Terminal desaturation

Metabolic Enzyme(s):
CYP1A2 (Cytochrome P450 1A2)
CYP2D6 (Cytochrome P450 2D6)
CYP3A4 (Cytochrome P450 3A4)

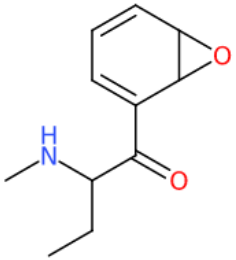

Reaction: Epoxidation of arene

Metabolic Enzyme(s):
CYP1A2 (Cytochrome P450 1A2)
CYP2B6 (Cytochrome P450 2B6)
CYP2C19 (Cytochrome P450 2C19)
CYP2E1 (Cytochrome P450 2E1)
CYP3A4 (Cytochrome P450 3A4)

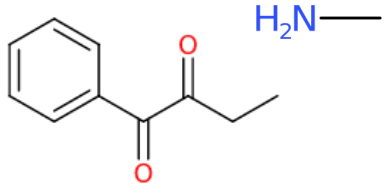

Reaction: N-dealkylation of acyclic secondary amine

Metabolic Enzyme(s):
CYP1A2 (Cytochrome P450 1A2)
CYP2B6 (Cytochrome P450 2B6)
CYP2C19 (Cytochrome P450 2C19)
CYP2D6 (Cytochrome P450 2D6)
CYP3A4 (Cytochrome P450 3A4)

Figure 4.14 Buphedrone metabolites with corresponding reaction types and metabolic enzymes inolved in the reaction predicted by BioTransformer

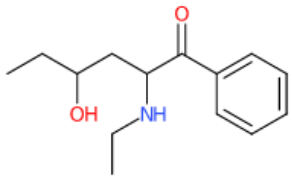

Reaction: Hydroxylation of antepenultimate aliphatic secondary carbon

Metabolic Enzyme(s):
CYP1A2 (Cytochrome P450 1A2)

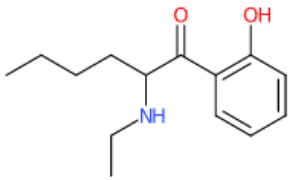

Reaction: o-Hydroxylation of monosubstituted benzene

Metabolic Enzyme(s):
CYP1A2 (Cytochrome P450 1A2)
CYP2C19 (Cytochrome P450 2C19)
CYP3A4 (Cytochrome P450 3A4)

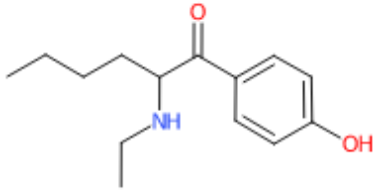

Reaction: p-Hydroxylation of monosubstituted benzene

Metabolic Enzyme(s):
CYP1A2 (Cytochrome P450 1A2)
CYP2C19 (Cytochrome P450 2C19)
CYP3A4 (Cytochrome P450 3A4)

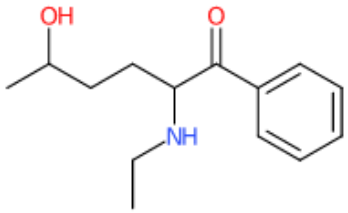

Reaction: Hydroxylation of penultimate aliphatic secondary carbon

Metabolic Enzyme(s):
CYP1A2 (Cytochrome P450 1A2)
CYP2B6 (Cytochrome P450 2B6)
CYP2C19 (Cytochrome P450 2C19)
CYP2D6 (Cytochrome P450 2D6)
CYP3A4 (Cytochrome P450 3A4)

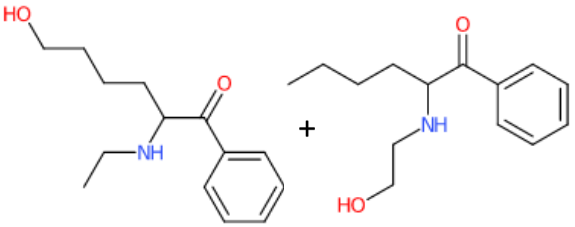

Reaction: Hydroxylation of terminal methyl

Metabolic Enzyme(s):
CYP1A2 (Cytochrome P450 1A2)
CYP2B6 (Cytochrome P450 2B6)
CYP2C19 (Cytochrome P450 2C19)
CYP2D6 (Cytochrome P450 2D6)
CYP3A4 (Cytochrome P450 3A4)

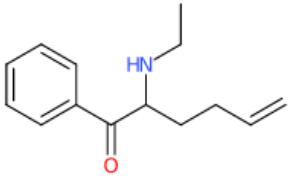

Reaction: Terminal desaturation

Metabolic Enzyme(s):
CYP1A2 (Cytochrome P450 1A2)
CYP2D6 (Cytochrome P450 2D6)
CYP3A4 (Cytochrome P450 3A4)

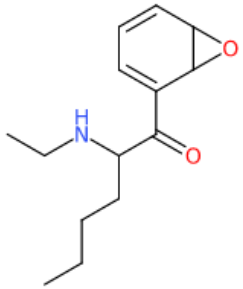

Reaction: Epoxidation of arene

Metabolic Enzyme(s):
CYP1A2 (Cytochrome P450 1A2)
CYP2B6 (Cytochrome P450 2B6)
CYP2C19 (Cytochrome P450 2C19)
CYP3A4 (Cytochrome P450 3A4)

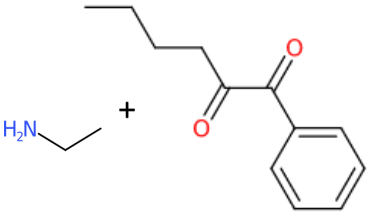

Reaction: N-dealkylation of acyclic secondary amine

Metabolic Enzyme(s):
CYP1A2 (Cytochrome P450 1A2)
CYP2B6 (Cytochrome P450 2B6)
CYP2C19 (Cytochrome P450 2C19)
CYP2D6 (Cytochrome P450 2D6)
CYP3A4 (Cytochrome P450 3A4)

Figure 4.15 N-ethylhexedrone metabolites with corresponding reaction types and metabolic enzymes inolved in the reaction predicted by BioTransformer

According to the literature (Uralets et al., 2014; Zaitsu, 2018), the primary reactions of Phase I metabolism, both for buphedrone and N-ethylhexedrone, are β-keto reduction followed by N-dealkylation or N-dealkylation. The possibility of hydroxylation of the aromatic ring was also mentioned, but it appears to be less probable than for amphetamines, where it is one of the major pathways. This might be caused by the presence of the ketone group attached to the β-carbon that might prevent this metabolite from being formed (Zaitsu, 2018). Similar prediction was made by SmartCyp and XenoSite. Both programs indicated N-dealkylation as the most probable reaction. In case of Buphedrone, first analysis in SwissADME tool predicted the substance as a possible CYP1A2 inhibitor. SmartCyp predicted that the N-dealkylation reaction mentioned in literature may be catalyzed by the systems 3A4, 2D6 and 2C9. XenoSite provided even more detailed analysis listing specific cytochromes 1A2, 2A6, 2B6, 2C19, 2C8, 2C9, 2D6, 3A4 and HLM as the ones responsible for dealkylation. In the BioTransformer analysis only one metabolite formed from N-dealkylation is present in the results and in that case also CYP1A2 is listed as a possible catalyst for the reaction, but the metabolite differs from what was predicted in the literature and by other prediction tools. The programs however did not predict the reduction of the ketone group, even though it was the reaction most widely mentioned by literature (Uralets et al., 2014; Zaitsu, 2018). This might be due to the fact that the CYP 450 enzymes usually perform oxidation reactions (Stanley, 2017) and this reaction can occur spontaneously without the help of the enzymes.

N-ethylhexedrone has been indicated by SwissADME as inhibitor of both CYP1A2 and CYP2D6, whereas SmartCyp predicted that it is as a substrate for CYP3A4 and CYP2C9. XenoSite also detected a higher probability of the reaction being carried out by the CYP3A4 family, with also possible 2C9 and 2C19 activity. Dehydrogenation, reduction and stable oxydation were the most probable reactions predicted by the XenoSite rainbow prediction, which perfectly corresponds to the literature prediction (Zaitsu, 2018) and metabolites observed *in vivo* (Uralets et al., 2014). N-dealkylation was also predicted by BioTransformer, but with a different mechanism that was not found in literature nor in other *in silico* prediction tools.

The literature review and *in silico* predictions provided information that lead the team to choose the following metabolites to be synthetized, as they appeared to be the most suitable for the stability and microsomal studies: 2-(ethylamino)-1-phenylhexan-1-ol hydrochloride (**H1**), 2-amino-1-phenylhexan-1-ol hydrochloride (**H2**) 4-(2-(ethylamino)-1-hydroxyhexyl)phenol hydrochloride (**H3**), 4-2-amino-1-hydroxyhexyl)phenol hydrochloride (**H4**), 4-(2-amino-1-hydroxyhexyl)phenol hydrochloride (**H5**), 2-(methylamino)-1-phenylbutan-1-ol hydrochloride (**B1**), 2-amino-1-phenylbutan-1-one hydrochloride (**B2**), 2-amino-1-phenylbutan-1-ol hydrochloride (**B3**) and 4-(1-hydroxy-2-(methylamino)butyl)phenol hydrochloride (**B4**) (Figure 3.1). Those metabolites were later

searched for as the most probable to appear in the samples as a result of degradation and microsomal activity.

4.2 *In vitro* stability studies

4.2.1 Short term Stability study of buphedrone and N-etylhexedrone

The short-term, 2 h, stability study of buphedrone and N-ethylhexedrone at physiological temperature of 37 °C, was evaluated by performing incubation studies in 20% of isotonic 0.01 M phosphate buffer pH 7.4 of each studied SC (final concentration 15 μM). Because the water used has a pH with the value around 7.0, the final pH of the testing solution was estimated to be slightly less than 7.4. Samples collected at several time points were analysed by liquid chromatography coupled with mass spectrometry (HPLC-MS/MS), in positive mode, and the peak area of each identified peak was measured and processed by the corresponding computer software.

When the amount of either buphedrone or N-ethylhexedrone was assayed by HPLC-MS/MS in samples taken during the incubation assay a decrease by around 20% comparing to the initial amounts was observed for both studied SCs. When all the synthetized buphedrone and N-ethylhexedrone metabolites were searched for, none were detected up to the limit of detection of the method. In addition, the stability of N-ethylhexedrone metabolites resulting from beta-keto reduction (H1) and N-dealkylation (H2) (Figure 3.1) was also evaluated and the results obtained suggested these metabolites were stable under the same conditions (Figure 4.16).

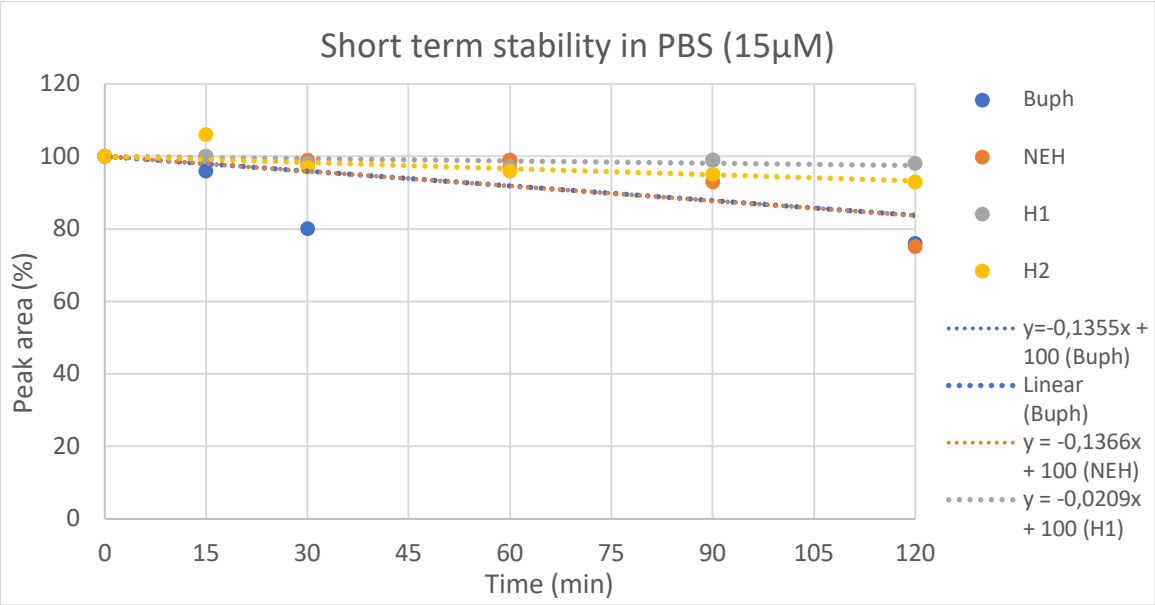

Figure 4.16 Assessed amount (%) of tested compounds during the short-term (2h) stability study at 37 °C in 20% of 0.01M phosphate buffer, pH ~7. Start concentration was 15µM (all data derived from single assays)

4.2.2 Long term stability study of buphedrone and N-ethylhexedrone

The long-term stability of buphedrone and N-ethylhexedrone at physiological temperature of 37 °C, was evaluated for 48 h, by performing incubation studies in isotonic phosphate buffer pH 7.4 of each studied SC (final concentration 100 µM). The same analyzing procedure as the one used in the short-term stability protocol was applied in this study. This long-term stability study was used as a control study for the plasma stability assay.

When the amount of buphedrone was assayed by HPLC-MS/MS in samples taken during the incubation assay the results suggested a relatively stable compound under the studied condition (Figure 4.17). At 24 h and after 48 h the amount of buphedrone remaining in the sample test was 97% and 82% of the initial amount (100 µM), respectively (Table 4.2).

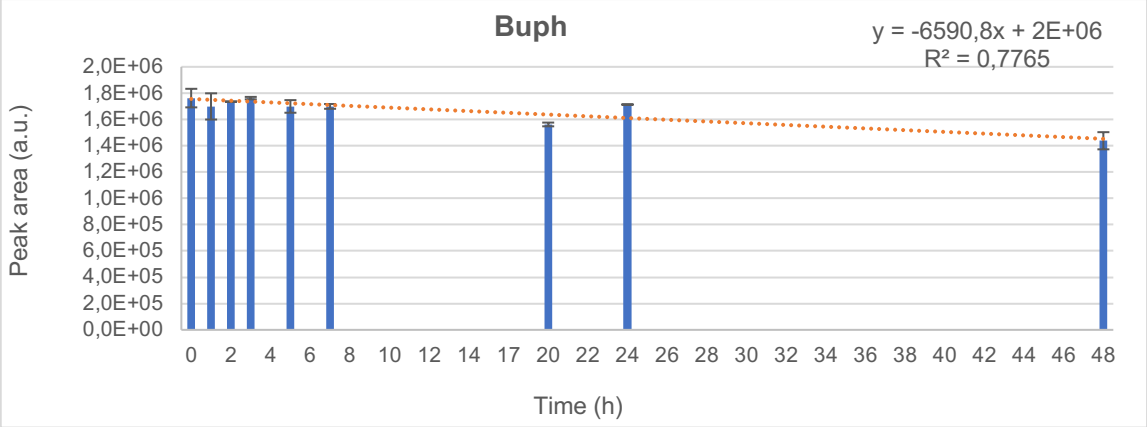

Figure 4.17 Long-term stability of buphedrone at 37 °C in 0.01 M isotonic phosphate buffer, pH 7.4 (starting concentration 100 μM) (results expressed as peak area (a.u.) and presented as average ± stdev, were obtained from duplicate assay)

When the presence of metabolites was search for, only the metabolite resulting from N-dealkylation of buphedrone (B2) was detected among all studied metabolites (B1 to B4) (Figure 4.18). Results show that same amount of metabolite B2 was detected at all time-points. At time zero the concentration of B2 corresponded to 0.08% of the parent compound, buphedrone, and until 3 h there was little variation in the amount of the metabolite, suggesting that buphedrone metabolite B2 is stable up to 3 hours, from when it seems to start to decrease reaching 56% of the initial concentration at 48h (Table 4.2).

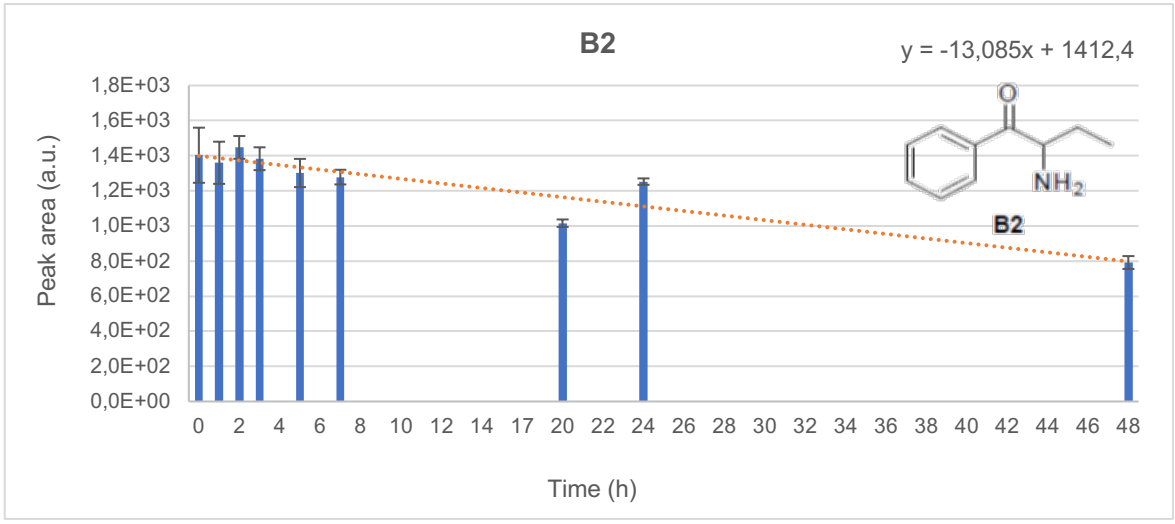

Figure 4.18 Detection and assessment of buphedrone N-dealkylated metabolite (B2) during the long-term stability study of buphedrone 100 μM at 37 °C in 0.01 M isotonic phosphate buffer, pH 7.4 (results expressed as peak area (a.u.) and presented as average ± stdev, were obtained from duplicate assay)

When the amount of the NEH was assessed by HPLC-MS/MS in samples taken during the incubation assay at 37 ºC in isotonic phosphate buffer (pH 7.4) the results suggested a relatively stable compound, under the studied condition, until 24 h (Figure 4.19). At 24 h and after 48 h the amount of N-ethylhexedrone remaining in the sample test was 94% and 66% of the initial amount (100 μM), respectively (Table 4.2).

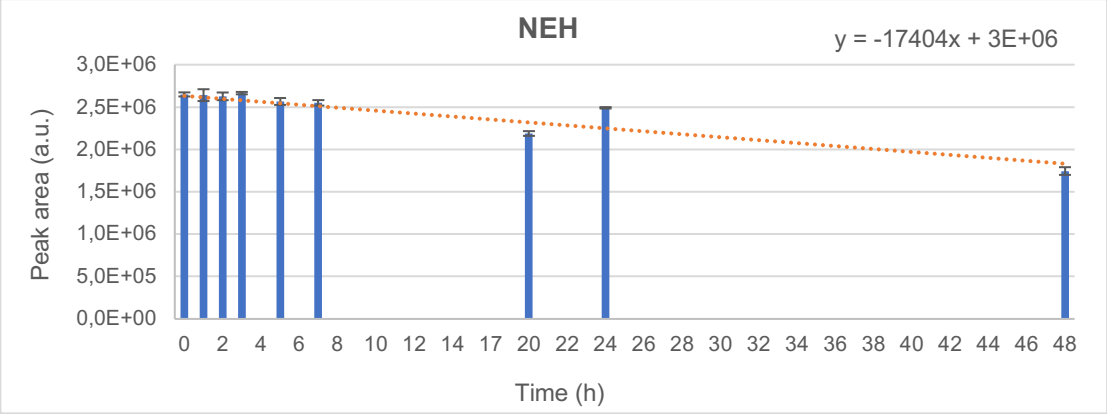

Figure 4.19 Long-term stability of N-ethylhexedrone at 37 ºC in 0.01 M isotonic phosphate buffer, pH 7.4 (starting concentration 100 μM) (results expressed as peak area (a.u.) and presented as average ± stdev, were obtained from duplicate assay)

When the presence of metabolites was search for, among all studied N-ethylhexedrone metabolites (H1 to H5) (Figure 3.1) only the metabolite resulting from N-dealkylation (H2) was detected (average ± stdev, were obtained from a duplicate assay.). The same amount of metabolite H2 was detected at all time-points up to 3 hours including time zero at a concentration corresponding to 0.05% of the parent compound, N-ethylhexedrone. The obtained results suggest that this N-ethylhexedrone metabolite H2 is stable up to 3 hours, from when it seems to start to decrease reaching 19% of the initial concentration at 48h (Table 4.2).

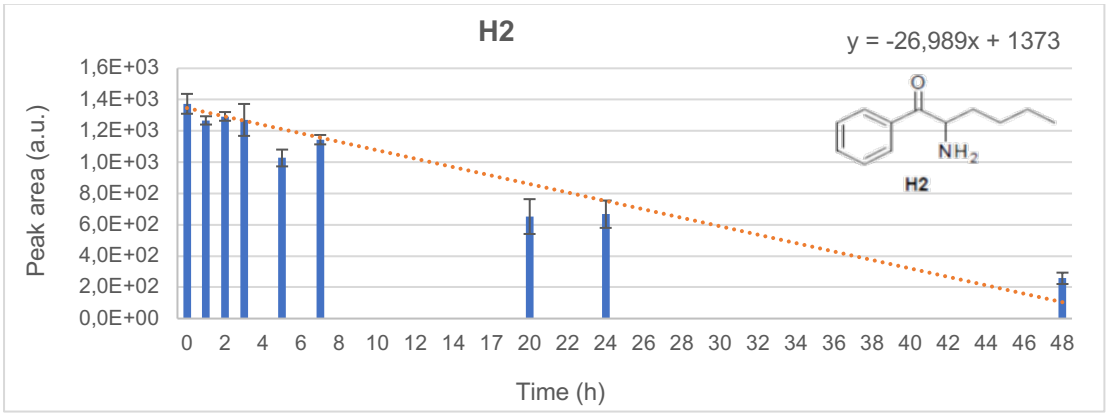

Figure 4.20 Detection and assessment of N-ethylhexedrone N-dealkylated metabolite (H2) during the long-term stability study of N-ethylhexedrone 100 μM at 37 ºC in 0.01 M isotonic phosphate buffer, pH 7.4. results expressed as peak area (a.u.) and presented as average ± stdev, were obtained from a duplicate assay.

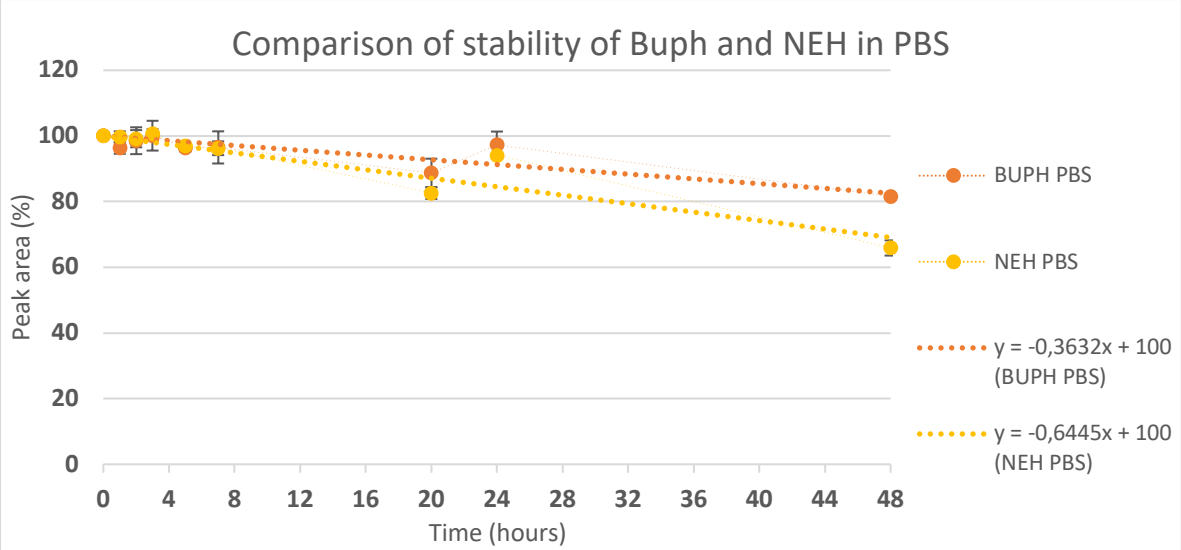

Figure 4.21 Comparison of the stability of Buph and NEH in phosphate buffer (0.01 M) (results expressed as percentage of peak area and presented as average ± stdev, were obtained from duplicate assay)

In addition, the percentages of substrates persisting in the sample after 2 h, 7 h, 24 h and 48 h were calculated using both the data obtained from the assay and the estimated values based on the line equation for each assay (Table 4.2). From that data, it can be concluded that both buphedrone and N-ethylhexedrone are quite stable for 24 h at 37ºC in isotonic phosphate buffer pH 7.4. After 48h for buphedrone the estimated reduction reached 84% and for NEH 72,8%. This shows that both those compounds are quite stable in PBS up to around 24h (Figure 4.21). On the contrary, the metabolite resulting from N-dealkylation of NEH (H2), detected in the NEH assay, is very unstable in PBS at 37ºC, having been estimated that near 50 % and only 5.6% would still be present in the sample after 24h and 48h, respectively. This might be explained by the fact that H2 is a primary amine and a weaker base and this could change its reactivity comparing to the secondary amines, such as N-ethylhexedrone.

Table 4.2 Amount (%) of tested compounds present at different times of the stability study in phosphate buffer (0.01 M). The results expressed as average ± stdev, correspond to duplicate assay while their estimated values were calculated from the obtained line equations.

	% Buph	% Buph estimated	% B2	% B2 estimated	% NEH	%NEH estimated	% H2	%H2 estimated
2h	98.56 ± 4.09	99.3	103.57 ± 6.97	98.4	99.16 ± 2.61	98.8	94.20 ± 2.33	96.1
7h	96.51 ± 4.9	97.7	91.87 ± 13.26	94	96.26 ± 2.09	95.9	83.34 ± 1.67	86.2
24h	97.29 ± 4.05	92.1	89.78 ± 8.74	79	94.04 ± 0.54	86.1	48.50 ± 4.12	52.8
48h	81.58 ± 0.44	84.2	56.64 ± 3.73	57.8	65.89 ± 2.31	72.1	18.69 ± 1.78	5.6

4.3 *In vitro* Plasma stability studies

This study aimed to access plasma stability of selected synthetic cathinones, N-ethylhexedrone (NEH) and buphedrone (Buph). Both SC were incubated at 37 ºC in 80% human plasma, derived from different healthy individuals, diluted with 0.01 M pH 7.4 isotonic phosphate buffer. Samples collected at several time points were analysed by liquid chromatography coupled with mass spectrometry (HPLC-MS/MS), in positive mode, following protein precipitation.

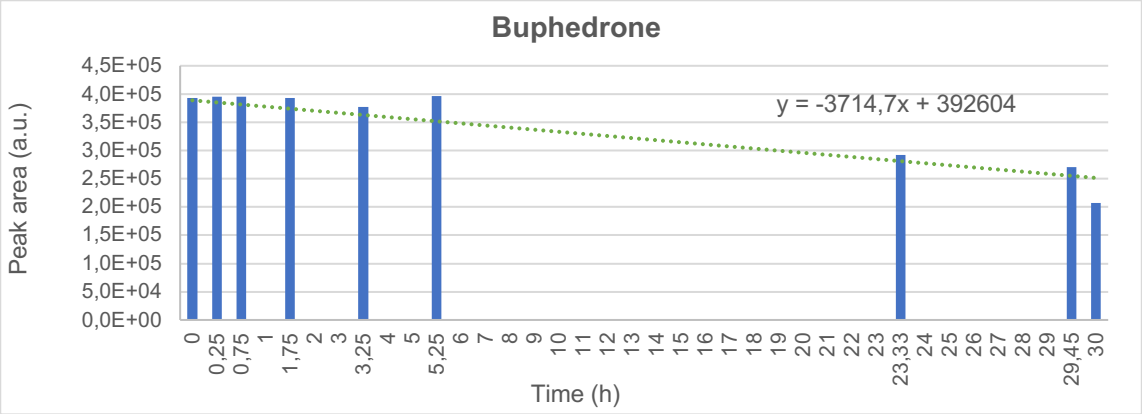

Figure 4.22 Plasma Stability of buphedrone at a final concentration of 10^{-5} M. Samples, incubated at 37ºC, were collected at different time points and analysed by HPLC-MS/MS.

The in vitro plasma studies with buphedrone were performed at both 10^{-4} M and 10^{-5} M final concentrations. The evaluation of the buphedrone content in samples collected during the study shows a compound relatively stable at 37 ºC in plasma up to 3-5 hours (Table 4.4 and Table 4.5) and a linear decay of buphedrone content which represents near 25% to 55% lost after 24 h incubation in plasma, respectively for each studied concentration (**Error! Reference s ource not found.** and Figure 4.24).

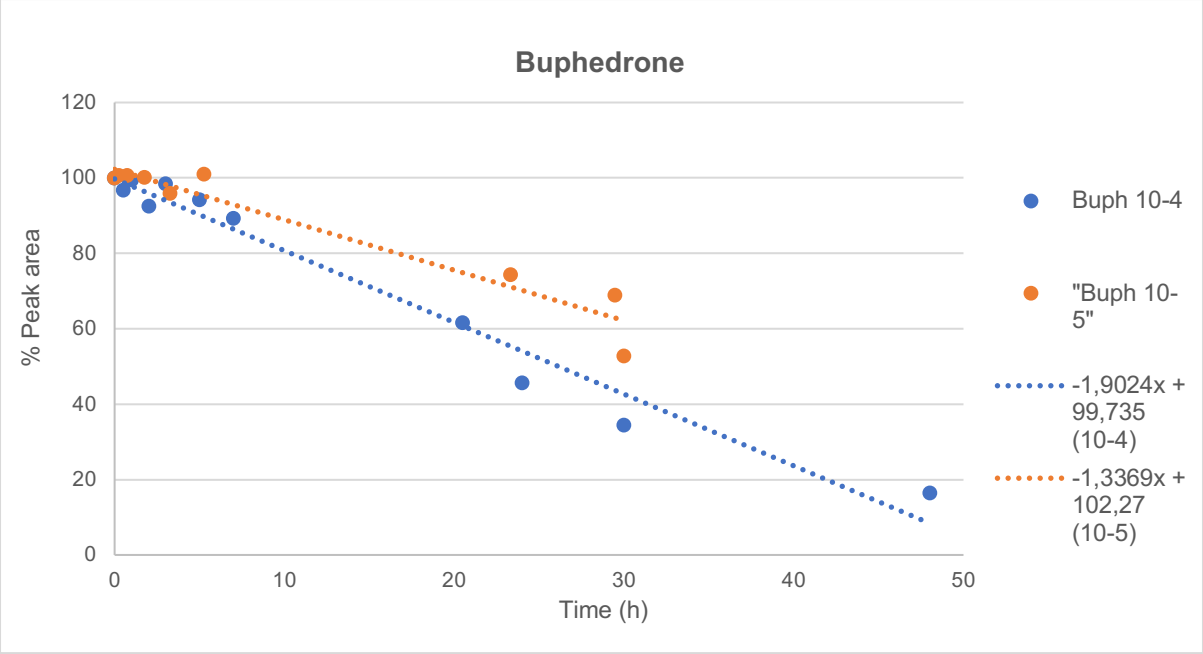

Figure 4.23 Plasma stability of buphedrone at starting concentration of 10^{-5} M and 10^{-4} M (results are expressed in percentage of the peak area)

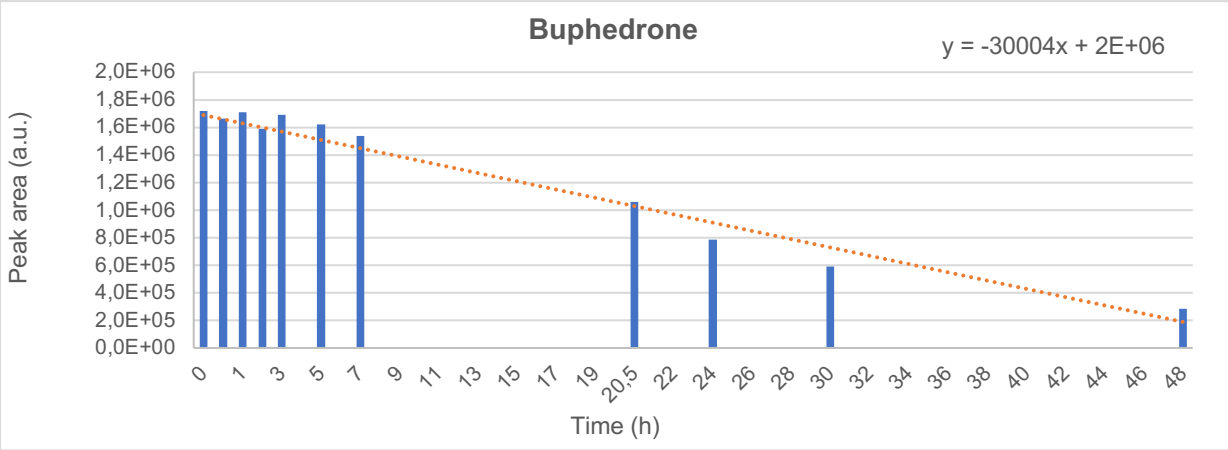

Figure 4.24 Plasma stability of buphedrone at final concentration 10^{-4} M. Results expressed as peak areas (a.u.) over time.

Table 4.3 Assessement of buphedrone content of samples collected from human plasma incubated at 37°C . Buphedrone starting concentration of 10^{-4} M

Time (h)	0.5	1.0	2.0	3.0	5.0	7.0	20.5	24	30	48
% Buph	96.7	99.5	92.5	98.4	94.3	89.3	61.6	45.6	34.4	16.4
%Buph estimated	99.2	98.5	97.0	95.5	92.5	89.5	69.2	64.0	55.0	27.8

The buphedrone kinetics in plasma was assessed (Figure 4.25) and corresponding half-life calculated for each studied concentration in 1.5 days when starting concentration of buphedrone was 10^{-5} M and a shorter half-life of near 1 day (0.9 days) when starting concentration of buphedrone was 10^{-4} M.

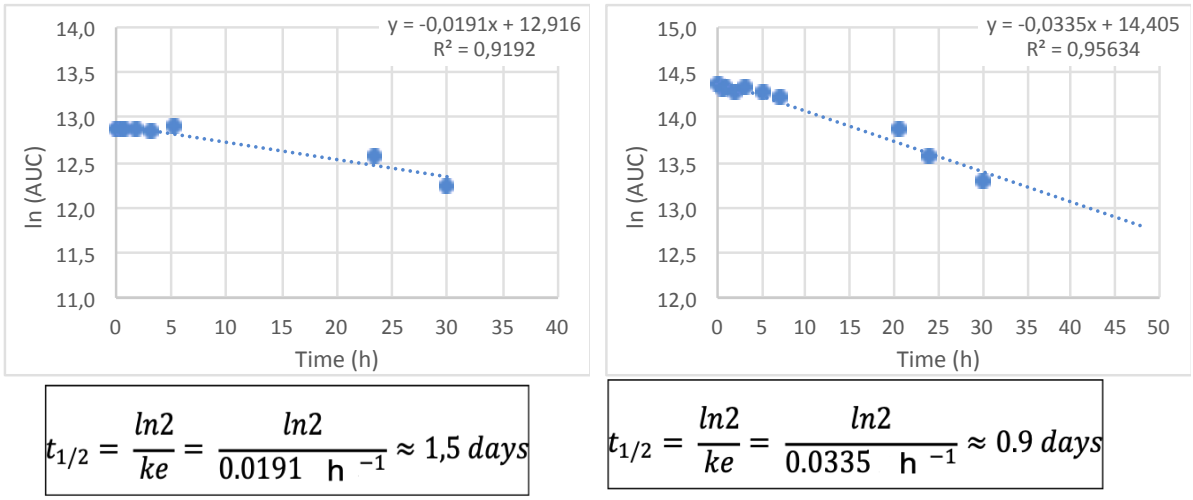

$$t_{1/2} = \frac{ln2}{ke} = \frac{ln2}{0.0191 \quad h^{-1}} \approx 1{,}5 \; days$$

$$t_{1/2} = \frac{ln2}{ke} = \frac{ln2}{0.0335 \quad h^{-1}} \approx 0.9 \; days$$

Figure 4.25 Buphedrone kinetics assessment in plasma at concentration 10^{-5} M (left) and 10^{-4} M (right).

When metabolites were search for, from all studied buphedrone metabolites, B1 to B4 (Figure 3.1), only metabolite resulting from N-dealkylation (B2), was detected (Figure 4.26). It can be noticed that the metabolite is already present at time 0, at a concentration corresponding to 0.1% of the parent compound, buphedrone. The same was observed in the long-term stability study, which may indicate that the sample was initially contaminated. We observed that the amount of metabolite B2 was stable up to 3 h of incubation, rises up to 154% at 20.5 hours, then goes back to base line amounts and at 48h decreases to about 79% of the initial detected value. No formation of any other metabolites was observed.

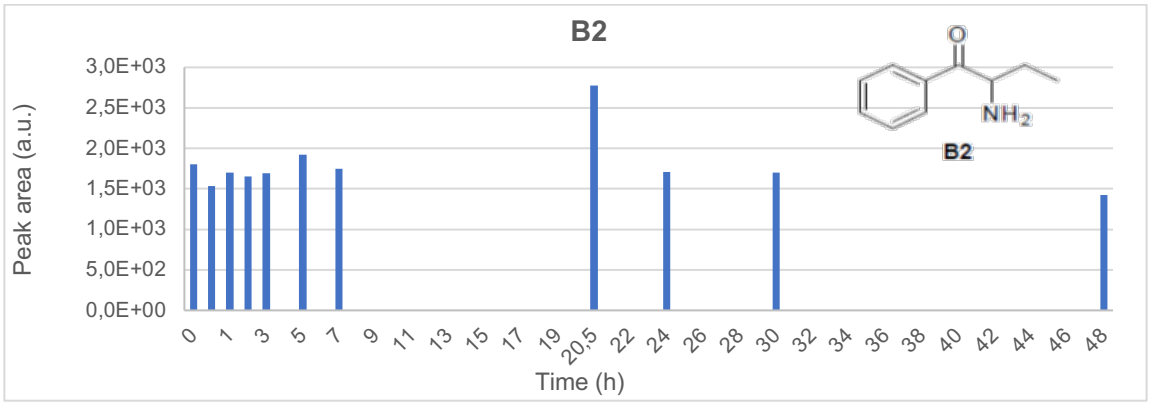

Figure 4.26 Detection and assessment of buphedrone N-dealkylated metabolite (B2) during the plasma stability study of buphedrone at final concentration of 10^{-4} M.

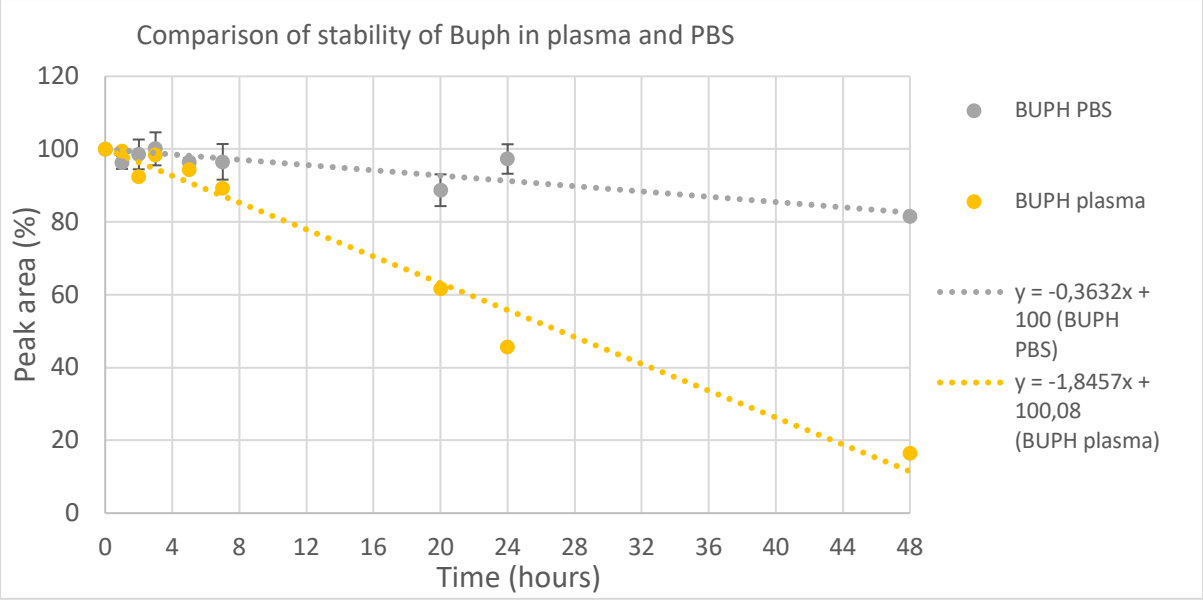

Figure 4.27 Stability of buphedrone in phosphate buffer (0.01 M, pH 7.4) and in plasma. Buphedrone starting concentration 100 μM. Results expressed as percentage of the starting concentration were obtained either from duplicate (average ± stdev) or single assay, respectively.

The in vitro plasma study with N-ethylhexedrone was performed at 10^{-4} M final concentrations (Figure 4.28). The evaluation of the N-ethylhexedrone content in samples collected during the study shows a compound relatively stable at 37ºC in plasma up to 5 h (Table 4.4) and a linear decay of N-ethylhexedrone content reaching an estimated of approximately 20% loss after 24h and 35% loss after 48h of incubation in human plasma of the initial substrate present.

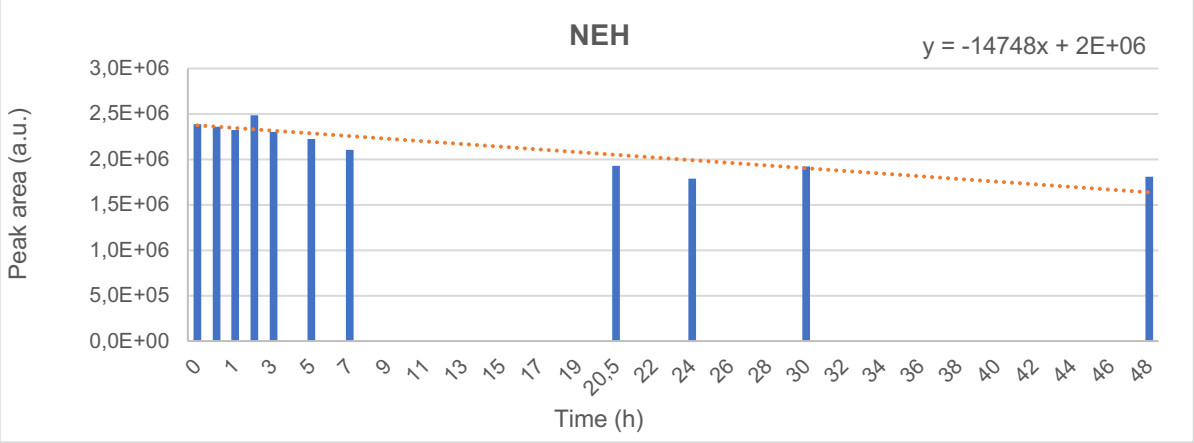

Figure 4.28 Plasma stability of N-ethylhexedrone at final concentration at 10^{-4} M. Results expressed as peak areas (a.u.) over time, were obtained from single assay.

Table 4.4 Assessement of N-ethylhexedrone content of samples collected from human plasma incubated at 37°C. N-ethylhexedrone starting concentration of 10^{-4} M

Time (h)	0.5	1.0	2.0	3.0	5.0	7.0	20.5	24	30	48
% NEH	98.6	100.7	97.2	96.3	93.1	88.2	80.7	74.9	80.5	75.8
%NEH estimated	99.6	99.3	98.5	97.8	96.3	94.8	84.9	82.3	77.9	64.6

The N-ethylhexedrone kinetics in in vitro human plasma was assessed (Figure 4.29) and corresponding half-life calculated in near 3 day (3.2 days) when the starting concentration of N-ethylhexedrone was 10^{-4} M.

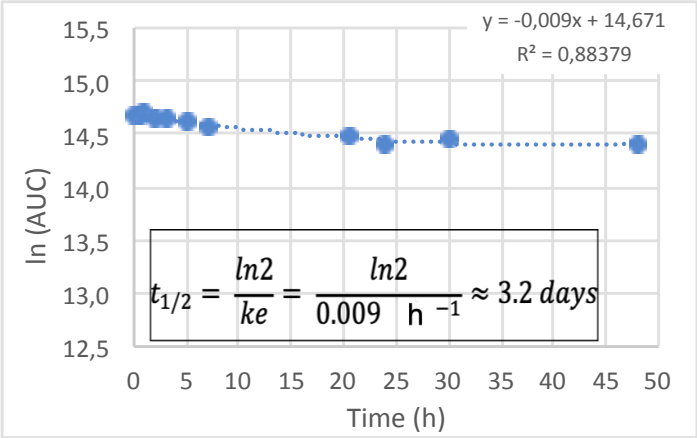

Figure 4.29 N-ethylhexedrone kinetics assessment in plasma at concentration 10^{-4} M.

When looking for metabolites, of all studied N-ethylhexedrone metabolites only the presence of metabolite resulting from N-dealkylation (H2) and the one resulting from keto-reduction and oxidation in the para position of the aromatic ring (H4) were detected (Figure 4.30 and Figure 4.31, respectively). The presence of H2 metabolite was detected at all time-points, including at time 0, at a concentration corresponding to 0.07% of the parent compound, N-ethylhexedrone. Identical results were obtained in the long-term stability study, which may indicate initial contamination of the sample. However, the amount of this metabolite, stable during the incubation, increases at time 20.5 h and keeps growing until the end of the assay, which suggest formation of that metabolite in the sample. The final amount of metabolite H2 after 48 h is 183,5% of the initial value detected at time 0 (Table 4.6).

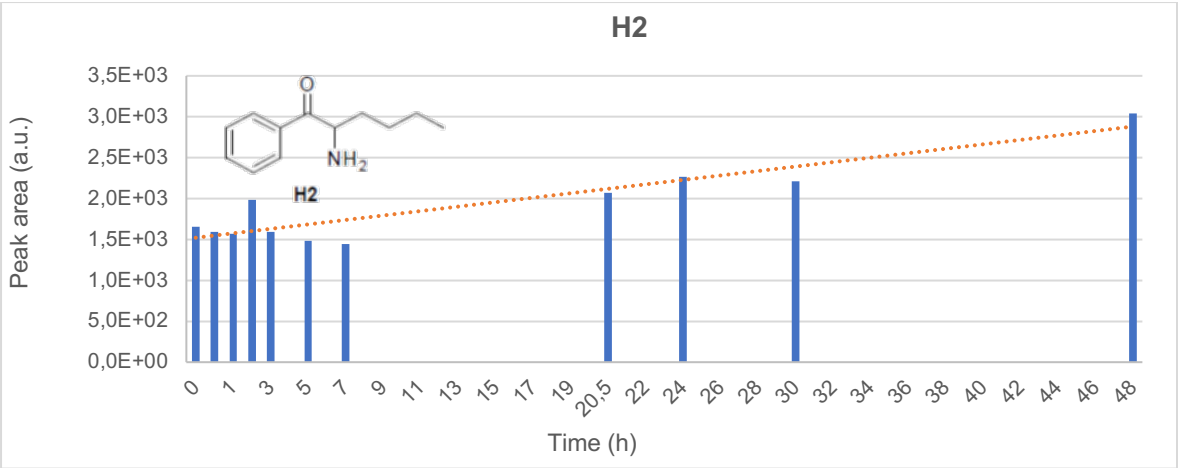

Figure 4.30 Detection and assessment of NEH N-dealkylation metabolite (H2) during the plasma stability study of NEH (10^{-4} M). Results expressed as peak areas (a.u.) over time. Data obtained from a single assay.

The presence of metabolite resulting from keto-reduction and oxidation in the para position of the aromatic ring of NEH (H4) was detected at time 3 h, and its content decreased below the limit of detection after the time of 7 h (Figure 4.31). The presence of that metabolite is rather unusual, as according to the literature it requires first the appearance of metabolite H1, that has not been detected (Zaitsu, 2018).

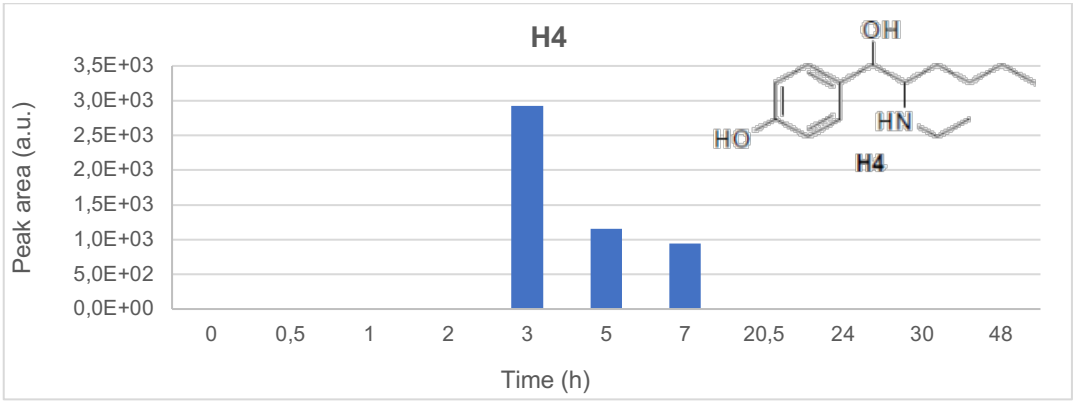

Figure 4.31 Detection and assessment of NEH metabolite resulting from β-keto-reduction and oxidation in the para position of the aromatic ring (H4) during the plasma stability study of NEH (10^{-4} M). Results expressed as peak areas (a.u.) over time. Data obtained from a single assay.

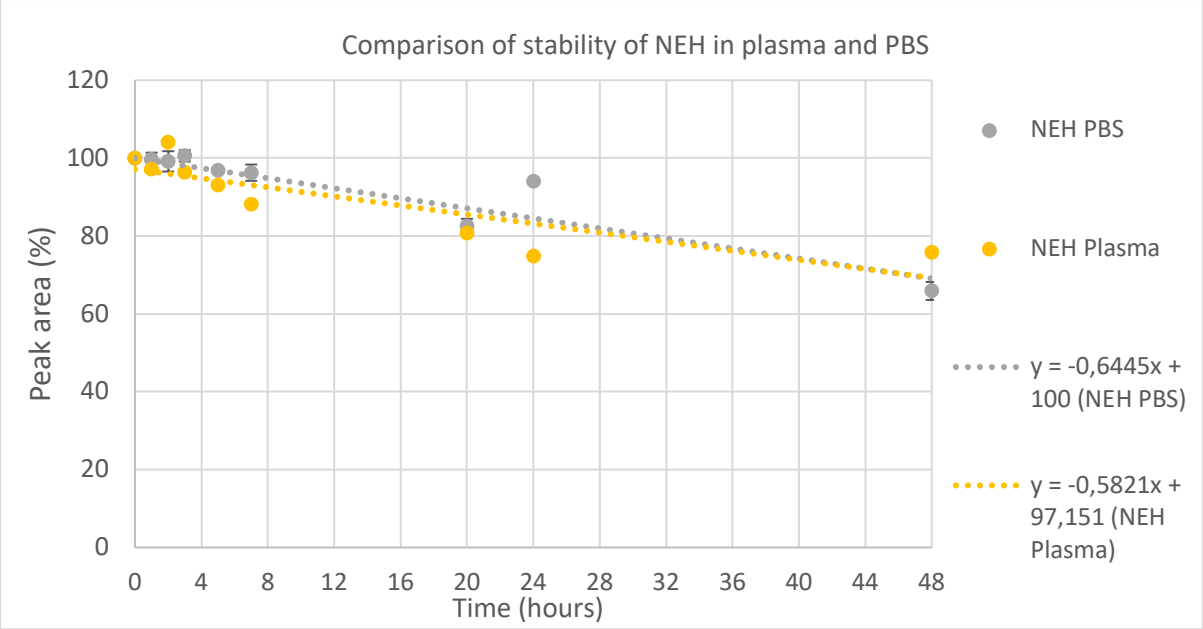

Figure 4.32 Stability of N-ethylhexedrone in phosphate buffer (0.01 M, pH 7.4) and in plasma. Starting concentration 100 μM. Results obtained either from duplicate or single assay, respectively.

Table 4.5-Assessment of the content of investigated compounds present in samples collected from human plasma incubated at 37°C . Starting concentration for buphedrone and N-ethylhexedrone was 10^{-4} M

	% Buph	% Buph estimated	% B2	% NEH	% NEH estimated	% H2
2h	89.3	97	97	104.1	98.5	119.6
7h	89.3	89.5	97	88.2	94.8	87.1
24h	45.6	64	94.6	74.9	82.3	136.8
48h	16.5	28	79.1	75.8	64.6	183.5

From the obtained data it can be seen that both buphedrone and N-ethylhexedrone are quite stable at 37 °C in isotonic phosphate buffer pH 7.4 after 2 hours, as well as in plasma and PBS (in all cases the percentage of the initial amount of substance is around 99% for NEH and between 92%and 100% for Buph) (Table 4.2 and 4.5). Interestingly, it was observed that buphedrone degrades quickly in plasma (after 48 h only 16% of the initial value is still present in the sample), but is rather stable in PBS (after 48 h still 82% of the initial amount is present)(Figure 4.27). For N-ethylhexedrone, it seems to be more or less as stable in plasma (76% after 48h) as in PBS (66% after 48h) (see Figure 4.32). In addition to the stability studies in PBS, when the stability of buphedrone and N-ethylhexedrone at 15 μM was evaluated in 20% PBS at 37°C for 2 h, a decrease in concentrations to 76% and 75% of buphedrone and N-

ethylhexedrone was observed, respectively (Table 4.2), but no metabolites were detected. The disappearance of the compounds in both cases is around 25% but since no metabolites, out of the synthetized ones, were detected, it suggests that the appearance of those metabolites in *in vitro* metabolism assays is in fact the result of the microsomal activity. The difference in the stability of investigated compounds in short term and in long term is most probably caused by fact that in long term the concentration of PBS in the sample was almost 100% (0,01 M) and in short term it was around 20% (2,2 mM). There is little data to compare if the concentration of synthetic cathinones have any effect on their stability. Glicksberg and Kerrigan (2017) in both of their studies, carried out in blood and urine, concluded that no concentration differences affected the stability observed for any of the 22 synthetic cathinones investigated.

It has been noticed that while investigating long-term (48h) plasma stability of N-ethylhexedrone that the metabolite resulting from β-keto-reduction and oxidation of the benzene ring in the para position (H4), appears after 3 hours, but it seems to be quite unstable and its presence was not detected after 7 hours. It is surprising because, as predicted by literature (Zaitsu, 2018) and the carried out experiments its appearance requires first formation of the metabolite H1 (β-ketones are unlikely to undergo oxidation in the para position of the aromatic ring) that was not detected in the assay using the described detection method. It has also been noticed that throughout the whole duration of the assay, the amount of metabolite H2 constantly increases, but the formed amount does not explain the total disappearance of the N-ethylhexedrone. This could mean that probably there are other products being formed in the reaction mixture that we are not able to detect or that the substrates suffer degradation that might be caused by the temperature or the pH. Additionally, the disappearance of the substrate in plasma can be explained by other factors, such as its metabolic and chemical instability, which may cause the analyte to suffer oxidation, hydrolysis or isomerization over time (Reed, 2016). Moreover, the analyzed substance can also undergo aggregation, precipitation or by non-covalently binding to plastic or glass surfaces, as well as biological ones, such as proteins and lipids present in plasma, thus reducing the amount of the substrate in the investigated sample (Reed, 2016).

Plasma stability studies have shown that buphedrone is the least stable compound in plasma and after 48h only 16% of the initial amount of the compound is still present in the sample. N-ethylhexdrone appears to be much more stable and in the final sample still around 75% is still present. Under the studied conditions (37°C, pH 7.4), NEH has almost the same stability in plasma as in PBS, while buphedrone appears to be more stable in PBS than in plasma.

One study investigating stability of synthetic cathinones in blood at different concentrations, temperatures and analytes, with the analysis carried out by LC/Q-TOF-MS, proved that the factor that most influences their stability was temperature (Glicksberg &

Kerrigan, 2017). Pyrrolidinyl analogs of cathinone were significantlly more stable than the N-alkylated ones. In that study the stability of buphedrone was estimated to 4 months at 4°C, 3,4 days at 20°C and 14h at 32°C in whole blood and the values were very similar for that group of cathinones. For similar temperature (32°C) and lower concentrations (100 ng/L and 1000 ng/L, which corresponds to 0.56 μM and 5.6 μM, respectively), the blood stability of buphedrone was estimated to reach 14h, while in our investigation it was 0,9 day (~22h) for the concentration 10^{-4} and 1,5 day (36h) for the concentration 10^{-5}. Those information regarding stability in biosamples are of huge importance because the biological material that is collected from the users often needs to be transported and stored before being analysed and, as shown, the conditions that the sample is kept in have a very siginficant impact on the content of the sample. Those results suggest that the best conditions to store synthetic cathinones such as buphedrone in blood is an environment with a low temperature and low pH (~4) (Glicksberg & Kerrigan, 2017, 2018).

In a study by the same group in human urine (Glicksberg & Kerrigan, 2018), evaluating the effects of concentration, pH, temperature and analyte-dependent effects stability of 22 synthetic cathinones the authors found that those compounds were more stable at low temperatures in acidic urine (pH 4). In both studies, in blood and in urine, they concluded that the concentration differences did not affect the stability for any of the 22 synthetic cathinones investigated. They also noticed that ring substituted and unsubstituded cathinones containing secondary amines were significantly less stable that the ones containing a pyrrilodine ring and a tertiary amine. That group of cathinones, such as buphedrone used in the study, was very unstable at 32°C (almost no sample remaining after 6 months at pH 4 and no sample remaining after 5 days at pH 8). At ambient temperature buphedrone was stable for 2 months. All cathinones proved to be very stable at pH 4 at 4°C and -20°C, so those conditions may indicate the right conditions for storage of those substances.

4.4 In vitro metabolism studies using liver microsomes

The in vitro metabolism assay was performed during 120 min, according to the guidelines provided by the manufacturer. Samples collected at several time points were analysed by liquid chromatography coupled with mass spectrometry (HPLC-MS/MS), in positive mode, following protein precipitation. In order to establish the optimal conditions for the assay, several substrate concentrations were tested, namely 5, 10 and 15 μM of either buphedrone or N-ethylhexedrone.

4.4.1 Microsomal metabolism studies with mice liver microsomes using buphedrone and N-ethylhexedrone as substrates

The evaluation of the buphedrone content in samples collected during the *in vitro* metabolism study with mice liver microsomes using 5 μM buphedrone as substrate shows almost no variation on buphedrone content (Figure 4.33), with exception of a 20% decrease of the initial amount at time 30 min, which could be an artifact. When formation of buphedrone metabolites (B1 to B4, Figure 3.1) was investigated, metabolite resulting from N-dealkylaion (B2) was detected and results suggest its formation with stabilizing rate formation at 90 min and maximum at 120 min (Figure 4.33). The detected presence of B2 metabolite at time 0, corresponded to 0.12% of the parent compound, buphedrone. No other investigated metabolite was formed in detectable amounts.

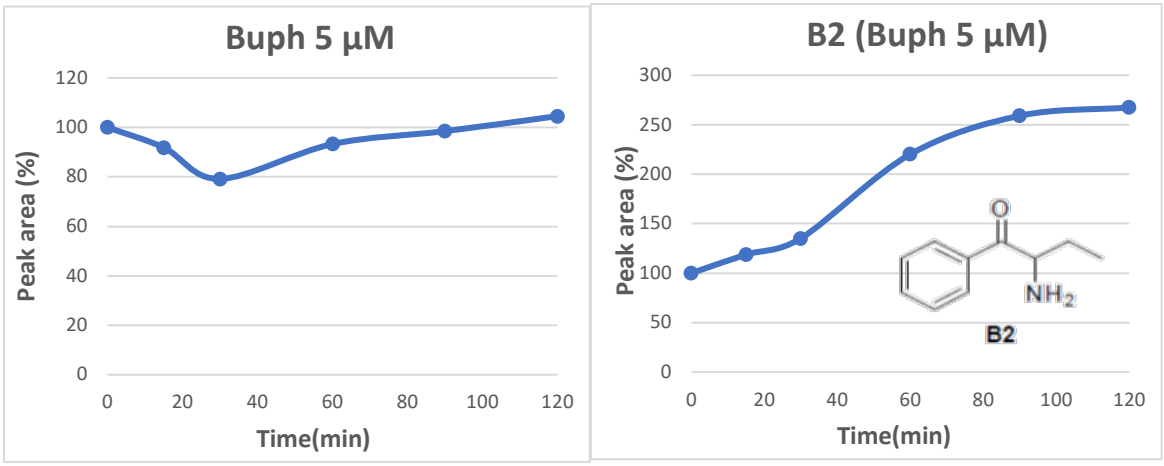

Figure 4.33 Buphedrone *in vitro* metabolism assay using mice liver microsomes: buphedrone content variations (left) and detected metabolite resulting from N-dealkylation (B2, right). Results, obtained from a single assay, are expressed in peak area percentage (value at time 0 assumed as 100%) over time. Initial concentration of the substrate was 5 μM.

The evaluation of the N-ethyhexedrone content in samples collected during the *in vitro* metabolism study with mice liver microsomes using 5 μM N-ethyhexedrone as substrate shows almost no variation on N-ethyhexedrone initial content (Figure 4.34). Again, like with buphedrone, when formation of N-ethyhexedrone metabolites (H1 to H5, Figure 3.1) was investigated, metabolite resulting from N-dealkylation (H2), was detected and the results suggest its formation as its amount increases along time (Figure 4.34, right). No other metabolites were detected in those assays.

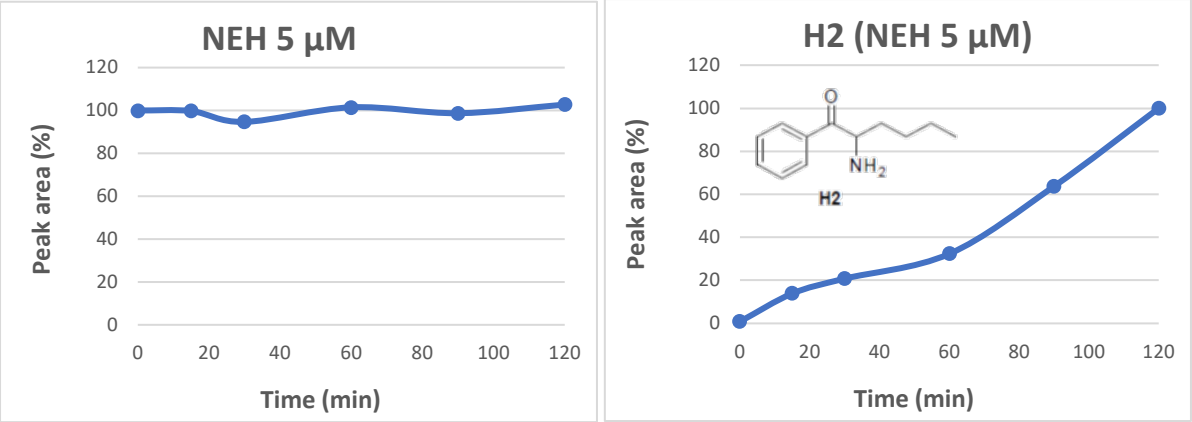

Figure 4.34 N-ethylhexedrone *in vitro* metabolism assay using mice liver microsomes: N-ethylhexedrone content variation (left) and detected metabolite resulting from N-dealkylation (H2, right). Results, obtained from a single assay, are expressed in peak area percentage (value at time 120 assumed as 100% for metabolite H2) over time. Initial concentration of the substrate was 5 µM.

These preliminary results obtained in the *in vitro* metabolism studies with mice liver microsomes show that even at very low concentrations, the metabolites resulting from N-dealkylation, B2 and H2, are detected and their amount appears to increase along time. However, no significant decrease in the substrate initial concentration was observed. No other investigated metabolite was formed in detectable amounts. For a better understanding of the metabolism processes that seems to be occurring in the microsomal reaction mixture at this substrate concentration, it would be necessary to carry out further assays in order to observe either the decrease of the substrate or the formation of any other metabolite. Because the amounts of compounds that were being detected were near the limit of quantification it was decided to repeat the microsomal metabolism studies at increased initial substrate concentrations.

In the assays performed with substrate concentrations of 10 µM for both buphedrone (Figure 4.35) and N-ethyhexedrone (Figure 4.36) we observed again the formation of metabolites resulting from N-dealkylation: B2 and H2. The detected presence of B2 metabolite at time 0, corresponded to 0.02% of the parent compound, buphedrone. No other investigated metabolites were detected.

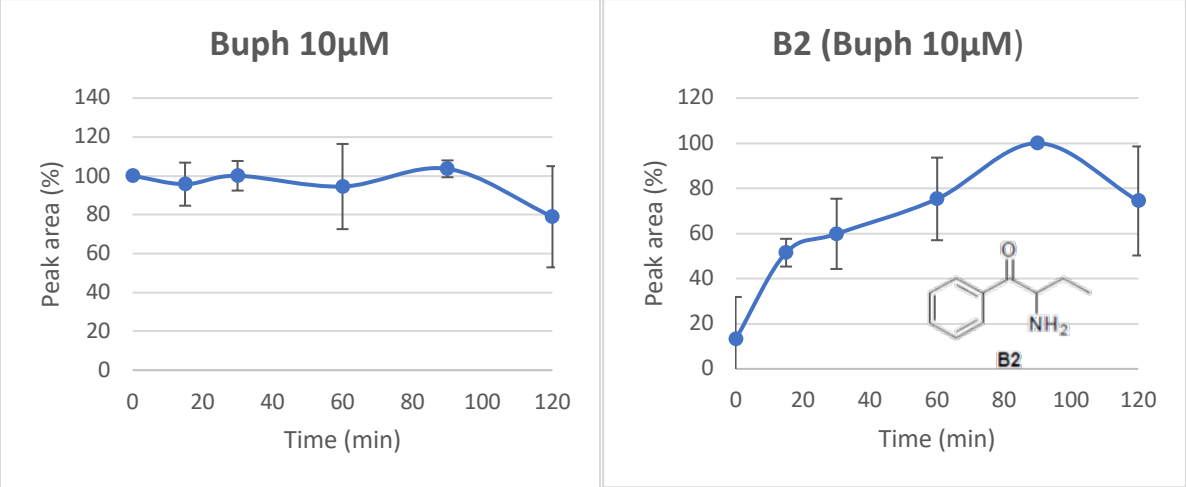

Figure 4.35 Buphedrone *in vitro* metabolism assay using mice liver microsomes: Buphedrone content variations (left) and detected metabolite resulting from N-dealkylation (B2, right) (results expressed as percentage of peak area and presented as average ± stdev, were obtained from duplicate assay; for metabolite B2 the highest value at time 90 assumed as 100%). Initial concentration of the substrate was 10 μM.

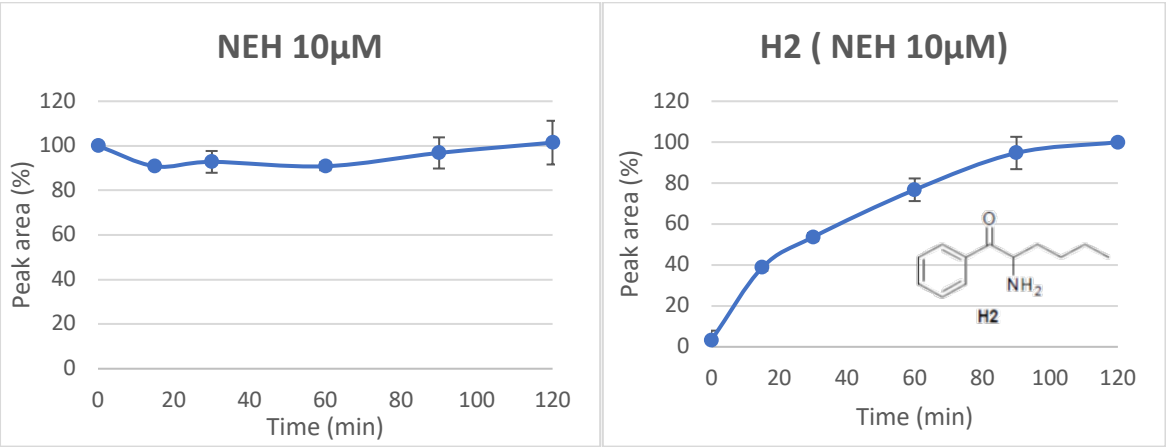

Figure 4.36 N-ethylhexedrone *in vitro* metabolism assay using mice liver microsomes: N-ethylhexedrone content variation (left) and detected metabolite resulted from N-dealkyation (H2, right) (results expressed as percentage of peak area and presented as average ± stdev, were obtained from duplicate assay; for metabolite H2 the highest value at time 120 assumed as 100%). Initial concentration of the substrate was 10 μM.

In order to further evaluate the mice microsomal metabolism of buphedrone and N-ethylhexedrone three assays were performed at initial concentration of 15 μM of substrate

(each parent compound), expecting to detect the formation of any other of the predicted metabolites, apart from the B2 and the H2.

The evaluation of the buphedrone content (15 μM) in samples collected during the *in vitro* metabolism study with mice liver microsomes using buphedrone as substrate shows almost no variation on buphedrone content (Figure 4.37), with exception at the end of the experiment, after 2h, the amount of the substance decreased by 9% of the initial amount (see Table 4.6) but with no statistical significance (p=0,29).

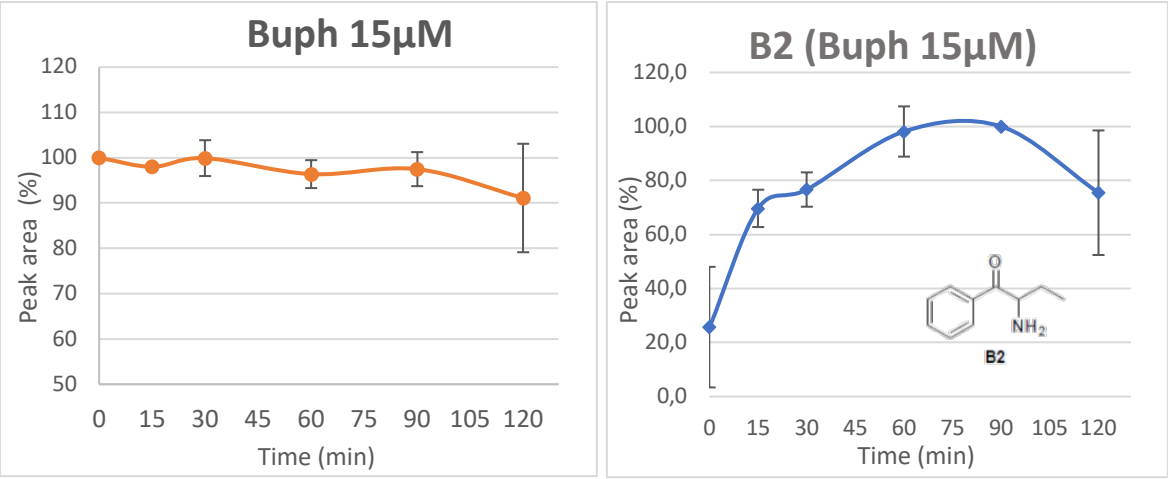

Figure 4.37 Buphedrone *in vitro* metabolism assay using mice liver microsomes: Buphedrone content variations (left) and detected metabolite resulting from N-dealkylation (B2, right) (results expressed as percentage of peak area and presented as average ± stdev, were obtained from duplicate assay; for metabolite B2 the highest value at time 90 assumed as 100%). Initial concentration of the substrate was 15 μM.

When we searched for metabolites that could be formed from buphedrone (B1 to B4), only the presence of the metabolite resulting from N-dealkylation, B2, was found (Figure 4.37, right) (and its assessed amounts in each sample suggest formation of the metabolite B2, in both analyzed assays (in one assay it was not possible to detect any metabolites). After around 60min the amount of the metabolite becomes stable reaching its peak of formation at 90 min. The maximum amount detected of B2 metabolite corresponds to 0.14% of the parent compound, buphedrone. One of the possible explanations for the decreasing rate of formation of metabolite B2 after 90 min can be the saturation of the enzymes. The detected presence of B2 metabolite at time 0, corresponded to 0,03% of the parent compound, buphedrone. No other metabolite, out of the synthetized ones, was formed in detectable amounts.

The evaluation of the N-ethylhexedrone (15μM) content in samples collected during the *in vitro* metabolism study with mice liver microsomes using N-ethylhexedrone as substrate shows almost no variation on N-ethylhexedrone content (Figure 4.38) At the end

of the assay the amount of the substrate still present in the sample was 97.35% of the initial amount (see Table 4.6) but with no statistical significance (p=0.24).

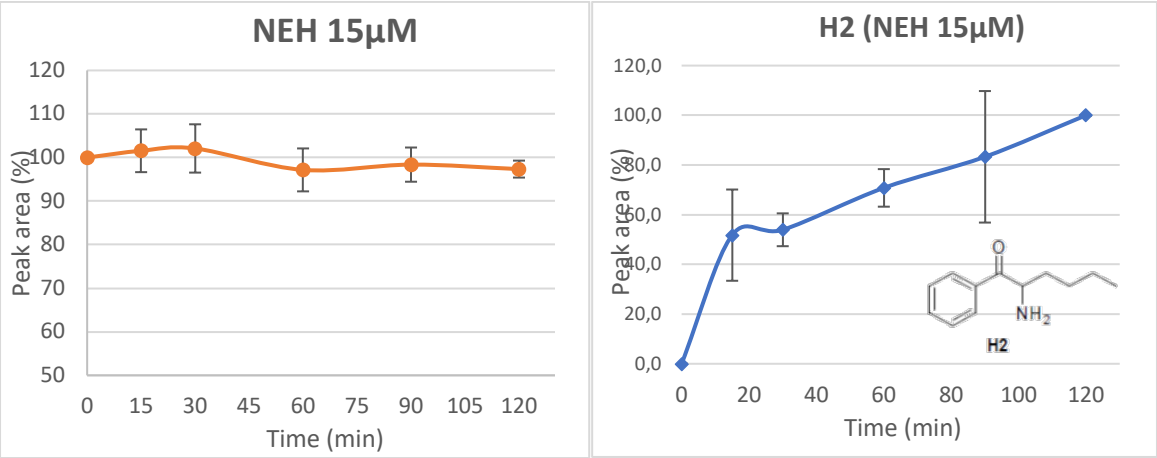

Figure 4.38 N-ethylhexedrone *in vitro* metabolism assay using mice liver microsomes: N-ethylhexedrone content variation (left) and detected metabolite resulted from N-dealkylation (H2, right) (results expressed as percentage of peak area and presented as average ± stdev, were obtained from duplicate assay; for metabolite H2 the highest value at time 120 assumed as 100%) over time. Initial concentration of the substrate was 15 µM.

When the formation of N-ethylhexedrone metabolites was investigated, only the metabolite resulting from keto-reduction (H1) and that resulting from N-dealkylation (H2) were detected among all the selected and studied N-ethylhexedrone metabolites (H1 to H5, Figure 3.1). Assessed amounts of metabolite H2 in each time sample (Figure 4.38) suggest its formation as its rate of formation is increasing throughout the whole duration of the assay. The maximum amount detected of H2 metabolite corresponding to 0.29% of the parent compound, N-ethylhexedrone. One of the three assays was excluded because no metabolites were found.

Assessed amounts of the metabolite resulting from keto-reduction (H1) in each time sample (Figure 4.39) suggest its formation from time 30 min with an increasing rate of formation with a maximum at 120 min. The maximum amount detected of formed H1 metabolite seems to be slightly lower than formed metabolite H2, corresponding to 0.21% of the parent compound N-ethylhexedrone. No other metabolite, out of the synthetized ones, was formed in detectable amounts during the in vitro metabolism assays with mice microsomes.

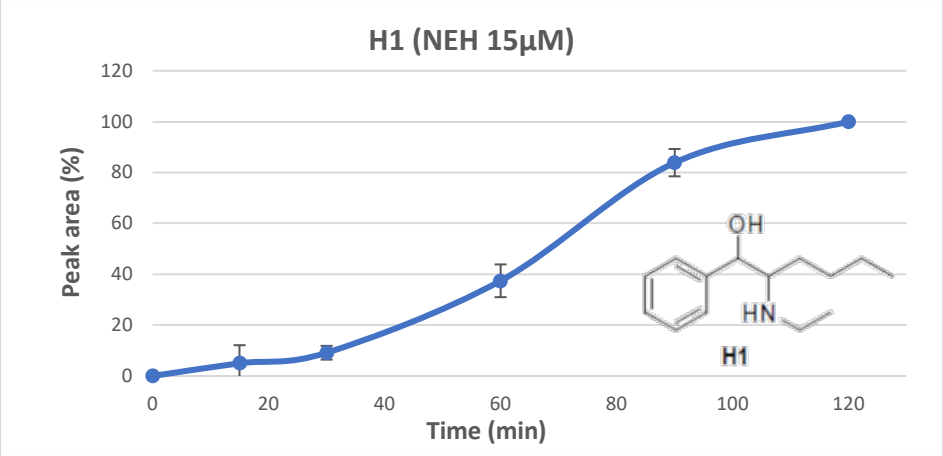

Figure 4.39 Formation of the metabolite resulting from β-keto reduction (H1) in the N-ethylhexedrone *in vitro* metabolism assay using mice liver microsomes (results expressed as percentage of peak area and presented as average ± stdev, were obtained from a duplicate assay, for metabolite H1 the highest value at time 120 assumed as 100%) over time. Initial concentration of the substrate N-ethylhexedrone was 15 μM

When comparing the amount of metabolites resulting from N-dealkylation of either buphedrone (B2) or N-ethylhexedrone (H2) (both formed under the same conditions: 120 min duration of in vitro metabolism using MLM) (Figure 4.40) it was noticed that the rate of formation of the N-ethylhexedrone H2 was relatively higher than that of buphedrone metabolite B2. Both seem to reach a stable level after 90min. Although it seems that the rate of disappearance of N-ethylhexedrone is smaller than that of buphedrone, relatively higher amount of the substrate H2, resulting from N-dealkylation, is observed (Figure 4.40). The rate of formation of the metabolite seems to stabilize after 90min. This might be caused by the saturation of the microsomal enzymes and their decreased activity over time, as 120 min was the maximum time of the microsomal assay suggested by the manufacturer.

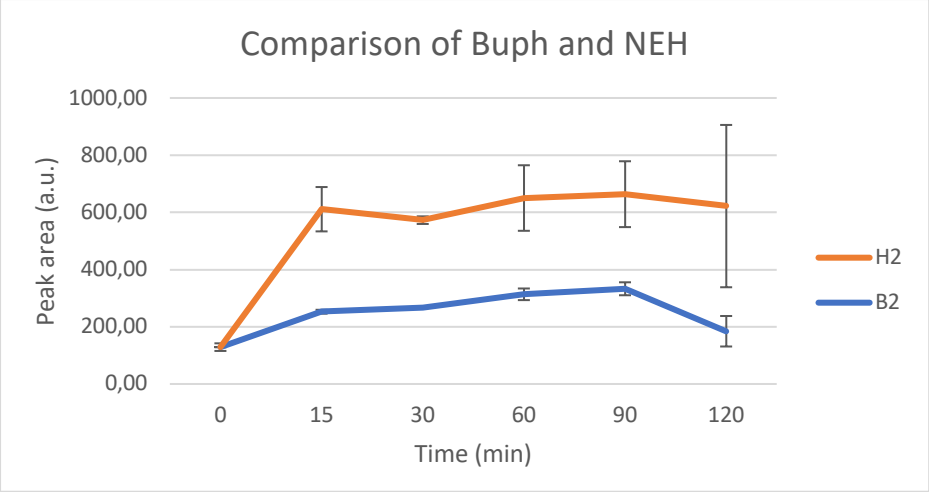

Figure 4.40 Variation of formed N-dealkylated metabolites B2 and H2. Start substrate concentrations of 15μM (results expressed as the peak area (a.u.) and presented as average ±SDEV. Data corresponds to the results obtained from 2 independent assays for both substrates.

4.4.2 Microsomal metabolism studies with mice liver microsomes using N-ethylhexedrone beta-keto-reduced metabolite as a substrate

In order to evaluate the microsomal stability and find other metabolites of the parent drug N-ethylhexedrone, as well as to observe further changes that might happen to the molecule in a prolonged period of time (more than 2 h), the metabolites detected in the previous assays resulting from β-keto-reduction (H1) and N-dealkylation (H2) were investigated in *in vitro* metabolism studies with MLM in the same way as the parent compound, N-ethylhexedrone, was investigated and at the same concentration, 15 μM. When the metabolite H1 was used as substrate, a steady decrease in the amount of substrate during the whole time of the assay was noticed (Figure 4.41). The amount of the compound after 120 min decreased to 88% of the initial amount (see Table 4.6), which suggests that it can be more easily metabolized in those conditions than N-ethylhexedrone. Among all searched metabolites (H2-H5, Figure 3.1), only the metabolite resulting from oxidation of the benzene ring in the *para* position (H4) was detected. The amount of metabolite H4 seems to be increasing during the whole duration of the assay (Figure 4.41) suggesting that it is been formed during the microsomal assay. The formation of this H4 metabolite has been seen previously, during the plasma stability assay.

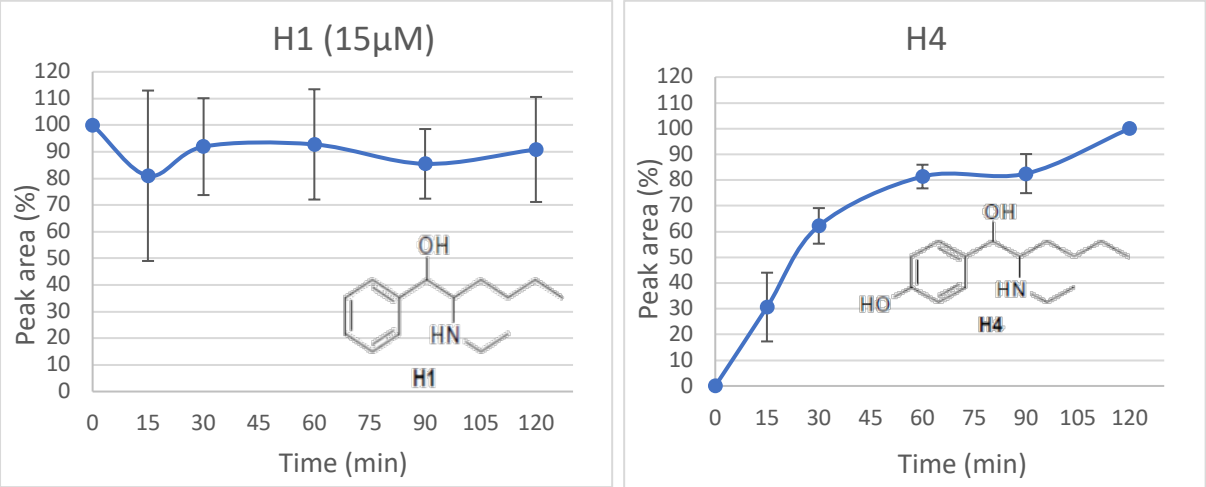

Figure 4.41 ***In vitro*** **metabolism assay of the β-keto-reduced N-ethylhexedrone metabolite (H1) using mice liver microsomes: H1 content variation (left) and detected metabolite resulted from hydroxylation in the** ***para*** **position (H4, right) (results expressed as percentage of peak area and presented as average ± stdev, were obtained from duplicate assay; for metabolite H4 the highest value at time 120 assumed as 100%) over time. Initial concentration of the substrate was 15 µM.**

4.4.3 Microsomal metabolism studies with mice liver microsomes using N-ethylhexedrone N-dealkylated metabolite as a substrate

Because the metabolite formed by dealkylation of N_ethylhexedrone (H2), was the metabolite that was detected in most cases of both the *in vitro* metabolism and the stability studies, a further investigation of that compound's metabolism was carried out using MLM. The study investigating the N-dealkylated metabolite H2 indicates a steady decrease in the amount of substrate (Figure 4.42), resulting in the presence of 87% of the initial amount of the compound after 120 min (see Table 4.6). Among all available metabolites (H1-H5, Figure 3.1) only one was detected, the metabolite resulting from reduction of the β-keto group (H3). As this is a spontaneous reaction for many cathinones, the presence of that metabolite can be seen already at the time 0 (Figure 4.42). It might have already been in the sample as a contamination or product of spontaneous degradation. The detected amount of H3 metabolite at time 0, corresponded to 1.09% of the parent compound, H2. This result might suggest that the sample has already undergo some level of degradation before being analyzed. However, an increase to about 143% of the initial value can be noticed in the assay, which indicates that the metabolite is also formed as a result of microsomal activity.

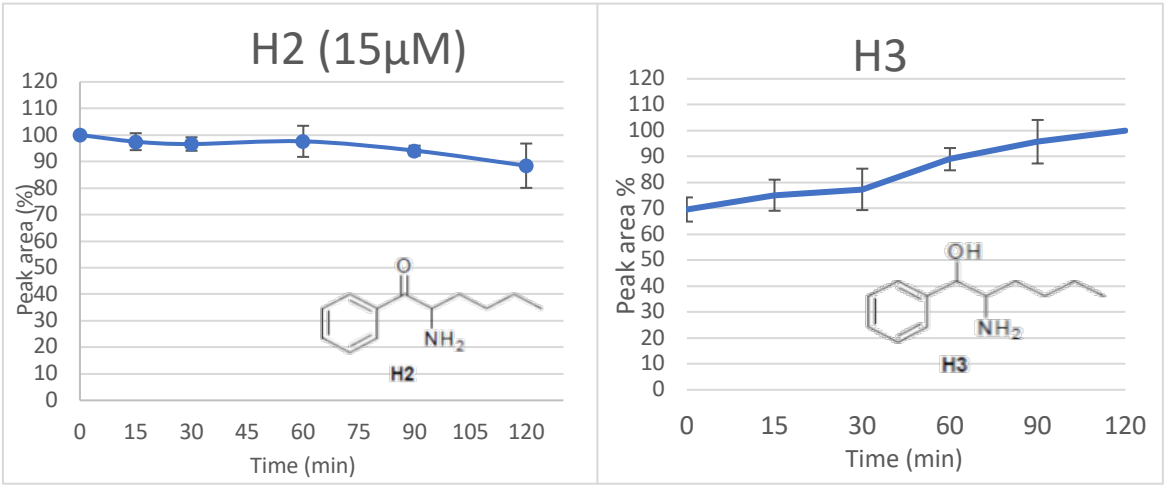

Figure 4.42 ***In vitro*** **metabolism assay of the N-dealkylated N-ethylhexedrone metabolite (H2) using mice liver microsomes: H2 content variation (left) and detected metabolite resulted from β-keto-reduction (H3, right) (results expressed as percentage of peak area and presented as average ± stdev, were obtained from duplicate assay; for metabolite H3 the highest value at time 120 assumed as 100%) over time. Initial concentration of the substrate was 15 µM.**

In order to confirm the stability of the metabolites compounds used as substrate in the in vitro metabolism studies with MLM, both metabolites, H1 and H2, were also incubated (37ºC) in 20% PBS during the time of 120 min (Table 4.2). For the metabolite resulting from NEH β-keto-reduction (H1) we can observe a slight decrease of the amount over time, but no metabolites were detected. For the N-dealkylated metabolite (H2) there was also a decrease of the amount of the substrate in time and the presence of metabolite H3 was detected at all time-points, which might confirm that it was already present in the sample as a contamination or product of spontaneous degradation. There is almost no noticeable decrease in sample with microsomes without cofactors.

4.4.4 Microsomal metabolism studies with human liver microsomes using buphedrone and N-ethylhexedrone as substrates

When buphedrone metabolism was evaluated through in vitro metabolism studies using HLM instead of MLM, the evaluation of the buphedrone content in samples collected during the study using 15 µM buphedrone as substrate shows almost no variation on buphedrone content (Figure 4.43**Error! Reference source not found.**), with exception of a 20% decrease of the initial amount at time 60 min, which could be an artifact, as the STDEV for this time-point was high and is not statistically different from the others. Similar results were obtained when N-ethylhexedrone was used as substrate at initial concentration of 15 µM

(Figure 4.44**Error! Reference source not found.**). In both cases we did not observe a significant decrease in the amount of the substrate in time.

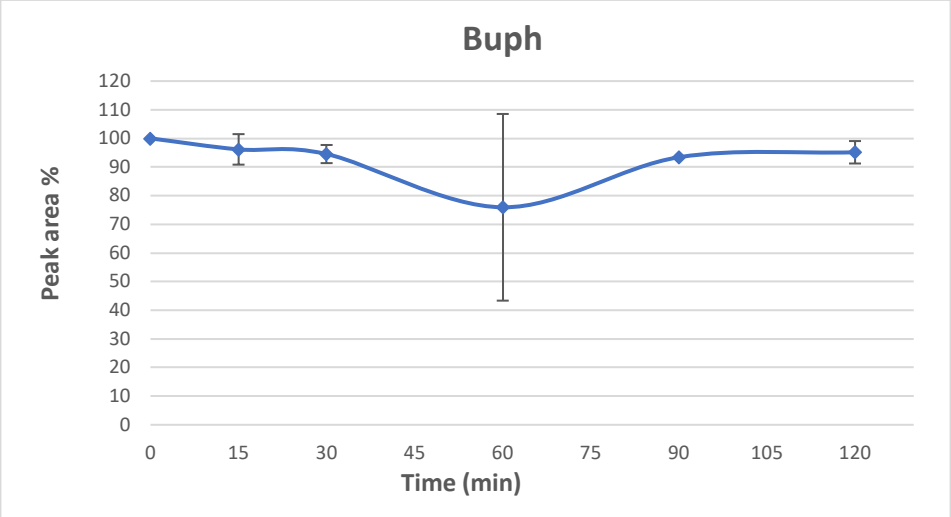

Figure 4.43 Buphedrone content variation during *in vitro* metabolism assay using human liver microsomes. Results expressed as percentage of peak area and presented as average ± stdev, were obtained from duplicate assay. Initial concentration of the substrate was 15 μM.

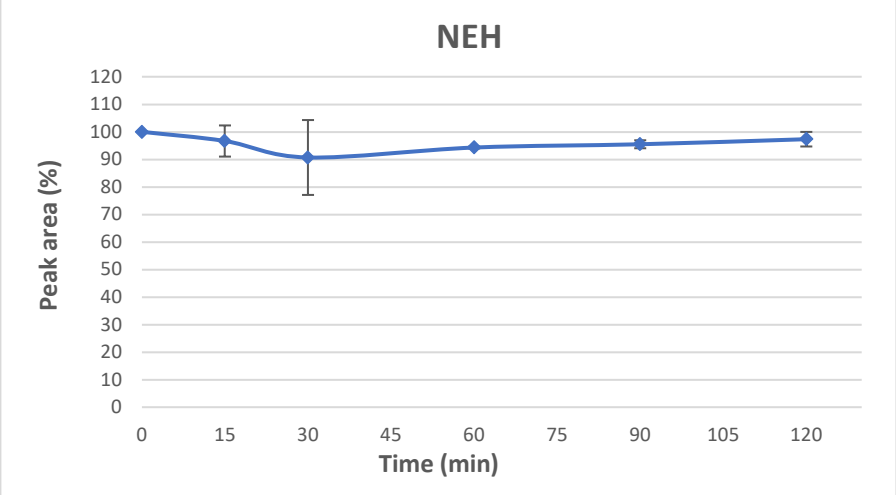

Figure 4.44 N-ethylhexedrone content variation during *in vitro* metabolism assay using human liver microsomes. Results expressed as percentage of peak area and presented as average ± stdev, were obtained from duplicate assay. Initial concentration of the substrate was 15 μM.

When searching form metabolites, only for N-ethylhexedrone we were able to detect the metabolite formed by the reduction of the β-keto group (H1), out of all the metabolites synthetized (Figure 4.45). The formation of this metabolite H1 was detected both in the testing sample as well as in the negative control. The maximum amount of metabolite H1 detected in

the microsomal mixture (testing sample), was at time 120 min, and corresponds to 0,38% of the initial value of N-ethylhexedrone and 152% more than the maximum amount detected in the negative control. We can assume that the metabolite H1 is partially spontaneously formed in the in vitro microsome metabolism used conditions (pH 7.4, 37ºC) after 60min.

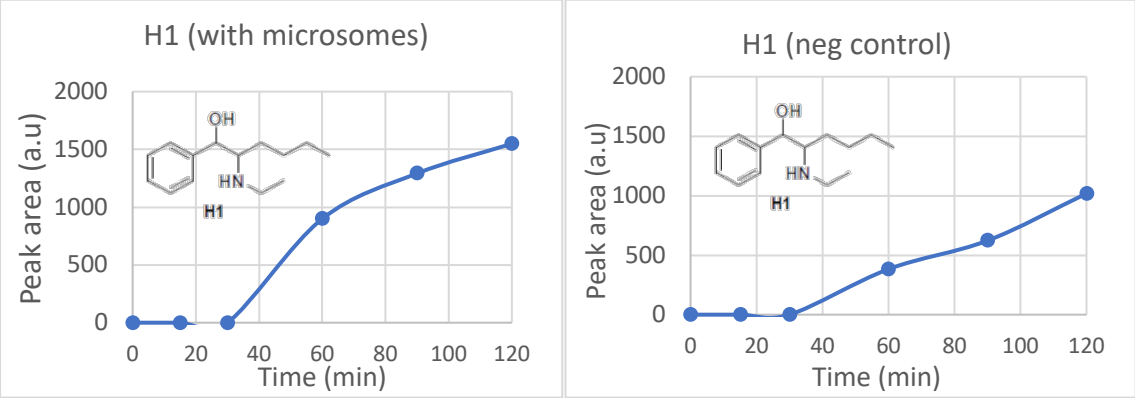

Figure 4.45 Metabolite H1 content variation during in vitro metabolism assay using human liver microsomes (left) and in the negative control without cofactors (right). Results expressed in peak area (a.u.) over time were obtained from a single assay. Initial concentration of the substrate was 15 μM.

Table 4.6 Percentage of the initial amount of substrate remaining in the microsomal reaction mixture after 2h.

	Mice 2h (15μM)	Mice 2h (10μM)	Mice 2h (5μM)	Human 2h (15μM)
% Buph	91.1	78.9	104.6	99.0
% NEH	97.4	101.4	102.7	100.6
% H1	88.2	-	-	-
% H2	87.3	-	-	-

To summarize the results obtained in the carried out *in vitro* metabolism studies, in case of N-ethylhexedrone, the metabolite that was mainly formed by the activity of mice microsomes was the β-keto reduced metabolite (H1), but the amount of the N-dealkylated metabolite H2 detected was only slightly lower. Further investigation of metabolism of the two forming compounds, β-keto reduced H1 and N-dealkylated H2, showed that in an *in vitro* study with mice microsomes metabolite H2 undergoes β-keto reduction giving rise to metabolite H3 and the metabolite H1 is further metabolized by hydroxylation of the aromatic ring in the *para* position giving rise to metabolite H4. The results roughly correspond to those obtained in literature (Uralets et al., 2014; Zaitsu, 2018), but with pathway presented on the Figure 4.46.

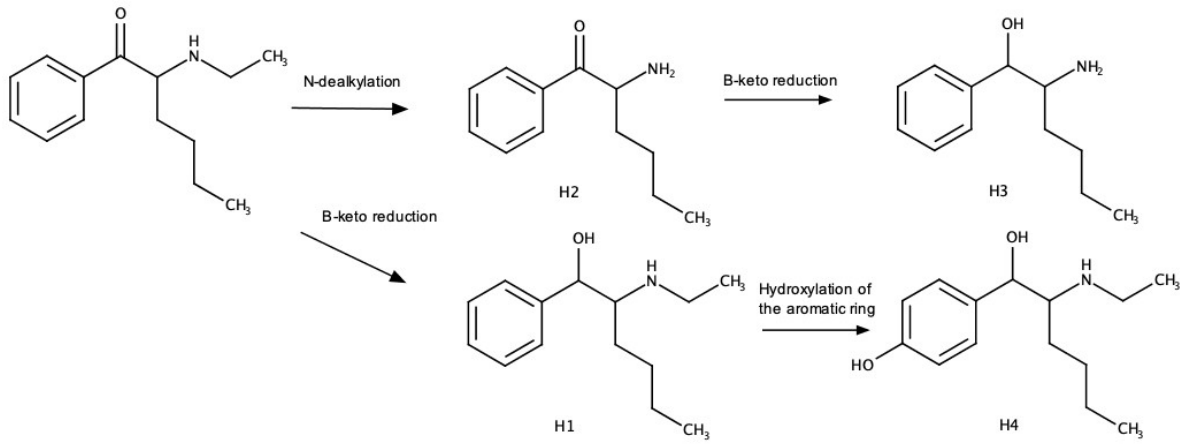

Figure 4.46 Proposed metabolic pathway of N-ethylhexedrone in mice liver microsomes as predicted by the carried-out in vitro metabolism experiments

Summarizing the metabolism studies using human microsomes instead of mice, only a very low amount of metabolite the β-keto reduced metabolite (H1) was detected. Additionally, its presence was also detected in the negative control, without microsomes co-factors, run at the same time, what might suggest that under those conditions used in the experiment, spontaneous formation of this product can occur, just as predicted by Zaitsu and Uralets (Uralets et al., 2014; Zaitsu, 2018). Uralets also found that this metabolite is found in human urine as a primary compound for this group of N-alkylated synthetic cathinones, and is more abundant than the parent drug, although the times of ingestion of the drugs were not known, that is why it is difficult to compare that data with the results obtained in our assays. Additionally, metabolites formed by β-keto reduction (H1) and N-dealkylation (H2), appear to be metabolized at the similar rate in mice microsomes (in both cases 88% of the initial sample present after 2 h). A rapid disappearance of metabolite H2 at 37ºC in PBS has also been observed with only 19% of the initial substrate remaining after 48 h in the sample. This could be caused by the fact that H2 is a primary amine and might behave differently in that environment, but it is only an assumption.

Uralets and colleagues (2014) have also shown that side chain substituted cathinones, such as buphedrone and N-ethylhexedrone, when metabolized by human organism, they primarily undergo β-keto reduction, followed by N-dealkylation, and little or no parent compound is detected in the urine sample. This was not confirmed in the assay carried out with human liver microsomes in our laboratory. We did not manage to observe formation of any of those metabolites in case of buphedrone and we detected only a very small amount of metabolite resulting from reduction of the β-keto group of N-ethylhexedrone (H1). Also, both compounds were very stable until up 2 hours of the duration of the experiment. This might

suggest that formation of those metabolites detected by Uralets is caused by some other enzymes or liver fraction that was not present or active in our assay, longer duration of the process or modified conditions that are different in the body, such as pH and temperature.

While investigating buphedrone, we have not observed formation of metabolites other than resulting from N-dealkylation (B2), out of the selected ones, in the assays with mice liver microsomes, and no metabolites were found in the assay with human liver microsomes, although they have been previously detected in human biological samples (Uralets et al., 2014). This might be caused by a short duration of the microsomal test (2h) and the fact that HLM do not reflect the whole complex metabolism that takes place in the human body.

The Table 4.6 shows that the optimal concentration of the substrate in mice microsomal assays seems to be 15 μM, because the values obtained in other assay do not always show disappearance of the substrate along time or induce a significant error, so this concentration is suggested for further investigation of the metabolism of those type of compounds in mice and human liver microsomes.

It is important to remember that the table only represents stability of the selected compounds in isolated environments (PBS and plasma) and does not fully depict the metabolism that can occur in living organisms.

5

5 Conclusions

According to the literature, the primary reactions of Phase I metabolism, both for buphedrone and N-ethylhexedrone, are N-dealkylation or β-keto reduction. The β-keto reduced form can also undergo further N-dealkylation or, less probable, hydroxylation in the *para* position of the aromatic ring (Uralets et al., 2014; Zaitsu, 2018). The same was also predicted by SmartCyp and XenoSite. Both programs indicated N-dealkylation as the most probable reaction. In case of buphedrone, first analysis in SwissADME tool predicted the substance as a possible CYP1A2 inhibitor. SmartCyp predicted that the N-dealkylation reaction mentioned in literature may be catalysed by the systems 3A4, 2D6 and 2C9. XenoSite provided even more detailed analysis listing specific cytochromes 1A2, 2A6, 2B6, 2C19, 2C8, 2C9,2D6, 3A4 and HLM as the ones responsible for dealkylation. In the BioTransformer analysis only one metabolite formed from N-dealkylation is present in the results and in that case also CYP1A2 is listed as a possible catalyst for the reaction, but the metabolite differs from what was predicted in the literature and by other prediction tools.

N-ethylhexedrone has been indicated by SwissADME as inhibitor of both CYP1A2 and CYP2D6, whereas SmartCyp predicted is as a substrate for CYP3A4 and CYP2C9. XenoSite also detected a higher probability of the reaction beings being carried out by the CYP3A4 family, with also possible 2C9 and 2C19 activity. Dehydrogenation, reduction and stable oxydation were the most probable reactions predicted by the XenoSite rainbow prediction, which corresponds to the literature prediction and metabolites observed *in vivo.* N-Dealkylation was also predicted by BioTransformer, but with a different mechanism that was not found in literature nor in other *in silico* prediction tools.

To evaluate the programs, it seems that XenoSite tool provided the most accurate and detailed analysis, corresponding to what was predicted in literature and later observed in *in vivo* and *in vitro* models. It also performed very well mapping the active sites of the molecule and predicting possible reaction sites for each enzyme family. BioTranformer seems to provide the least accurate analysis, as none of the metabolites predicted by that program were found in literature nor in any other prediction program or in the *in vitro* models. Interestingly, out of all the programs used, only XenoSite Rainbow Phase I prediction indicated reduction of the β-keto group as a possible reaction, although it was the first reaction mentioned in the literature (Uralets et al., 2014; Zaitsu, 2018) and it was also observed in *in vitro* assays performed for this study.

In the *in vitro* models we have observed that both buphedrone and N-ethylhexedrone are metabolized by liver microsomes only to a small degree, which might suggest that they are mostly excreted unchanged in urine, which was also suggested by literature (Pedersen et al., 2012; Uralets et al., 2014).

In all performed mice liver microsome assays, even the ones with the lowest concentration of 5 μM, metabolites resulting from N-dealkylation were found to be present and formed rather quickly (we usually noticed the formation of metabolites after 15min, although sometimes they were already present at time zero). Additionally, those metabolites appear to be more stable in 20% PBS and in blood plasma than their parent compounds (Table 4.2 and 4.7). Just as it was suggested by Uralets (Uralets et al., 2014) those metabolites seem to be better markers in biological samples than their parent compounds, especially when presence in blood is to be detected and when the time of consumption is not known.

The only metabolites that were detected in the mice liver microsome assay, formed from the parent compounds, buphedrone and N-ethylhexedrone, were the ones resulting from primary reduction (H1) and N-dealkylation (B2 and H2). This might be due to the short time of activity of the microsomes (120 min). However, when mice microsomal assay was performed using the β-keto reduced (H1) and N-dealkylated (H2) metabolites as substrates, we could detect further the metabolites resulting from subsequent β-keto reduction (H3) and hydroxylation in the para position of the aromatic ring (H4) to be formed, respectively, which roughly corresponded to the pathways predicted by literature (Pedersen et al., 2012; Meyeret al., 2010; Zawilska, 2018).

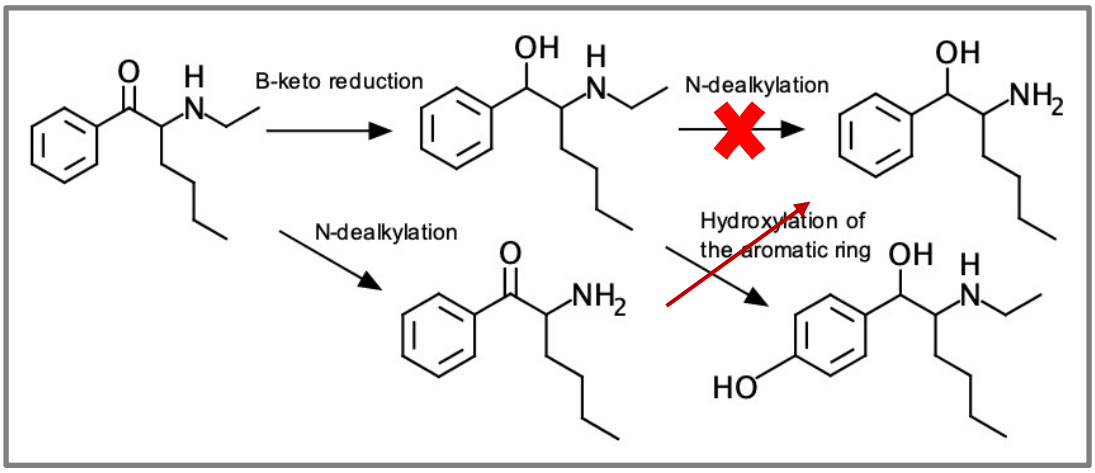

Figure 5.1 Comparison of the primarily predicted pathway for N-ethylhexedrone with the reactions actually observed in the *in vitro* mice microsomal assay

Further investigation of the metabolic pathway of buphedrone, similar to the one carried out for N-ethylhexedrone and its metabolites, is necessary, as in our laboratory we did not have buphedrone's metabolites available to carry out further assays. Moreover, different methods of compound identification, such as mass spectrometry and elucidation of the structures via fragmentation patterns should be carried out in order to find metabolites of parent compounds buphedrone and N-ethylhexedrone, other than looked for in this study, that can be formed from degradation of those drugs.

APPENDIX 1 – Structures of selected synthetic cathinones

Structure	Common name	Compound
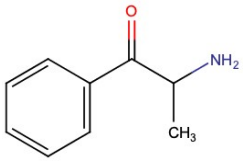	Cathinone	benzoylethanamine, or β-keto-amphetamine
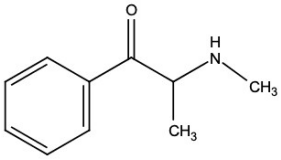	Methcathinone	α-methylamino-propiophenone or ephedrone
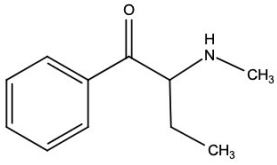	Buphedrone	α-methylamino-butyrophenone (MABP)
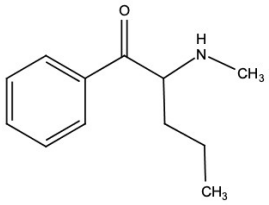	Pentedrone	α-methylamino-valerophenone
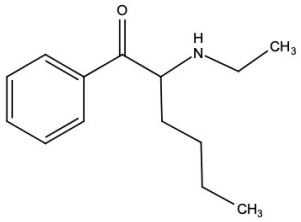	Hexen, NEH	N-ethylhexedrone

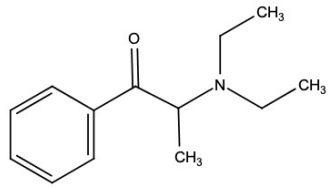	Diethylpropion	Amfepramone
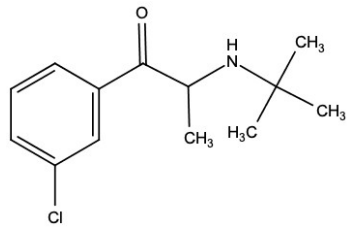	Bupropion	Amfebutamone; 3-Chloro-N-tert-butyl-β-keto-α-methylphenethylamine
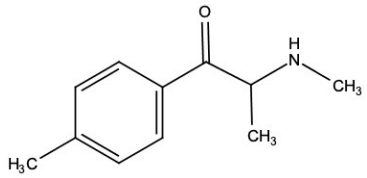	Mephedrone	4-methyl methcathinone (4-MMC)
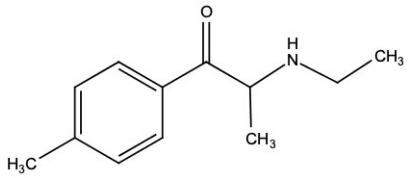	4-MEC	4-Methylethcathinone
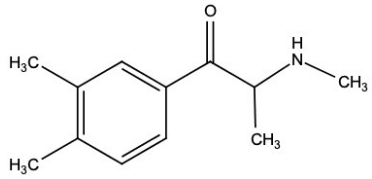	3,4-DMMC	3′,4′-dimethylmethcathinone
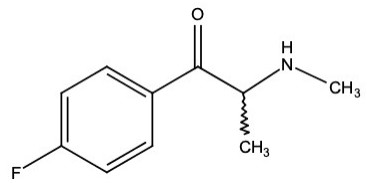	Flephedrone, 4-FMC	4-fluoromethcathinone

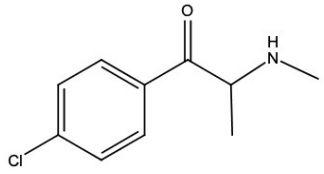	Clephedrone	4-Chloromethcathinone
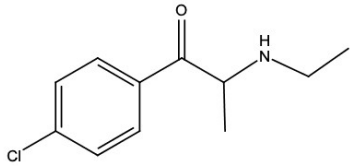	4-CEC	4-Chloroethcathinone
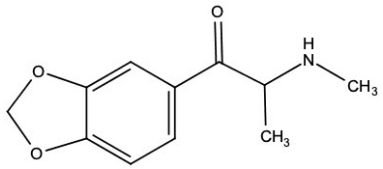	Methylone	3,4-methylenedioxy-N-methylcathinone", "MDMC", "βk-MDMA
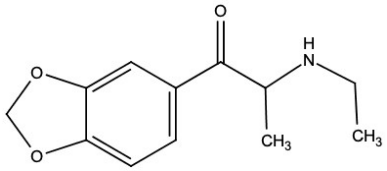	Ethylone	3,4-methylenedioxy-N-ethylcathinone (MDEC, βk-MDEA
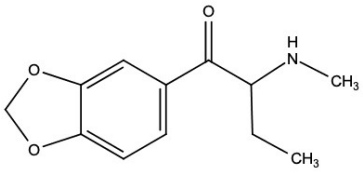	Butylone	β-keto-N-methylbenzodioxolylbutanamine (βk-MBDB)
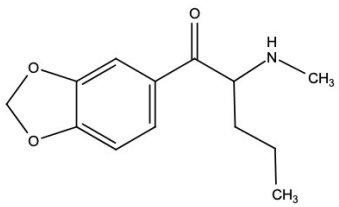	Pentylone	β-Keto-Methylbenzodioxolyl pentanamine, βk-Methyl-K, βk-MBDP
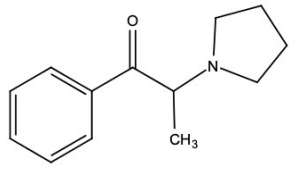	α-PPP	α-Pyrrolidinopropiophenone

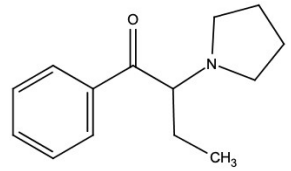	α-PBP	*alpha*-Pyrrolidinobutiophenone
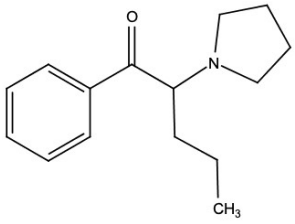	α-PVP	alpha-Pyrrolidinopentiophenone
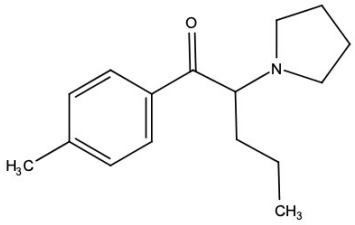	Pyrovalerone	Centroton, 4-Methyl-β-keto-prolintane
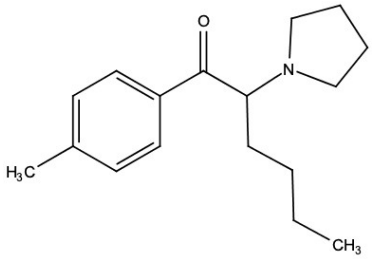	MPHP	4'-Methyl-α-pyrrolidinohexiophenone
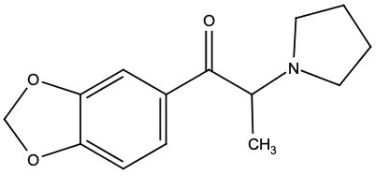	MDPPP	3',4'-Methylenedioxy-α-pyrrolidinopropiophenone
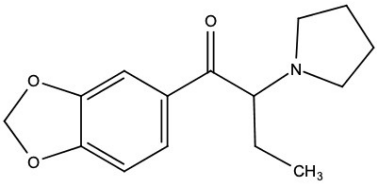	MDPBP	3',4'-Methylenedioxy-α-pyrrolidinobutyrophenone

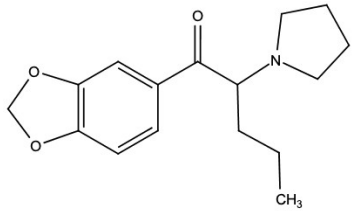	MDPV	Methylenedioxypyrovalerone
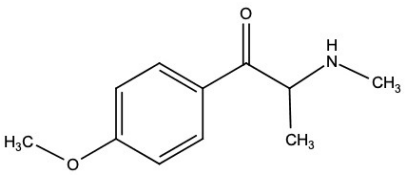	Methedrone	*para*- methoxymethcathinone

APPENDIX 2 – Structures of selected MDMA precursors and adulterants

Structure	Common Name	Compound
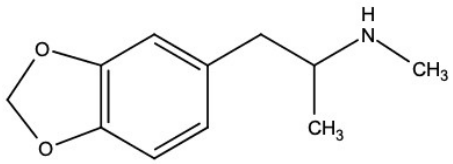	MDMA / Ecstasy	3,4-methylenedioxymethamphetamine
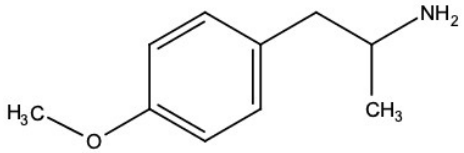	PMA	para-Methoxyamphetamine
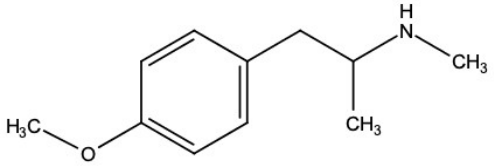	PMMA	para-Methoxy-N-methylamphetamine
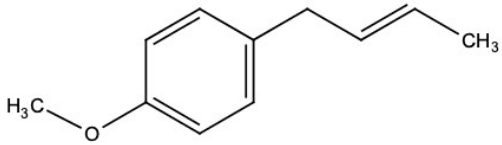	Anethole	*para*-Methoxyphenylpropene
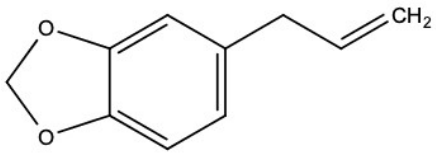	Safrole	3,4-Methylenedioxyphenyl-2-propene
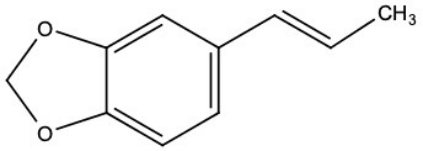	Isosafrole	3,4-Methylenedioxyphenyl-1-propene

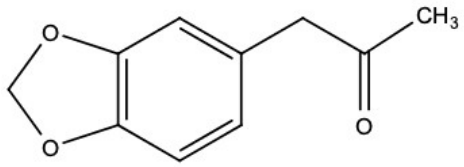	PMK	Piperonyl Methyl Ketone - 3,4-Methylenedioxyphenylpropan-2-one
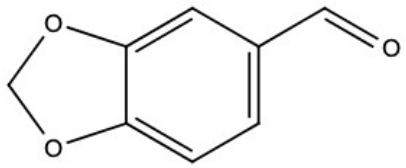	Piperonal	1,3-Benzodioxole-5-carbaldehyde
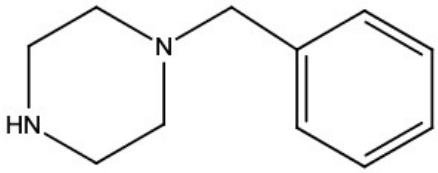	BZP	Benzylpiperazine
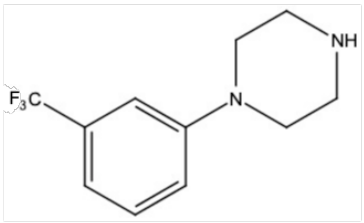	TFMPP	Trifluoromethylphenylpiperazine
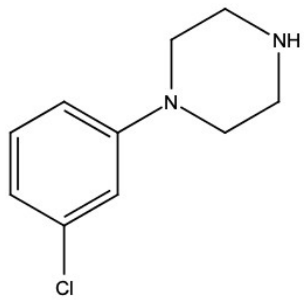	mCPP	meta-Chlorophenylpiperazine

APPENDIX 3 – Positive control studies performed during *in vitro* mice and human liver microsomal assays.

In the microsomal assays both phenacetine and propranolol were sued as positive controls, interchangeably. The phenacetine control was run 5 times and propanolol – 2 times. Although phenacetine is a known substrate of CYP1A2 isoform and propranolol of isoform CYP2D6, often the observed disappearance of the substrate was scarce (Figure VI,V, VII) even when using different starting substrate concentrations, which also corresponded to the little disappearance of the investigated compounds. As no metabolites were searched for from the positive studies, below we present the disappearance of the positive controls along the duration of the assays.

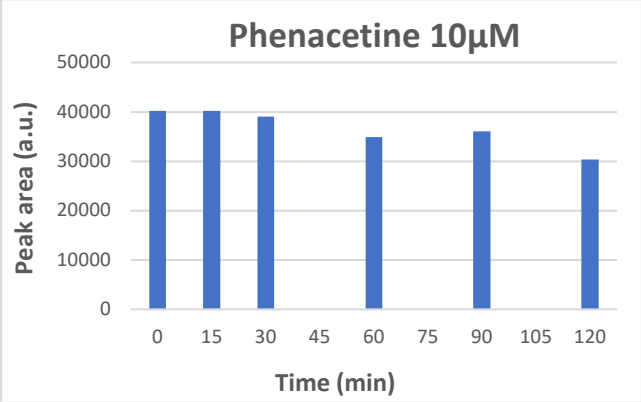

Figure I Phenacetine content variation as a positive control during the *in vitro* microsomal assay using mice liver microsomes. Results expressed as percentage of peak area (a.u.) were obtained from a single assay. Initial concentration of the substrate was 10μM.

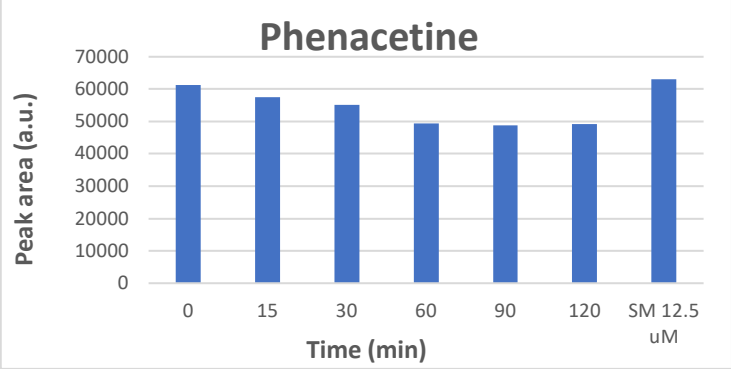

Figure II Phenacetine content variation as a positive control during the in vitro microsomal assay using mice liver microsomes. Results expressed as percentage of peak area (a.u.) were obtained from a single assay. Initial concentration of the substrate was 12,5μM and the last peak represents the dilution of the standard solution in order to simulate time zero (SM 12.5μM).

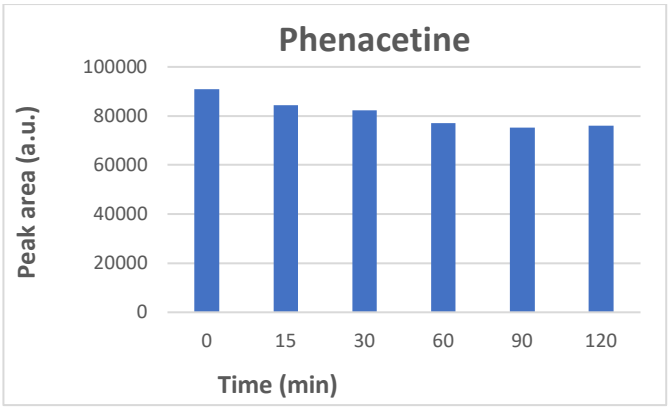

Figure III Phenacetine content variation as a positive control during the in vitro microsomal assay using mice liver microsomes. Results expressed as percentage of peak area (a.u.) were obtained from a single assay. Initial concentration of the substrate was 15μM.

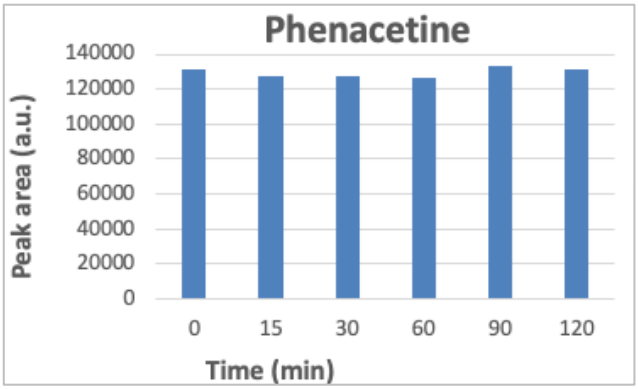

Figure IV Phenacetine content variation as a positive control during the in vitro microsomal assay using human liver microsomes. Results expressed as percentage of peak area (a.u.) were obtained from a single assay. Initial concentration of the substrate was 15μM.

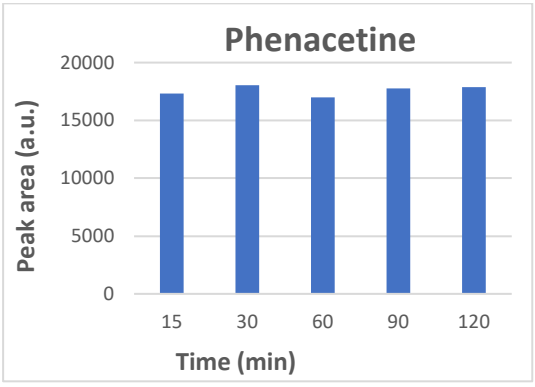

Figure V Phenacetine content variation as a positive control during the in vitro microsomal assay using human liver microsomes. Results expressed as percentage of peak area (a.u.) were obtained from a single assay. Initial concentration of the substrate was 15μM.

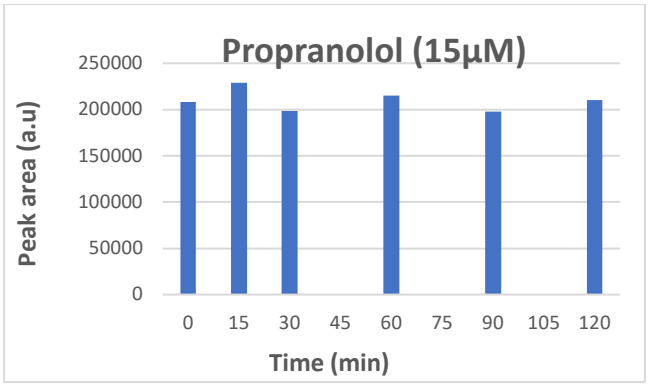

Figure VI Propanolol content variation as a positive control during the in vitro microsomal assay using mice liver microsomes. Results expressed as percentage of peak area (a.u.) were obtained from a single assay. Initial concentration of the substrate was 15μM.

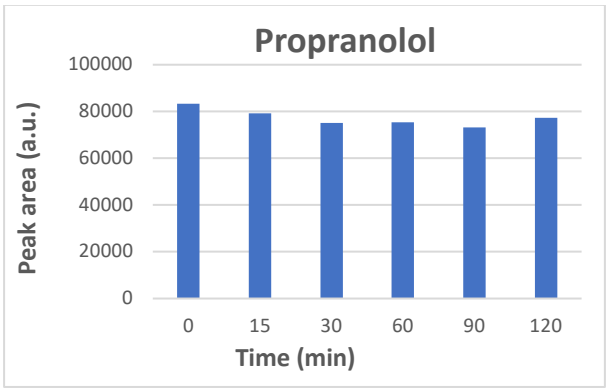

Figure VII Propanolol content variation as a positive control during the in vitro microsomal assay using mice liver microsomes. Results expressed as percentage of peak area (a.u.) were obtained from a single assay. Initial concentration of the substrate was 15μM.

Bibliography

Al-motarreb, A., Baker, K., & Broadley, K. J. (2002). *Khat : Pharmacological and Medical Aspects and its Social Use in Yemen*. *413*(April), 403–413.

Barron, L. (2015). Lack of safrole can't stop menace | Phnom Penh Post. Retrieved December 12, 2019, from The Phnom Penh Post website: https://www.phnompenhpost.com/national/lack-safrole-cant-stop-menace

Baumann, M. H., Rothman, R. B., Brandt, S. D., Ruoho, A. E., Partilla, J. S., Sink, J. R., … Shulgin, A. T. (2011). The Designer Methcathinone Analogs, Mephedrone and Methylone, are Substrates for Monoamine Transporters in Brain Tissue. *Neuropsychopharmacology*, *37*(5), 1192–1203. https://doi.org/10.1038/npp.2011.304

Baumann, M. H., Walters, H. M., Niello, M., & Sitte, H. H. (2018). Neuropharmacology of synthetic cathinones. In *Handbook of Experimental Pharmacology* (Vol. 252, pp. 113–142). https://doi.org/10.1007/164_2018_178

Bentur, Y., Bloom-Krasik, A., & Raikhlin-Eisenkraft, B. (2008). Illicit cathinone ("Hagigat") poisoning. *Clinical Toxicology*, *46*(3), 206–210. https://doi.org/10.1080/15563650701517574

Chatwin, C., Measham, F., O'Brien, K., & Sumnall, H. (2017). New drugs, new directions? Research priorities for new psychoactive substances and human enhancement drugs. *International Journal of Drug Policy*, *40*, 1–5. https://doi.org/10.1016/j.drugpo.2017.01.016

Coppola, M., & Mondola, R. (2012). 3,4-Methylenedioxypyrovalerone (MDPV): Chemistry, pharmacology and toxicology of a new designer drug of abuse marketed online. *Toxicology Letters*, *208*(1), 12–15. https://doi.org/10.1016/j.toxlet.2011.10.002

Cuimei, L., Wei, J., Tao, L., Zhendong, H., & Zhenhua, Q. (2017). Identification and analytical characterization of nine synthetic cathinone derivatives N-ethylhexedrone, 4-Cl-pentedrone, 4-Cl-α-EAPP, propylone, N-ethylnorpentylone, 6-MeO-bk-MDMA, α-PiHP, 4-Cl-α-PHP, and 4-F-α-PHP. *Drug Testing and Analysis*, *9*(8), 1162–1171. https://doi.org/10.1002/dta.2136

Daina, A., Michielin, O., & Zoete, V. (2017). SwissADME: A free web tool to evaluate pharmacokinetics, drug-likeness and medicinal chemistry friendliness of small molecules. *Scientific Reports*, *7*(March), 1–13. https://doi.org/10.1038/srep42717

Dargan, P. I., & Wood, D. M. (2013). Novel Psychoactive Substances: Classification, Pharmacology and Toxicology. In *Novel Psychoactive Substances: Classification, Pharmacology and Toxicology*. https://doi.org/10.1016/C2011-0-04205-9

EMCDDA. (2015). Injection of synthetic cathinones. *Perspectives on Drugs*. https://doi.org/10.1097/PSY.0b013e318160687c

EMCDDA. (2017). *European Monitoring Centre for Drugs and Drug Addiction (EMCDDA). High-risk drug use and new psychoactive substances.* (June). https://doi.org/10.2810/583405

Emmerson, S., & Cisek, J. (1993). Methcathinone : A Russian Designer Amphetamine Infiltrates the Rural Midwest. *ANNALS OF EMERGENCY MEDICINE*, (December).

Eshleman, A. J., Nagarajan, S., Wolfrum, K. M., Reed, J. F., Swanson, T. L., Nilsen, A., & Janowsky, A. (2018). *Structure-activity relationships of bath salt components : substituted cathinones and benzofurans at biogenic amine transporters*.

European Monitoring Centre for Drugs and Drug. (2019). European Drug Report. In *European Union Publications Office*. https://doi.org/10.1097/JSM.0b013e31802b4fda

European Monitoring Centre for Drugs and Drug Addiction. (2016). *Health responses to new psychoactive substances*. https://doi.org/10.2810/042412

European Monitoring Centre for Drugs and Drug Addiction. (2019). *EU Drug Markets Report 2019*. https://doi.org/10.2810/53181

Europol, & EMCDDA. (2005). *Joint Report on a new psychoactive substance : 4-methylmethcathinone*. 30. Retrieved from http://www.emcdda.europa.eu/system/files/publications/559/2010_Mephedrone_Joint_report_279863.pdf

Expert Committee on Drug Dependence. (2019). *Critical Review Report : N-ethylhexedrone*. (October), 21–25.

Ferreira, C., Rita, A., Florindo, P. R., Lopes, Á., Brites, D., & Quintas, A. (2019). Development of a high throughput methodology to screen cathinones ' toxicological impact. *Forensic Science International*, *298*, 1–9. https://doi.org/10.1016/j.forsciint.2019.02.022

Feunang, Y. D., Fiamoncini, J., Gil, A., Fuente, D., & Greiner, R. (2019). BioTransformer : a comprehensive computational tool for small molecule metabolism prediction and metabolite identification. *Journal of Cheminformatics*, 1–25. https://doi.org/10.1186/s13321-018-0324-5

Geisshusler, S., & Brenneisen, R. (1987). *The content of psychoactive phenylpropyl and phenylpentenyl khatamin~s in*. *19*.

Glicksberg, L., & Kerrigan, S. (2017). Stability of synthetic cathinones in blood. *Journal of Analytical Toxicology*, *41*(9), 711–719. https://doi.org/10.1093/jat/bkx071

Glicksberg, L., & Kerrigan, S. (2018). Stability of synthetic cathinones in Urine. *Journal of Analytical Toxicology*, *42*(2), 77–87. https://doi.org/10.1093/jat/bkx091

Herbert, K., Karl, Z., & Gerhard, L. (1965). *DE 1545591 Verfahren zur Herstellung von α-Aminoketonen mit heterocyclischer Aminogruppe*. Retrieved from https://worldwide.espacenet.com/textdoc?DB=EPODOC&IDX=DE1545591

Hyde, J. F., Browning, E., & Adams, R. (1928). SYNTHETIC HOMOLOGS OF d,l-EPHEDRINE. *Journal of the American Chemical Society*, *50*(8), 2287–2292. https://doi.org/10.1021/ja01395a032

Kalix, P. (1992). Cathinone, a Natural Amphetamine. *Pharmacology & Toxicology*, *70*(2), 77–86. https://doi.org/10.1111/j.1600-0773.1992.tb00434.x

Karila, L., Megarbane, B., Cottencin, O., & Lejoyeux, M. (2014). Synthetic Cathinones: A New Public Health Problem. *Current Neuropharmacology*, *13*(1), 12–20. https://doi.org/10.2174/1570159x13666141210224137

Khat is big business in Ethiopia | Africa | DW | 10.07.2019. (n.d.). Retrieved December 12, 2019, from https://www.dw.com/en/khat-is-big-business-in-ethiopia/a-49523289

King, L. A., & Kicman, A. T. (2011). A brief history of "new psychoactive substances." *Drug Testing and Analysis*, *3*(7–8), 401–403. https://doi.org/10.1002/dta.319

Knights, K. M., Stresser, D. M., Miners, J. O., & Crespi, C. L. (2016). In vitro drug metabolism using liver microsomes. *Current Protocols in Pharmacology*, *2016*(September), 7.8.1-7.8.24. https://doi.org/10.1002/cpph.9

Kovács, K., Kereszty, É., Berkecz, R., Tiszlavicz, L., Sija, É., Körmöczi, T., … Institóris, L. (2019). Fatal intoxication of a regular drug user following N -ethyl-hexedrone and ADB-FUBINACA consumption. *Journal of Forensic and Legal Medicine*, *65*(May), 92–100. https://doi.org/10.1016/j.jflm.2019.04.012

Krikorian, A. D. (1984). *Review Paper KAT AND ITS USE: AN HISTORICAL PERSPECTIVE**. *12*.

Liechti, M. E. (2015). Novel psychoactive substances (designer drugs): Overview and

pharmacology of modulators of monoamine signalling. *Swiss Medical Weekly*, *145*(January), 1–12. https://doi.org/10.4414/smw.2015.14043

Lindsay, L., & White, M. L. (2012). Toxic Highs. *Clinical Pediatric Emergency Medicine*, *13*(4), 283–291. https://doi.org/10.1016/j.cpem.2012.09.001

Litman, A., Levav, I., Saltz-Rennert, H., & Maoz, B. (1986). The use of khat. An Epidemiological Study in Two Yemenite Villages in Israel. *Culture, Medicine and Psychiatry*, *10*(4), 389–396. https://doi.org/10.1007/bf00049272

Maheux, C. R., & Copeland, C. R. (2012). Chemical analysis of two new designer drugs: Buphedrone and pentedrone. *Drug Testing and Analysis*, *4*(1), 17–23. https://doi.org/10.1002/dta.385

Majchrzak, M., Celiński, R., Kuś, P., Kowalska, T., & Sajewicz, M. (2018). The newest cathinone derivatives as designer drugs: an analytical and toxicological review. *Forensic Toxicology*, *36*(1), 33–50. https://doi.org/10.1007/s11419-017-0385-6

Meyer, M. R., Manier, S. K., Maurer, H. H., Schäper, J., & Richter, L. H. J. (2018). Different in vitro and in vivo tools for elucidating the human metabolism of alpha-cathinone-derived drugs of abuse. In *Drug Testing and Analysis* (Vol. 10). https://doi.org/10.1002/dta.2355

Meyer, M. R., & Maurer, H. H. (2010). Metabolism of Designer Drugs of Abuse: An Updated Review. *Current Drug Metabolism*, *11*(5), 468–482. https://doi.org/10.2174/138920010791526042

Meyer, M. R., Peters, F. T., & Maurer, H. H. (2008). *The Role of Human Hepatic Cytochrome P450 Isozymes in the Metabolism of Racemic 3 , 4-Methylenedioxy- Methamphetamine and Its Enantiomers ABSTRACT :* *36*(11), 2345–2354. https://doi.org/10.1124/dmd.108.021543.excluded

Mikołajczyk, A., Adamowicz, P., Tokarczyk, B., Sekuła, K., Gieroń, J., Wrzesień, W., & Stanaszek, R. (2017). Determination of N-ethylhexedrone, a new cathinone derivative, in blood collected from drivers - Analysis of three cases. *Z Zagadnien Nauk Sadowych*, *109*(july 2015), 53–63.

Mirea, M., Wang, V., & Jung, J. (2019). The not so dark side of the darknet: a qualitative study. *Security Journal*, *32*(2), 102–118. https://doi.org/10.1057/s41284-018-0150-5

Oh, J. H., Hwang, J. Y., Hong, S. I., Ma, S. X., Seo, J. Y., Lee, S. Y., … Jang, C. G. (2018). The new designer drug buphedrone produces rewarding properties via dopamine D1 receptor activation. *Addiction Biology*, *23*(1), 69–79. https://doi.org/10.1111/adb.12472

Patel, N. B. (2000). *Mechanism of action of cathinone: the active ingredient of khat (catha edulis) n. b. patel*. *77*(6), 329–332.

Pedersen, A. J., Reitzel, L. A., Johansen, S. S., & Linnet, K. (2012). In vitro metabolism studies on mephedrone and analysis of forensic cases. *Drug Testing and Analysis*, *5*(6), 430–438. https://doi.org/10.1002/dta.1369

Penner, N., Woodward, C., & Prakash, C. (2012). Appendix: Drug Metabolizing Enzymes and Biotransformation Reactions. *ADME-Enabling Technologies in Drug Design and Development*, 545–565. https://doi.org/10.1002/9781118180778.app1

PEYTON III, J., & SHULGIN, A. (1996). *Patent No. WO9639133A1*. Retrieved from https://worldwide.espacenet.com/patent/search/family/023855559/publication/WO9639133A1?q=pn%3DWO9639133

RAND Europe. (2013). *The Role of The 'Dark Web ' in the Trade of Illicit Drugs*. 8. Retrieved from https://www.rand.org/content/dam/rand/pubs/research_briefs/RB9900/RB9925/RAND_RB9925.pdf

Reed, G. A. (2016). Stability of drugs, drug candidates, and metabolites in blood and plasma. *Current Protocols in Pharmacology*, *2016*(1), 7.6.1-7.6.12. https://doi.org/10.1002/cpph.16

Rydberg, P., Gloriam, D. E., Zaretzki, J., Breneman, C., & Olsen, L. (2010). SMARTCyp: A 2D

method for prediction of cytochrome P450-mediated drug metabolism. *ACS Medicinal Chemistry Letters*, *1*(3), 96–100. https://doi.org/10.1021/ml100016x

Sikk, K., & Taba, P. (2015). Homemade Methcathinone and Permanent Neurological Damage. In *The Neuropsychiatric Complications of Stimulant Abuse* (1st ed.). https://doi.org/10.1016/bs.irn.2015.02.002

Stanley, L. A. (2017). Drug Metabolism. In *Pharmacognosy: Fundamentals, Applications and Strategy*. https://doi.org/10.1016/B978-0-12-802104-0.00027-5

Swamidass, S. J., Azencott, C. A., Lin, T. W., Gramajo, H., Tsai, S. C., & Baldi, P. (2009). Influence relevance voting: An accurate and interpretable virtual high throughput screening method. *Journal of Chemical Information and Modeling*, *49*(4), 756–766. https://doi.org/10.1021/ci8004379

Toennes, S. W., Harder, S., Schramm, M., Niess, C., & Kauert, G. F. (2003). *Pharmacokinetics of cathinone , cathine and norephedrine after the chewing of khat leaves*. 125–130.

TripSit Factsheets - Buphedrone. (2019). Retrieved December 16, 2019, from http://drugs.tripsit.me/buphedrone

TripSit Factsheets - Hexen. (2019). Retrieved December 16, 2019, from http://drugs.tripsit.me/hexen

United Nations Office on Drugs and Crime. (2018). *Global Smart Update Volumne 19: Understanding the synthetic drug market: the NPS factor*. 1–12. Retrieved from https://www.unodc.org/documents/scientific/Global_Smart_Update_2018_Vol.19.pdf

UNODC. (2015). *The Challenge of Synthetic Drugs in East and South-East Asia and Oceania Trends and Patterns of Amphetamine-type Stimulants and New Psychoactive Substances*. 35. Retrieved from https://www.unodc.org/southeastasiaandpacific/en/2015/05/regional-ats-nps-launch/story.html%5Cnhttp://www.unodc.org/documents/southeastasiaandpacific/Publications/2015/drugs/ATS_2015_Report_web.pdf

Uralets, V., Rana, S., Morgan, S., & Ross, W. (2014). Testing for designer stimulants: Metabolic profiles of 16 synthetic cathinones excreted free in human urine. *Journal of Analytical Toxicology*, *38*(5), 233–241. https://doi.org/10.1093/jat/bku021

Valente, P., Maria, J., & Guedes De, P. (2013). *Khat and synthetic cathinones : a review*. https://doi.org/10.1007/s00204-013-1163-9

Wood, E. J. (1996). Harper's biochemistry 24th edition. In *Biochemical Education* (Vol. 24). https://doi.org/10.1016/s0307-4412(97)80776-5

Zaitsu, K. (2018). *Metabolism of Synthetic Cathinones*. https://doi.org/10.1007/978-3-319-78707-7_5

Zaitsu, K., Katagi, M., Tatsuno, M., Sato, T., Tsuchihashi, H., & Suzuki, K. (2011). Recently abused β-keto derivatives of 3,4- methylenedioxyphenylalkylamines: A review of their metabolisms and toxicological analysis. *Forensic Toxicology*, Vol. 29, pp. 73–84. https://doi.org/10.1007/s11419-011-0111-8

Zaretzki, J., Matlock, M., & Swamidass, S. J. (2013). *XenoSite: Accurately Predicting CYP-Mediated Sites of Metabolism with Neural Networks*. (1).

Zuba, D., Adamowicz, P., & Byrska, B. (2013). Detection of buphedrone in biological and non-biological material - Two case reports. *Forensic Science International*, *227*(1–3), 15–20. https://doi.org/10.1016/j.forsciint.2012.08.034